Brown and Beige Adipocytes:
Effects of Inflammation and Nutritional Intervention

A Dissertation Presented for the
Doctor of Philosophy
Degree
The University of Tennessee, Knoxville

Jiyoung Bae
December 2015

Copyright © 2015 by Jiyoung Bae.
All rights reserved.

DEDICATION

With gratitude, I would like to dedicate this dissertation to my mother, Yeon Suk Jeong, and my father, Kyung Jik Bae, for their unconditional love, encouragement, and support throughout my life. I believe a special dedication is necessary for my husband and best friend, Sumin Shin, and my loving son, Jacob Onyu Shin.

ACKNOWLEDGEMENTS

It is my pleasure to express my sincere appreciation to all those who helped and supported me throughout my doctoral studies.

First, I would like to express my deepest gratitude to my committee chair, major advisor, and mentor, Dr. Jiangang Chen, for his kind encouragement and guidance during the PhD program at the University of Tennessee. He is always there and has provided invaluable support when I needed it. I would like to extend my sincere gratitude to Dr. Ling Zhao for her continuous help, support, and advice in both research and life as a working mom. I have been very fortunate to work with her during my doctoral studies. I would also like to thank Dr. Jay Whelan and Dr. Brynn Voy for serving on my dissertation committee and providing me with guidance and invaluable knowledge.

I would like to thank my college advisor, Dr. Young Hee Kang, for introducing me to scientific research, recognizing my ability, and pushing me to pursue my graduate degree.

I would like to give special thanks to my extraordinary husband Sumin Shin. He has been my greatest source of support, encouragement, and comfort during the past years. I am also incredibly grateful to my parents, Kyung Jik Bae and Yeon Suk Jeong, my sister, Yong Seon Bae, and parents-in-law, Ill Keun Shin and In Ja Park. All of them have always supported and encouraged me throughout my life. Without their unwavering support and confidence, I would not be where I am today. Finally, I would like to recognize and thank my other family members and friends who provided love and encouragement throughout my educational journey.

ABSTRACT

Recent findings of brown adipocytes and brown-like or beige adipocytes, capable of dissipating energy as heat, in adult humans have promised new hope for obesity treatment and prevention. Understanding of the regulation of brown and beige adipocytes will provide novel strategies to reach the goal. Pattern recognition receptors (PRR) are responsible for inflammation in adipose tissue, which leads to adipose dysfunction and obesity associated chronic diseases. It has been shown that PRR activation induces inflammation, leading to insulin resistance in white adipocytes and white adipose tissue (WAT). However, the roles of PRR activation in brown adipocytes and brown adipose tissue (BAT) have not been studied. In addition, in vitro and in vivo studies have shown that bioactive food components can contribute to obesity prevention; however, very few bioactive food components have been studied for their beneficial effects in promoting development and function of brown and beige adipocytes.

This dissertation reports that (1) mRNA of PRRs and inflammatory cytokines/chemokines are upregulated in the BAT of both diet induced obesity mice model and ob/ob mice model; (2) activation of PRRs induces activation of NF-κB and MAPK signaling pathways, leading to upregulation of the proinflammatory genes, MCP-1, IL-6, RANTES, and TNF-α, in mature brown adipocytes; (3) activation of PRRs suppresses UCP-1 expression, leading to decreased mitochondrial respiration and thermogenesis in mature brown adipocytes; (4) chronic activation of PRRs reduces adipogenesis and suppresses expression of brown-specific genes in both classic brown adipocytes and multipotent stem cells. This dissertation further demonstrates that

naringenin, a flavanone mainly found in citrus fruits, enhances thermogenic activation in isoproterenol-stimulated 3T3-L1 adipocytes through PKA/p38 MAPK pathways.

The results suggest that PRR-mediated inflammation in brown adipocytes may be a potential target for regulating BAT development and function for obesity treatment and prevention. Dietary bioactive compounds, such as naringenin, could be beneficial in promoting functional BAT, thereby contributing to energy expenditure.

TABLE OF CONTENTS

INTRODUCTION 1

CHAPTER I LITERATURE REVIEW 4

1.1 Obesity and adipose tissue 5

1.1.1 Obesity and metabolic disease 5

1.1.2 Anatomy of adipose tissue: WAT and BAT 6

1.1.3 Functions of adipose tissue: WAT and BAT 8

1.2 Chronic inflammation in obesity 11

1.2.1 Adipose inflammation in obesity 11

1.2.2 Role of the pattern recognition receptor in adipose inflammation 14

1.3 Novel targets for obesity treatment and prevention: Brown and beige adipocytes 19

1.3.1 Browning and beige 19

1.3.2 Origins of brown and beige adipocytes 21

1.3.3 Regulation of BAT development and function 22

1.3.4 Regulation of the browning process 26

1.3.5 Nutritional intervention of BAT development and browning 30

1.4 References 35

CHAPTER II ACTIVATION OF PATTERN RECOGNITION RECEPTORS IN BROWN ADIPOCYTES INDUCES INFLAMMATION AND SUPPRESSES UNCOUPLING PROTEIN 1 EXPRESSION AND MITOCHONDRIAL RESPIRATION 53

2.1 Abstract 55

2.2 Introduction 57

2.3 Materials and methods 61

2.4 Results..... 67

2.5 Discussion 74

2.6 References 81

2.7 Appendix..... 85

CHAPTER III CHRONIC ACTIVATION OF PATTERN RECOGNITION RECEPTORS SUPPRESSES BROWN ADIPOGENESIS OF MULTIPOTENT MESODERMAL STEM CELLS AND BROWN PRE-ADIPOCYTES 96

3.1 Abstract 98

3.2 Introduction..... 99

3.3 Materials and methods 102

3.4 Results..... 107

3.5 Discussion 114

3.6 References 119

3.7 Appendix..... 123

CHAPTER IV NARINGENIN, A CITRUS FLAVANONE, ENHANCES ISOPROTERENOL STIMULATED THERMOGENIC ACTIVATION OF 3T3-L1 ADIPOCYTES VIA PKA/P38 PATHWAYS..... 134

4.1 Abstract 136

4.2 Introduction..... 137

4.3 Materials and Methods 139

4.4 Results..... 144

4.5 Discussion 147

4.6 References 151

4.7 Appendix..... 154

CONCLUSION AND FUTURE DIRECTION 162

VITA 164

LIST OF FIGURES

Figure 1 mRNA expression of selected PRRs are up-regulated in brown fat tissue of DIO and ob/ob mice 86

Figure 2 Expression of selected PRRs are up-regulated during brown adipocyte differentiation..... 87

Figure 3 PRR activation in brown adipocytes induces phosphorylation and activation of NF-κB and MAPK signaling..... 88

Figure 4 PRR activation in brown adipocytes up-regulates the expression and secretion of proinflammatory cytokines/chemokines 89

Figure 5 Inhibition of NF-κB attenuates mRNA expression of proinflammatory cytokines/chemokines induced by PRR activation 90

Figure 6 Inhibition of MAPK differentially attenuates mRNA expression of proinflammatory cytokines/chemokines induced by PRR activation..... 91

Figure 7 PRR activation suppresses both basal and isoproterenol-induced UCP-1 expression, but not mitochondrial biogenesis, in brown adipocytes 92

Figure 8 PRR activation suppresses mitochondrial respiration in brown adipocytes.... 94

Figure 9 Selected PRRs are expressed and functional during commitment and differentiation of multipotent mesodermal stem C3H10T1/2 cells 124

Figure 10 Chronic activation of NOD1, TLR4, or TLR2 suppresses brown-like adipocyte differentiation of C3H10T1/2 cells 126

Figure 11 Molecular insights into the mechanisms by which chronic PRR activation suppresses brown-like differentiation of C3H10T1/2..... 127

Figure 12 PRR activation only during the commitment phase is sufficient to lead to suppression of brown-like differentiation of C3H10T1/2 cells..... 128

Figure 13 Molecular insights into the mechanisms by which PRR activation only during the commitment suppresses brown-like differentiation of C3H10T1/2 cells 129

Figure 14 PRR activation suppresses the commitment to brown-like adipocytes of C3H10T1/2 cells..... 130

Figure 15 Chronic activation of NOD1, TLR4, or TLR2 suppresses terminal differentiation of immortalized brown preadipocytes derived from BAT of mice 131

Figure 16 Activation of PRR suppresses PPARγ transactivation through NF-κB pathway 133

Figure 17 Effect of naringenin on mRNA expression of brown adipose specific markers 155

Figure 18 Effect of naringenin on mitochondrial respiration in isoproterenol induced 3T3-L1 adipocytes..... 156

Figure 19 Effect of naringenin on PKA activation 157

Figure 20 The effect of naringenin on the phosphorylation of p38 MAPK..... 158

Figure 21 Effect of naringenin on PPARγ and PPRE transactivation 159

Figure 22 Regulation of UCP-1 gene expression by pharmacological inhibitors for PKA/p38 MAPK signaling pathway 160

Figure 23 Schematic diagram of activation of β-adrenergic receptor-stimulated signaling pathway and naringenin effects..... 161

INTRODUCTION

Obesity is a major health concern in the US: over 70% of adults are overweight (BMI of 25 to 29.9) or obese (BMI of 30 and over). Obesity leads to metabolic diseases including heart disease, stroke, and diabetes (National Institutes of Health, 2011). Obesity is caused by excess of energy intake that exceeds energy expenditure. Food is a major source of energy intake, while physical activity and basic metabolism rate are the major contributors to energy expenditure (Church et al., 2011; Hill, Wyatt, & Peters, 2012). Physiologically, obesity is defined as excessive fat accumulation mostly in adipose tissue; hence, excess of adipose tissue is a hallmark of obesity. White adipose tissue (WAT) and brown adipose tissue (BAT) are the main types of adipose tissue in humans. WAT stores excess energy in the form of triglycerides whereas BAT dissipates energy through non-shivering thermogenesis, or heat production (Y. H. Lee, Mottillo, & Granneman, 2014).

It is well recognized that obesity is associated with inflammation in adipose tissue, characterized by elevated proinflammatory cytokine/chemokine expression and infiltration of immune cells and that adipose inflammation is the starting point for dysfunction of adipose tissue and lipid metabolism, leading to obesity associated chronic diseases (Eto et al., 2009). It has been demonstrated that pattern recognition receptors (PRRs), including Toll-like receptors (TLRs) and Nucleotide-oligomerization domain-containing protein-like receptors (NLRs), play important roles in innate immune response and mediating adipose inflammation (Jin, Henao-Mejia, & Flavell, 2013; Takeuchi & Akira 2010). PRRs are responsible for the sensing of invading microbial pathogens leading to distinct inflammatory and immune responses in the host cells.

In contrast to WAT's function for energy storage, BAT is a specialized tissue whose function is to produce heat through nonshivering thermogenesis via the functions of uncoupling protein 1 (UCP-1). UCP-1 proteins are localized in the inner membrane of brown adipocyte mitochondria to uncouple ATP synthesis from respiration. Newborn infants have BAT and that BAT quickly regresses following birth. However, new evidence from positron emission tomography/computed tomography scanning has revealed symmetrical fat depots in adults that have classical BAT features (Cypess et al. 2009; van Marken Lichtenbelt et al. 2009). Therefore, BAT has become a novel target for obesity treatment and prevention. While it has been reported that activation of PRRs increases inflammatory response and insulin resistance in WAT and white adipocytes (Pierre et al., 2013; Song et al., 2006; Zhao et al. 2011), the role of PRR-mediated inflammation in regulating the function of BAT and brown adipocytes has not been studied.

Recent evidence has also reported inducible brown-like adipocytes, also known as beige adipocytes, in WAT in animals and humans (Giralt & Villarroya, 2013; Lo & Sun, 2013; Rosenwald & Wolfrum, 2014). When exposed to cold temperature, hormonal stimuli (e.g. irisin and T3) (Obregon, 2014a; Zhang et al., 2014), or pharmacological treatment (e.g. rosiglitazone, bone morphogenetic protein, and isoproterenol) (Elsen et al., 2014; Obregon, 2014b; J. Wu et al., 2012), beige adipocytes can adopt a brown adipocyte phenotype (i.e., browning) with increased UCP-1 expression, contributing to thermogenesis and energy expenditure. Identification and characterization of dietary bioactive components to increase the development and functions of both classical brown and beige adipocytes hold great promise for obesity treatment and prevention.

Therefore, this dissertation begins with an overview of the role of inflammation, functions of adipose tissue, and genetic, pharmacological, and nutritional regulators for BAT development and browning functions. The chapter II focuses on the role of acute PRR activation in inflammation and mitochondrial respiration in mature brown adipocytes. The chapter III focuses on the role of chronic PPR activation in brown adipogenesis using two brown adipogenesis cellular models: immortalized brown pre-adipocytes and multipotent mesodermal stem cells. The chapter IV reports the effects of naringenin, a citrus flavanone, on browning and thermogenic function in 3T3-L1 adipocytes.

CHAPTER I

LITERATURE REVIEW

1.1 Obesity and adipose tissue

1.1.1 Obesity and metabolic disease

Obesity has become a growing epidemic worldwide over the past few decades (Keating, Backholer, & Peeters, 2014; Ng et al., 2014; Seidell & Halberstadt, 2015). Currently, almost 70% of adults in the US are overweight and 25% are obese, with rates having almost tripled in the last two decades (Ezzati, Martin, Skjold, Vander Hoorn, & Murray, 2006). Obesity is caused by a positive energy balance when energy intake exceeds energy expenditure over a given period of time (Vandevijvere, Chow, Hall, Umali, & Swinburn, 2015). Food intake is a major source of energy intake, while physical activity and basic metabolism rate are the major contributors to energy expenditure (Church et al., 2011; Hill, Wyatt, & Peters, 2012). However, our understanding of the mechanisms by which the body acts to achieve and maintain energy balance is incomplete (Hill et al., 2012).

In humans, energy is spent in several forms. Energy is expended to support basal metabolism needs for the normal functioning of cells and organs at rest. It is also expended to absorb and metabolize consumed food, which is referring to the thermic effect of food. Energy is also consumed through physical activity (Hill et al., 2012; Joosen & Westerterp, 2006) and dissipated for adaptive thermogenesis in response to environmental changes, such as cold temperature and diet (Tseng, Cypess, & Kahn, 2010). There are three types of thermogenesis: shivering thermogenesis, non-shivering, and diet-induced heat dissipation (Cannon & Nedergaard, 2011; Tseng et al., 2010). Shivering thermogenesis is induced in skeletal muscles and is a process in which heat is generated by shivering to stay warm (Tseng et al., 2010; van den Berg, van Marken

Lichtenbelt, van Dijk, & Schrauwen, 2011). Non-shivering thermogenesis occurs in the brown adipose tissue (BAT) upon certain stimuli such as cold exposure (Mineo, Cassell, Roberts, & Schaeffer, 2012; Nguyen et al., 2011; Sammons & Price, 2014; Teulier et al., 2010; van der Lans et al., 2013; van Marken Lichtenbelt & Schrauwen, 2011), while overfeeding could trigger the diet-induced thermogenesis propensity of brown fat to achieve energy balance (Shingo Kajimura & Saito, 2014; Tseng et al., 2010).

Obesity is a well-known risk factor that leads to metabolic disorder, including diabetes (Shigetoh et al., 2009), hypertension (Re, 2009), cardiovascular diseases (Apovian & Gokce, 2012), and cancers (Basen-Engquist & Chang, 2011). Metabolic disorder has at least three of the following features: abdominal obesity (waist circumference > 40 inches in males or 35 inches in females), hypertriglyceridemia (≥ 150 mg/dL), low HDL cholesterol (< 40 mg/dL in men or < 50 mg/dL in women), hypertension (≥ 130/85 or on antihypertensive medication), or elevated fasting glucose (≥ 110 mg/dL or on medication for diabetes). Insulin resistance has been suggested as the primary factor responsible and precedes other aspects of metabolic disorder (National Institutes of Health, 2011).

1.1.2 Anatomy of adipose tissue: WAT and BAT

There are two major types of adipose tissue: white adipose tissue (WAT) and BAT, which contribute to energy balance in humans (Y. H. Lee, Mottillo, & Granneman, 2014). WAT exists throughout the body and has different functions depending on the anatomical site. WAT is mainly found in two places: visceral adipose tissue and subcutaneous adipose tissue. Visceral adipose tissue is predominantly located around the inner organs, such as the intestines, stomach, spleen, kidney, gonad, uterus,

ovaries, epididymis, testis, and pericardial. Subcutaneous adipose tissue is located around the abdomen, hips, thighs, legs, and other lower body parts. The function of subcutaneous adipose tissue is protecting organs in the body and lipid accumulation (Bjørndal, Burri, Staalesen, Skorve, & Berge, 2011; Gesta, Tseng, & Kahn, 2007). Visceral adipose tissue is more associated with metabolic issues such as insulin resistance than subcutaneous adipose tissue. In contrast, BAT exists in a distinct location depending on species (only higher mammals) and age (Gesta et al., 2007; Saely, Geiger, & Drexel, 2012).

BAT is most abundant in the interscapular region and is present throughout life in rodents. In humans, BAT is located in the interscapular region and found in the cervical, paravertebral, supraclavicular, periadrenal, suprarenal, and subscapular areas in infants. However, it is remarkably reduced with age, leading to a remarkable absence in adults (Cinti, 2001, 2007; Gesta et al., 2007; Lanthier & Leclercq, 2014; Y. H. Lee et al., 2014; Saely et al., 2012; Vosselman, van Marken Lichtenbelt, & Schrauwen, 2013). Infants do not have enough muscles for shivering when exposed to cold temperatures, making heat production from BAT essential for maintaining temperature homeostasis (Devlin, 2015; Hu, Yin, et al., 2013; Zafrir, 2013). However, recent studies have detected BAT in adults using 2-deoxy-2-(^{18}F)fluoro-D-glucose integrated with Positron Emission Tomography associated with Computed Tomography (^{18}F-FDG PET/CT). FDG is the most common radiotracer and makes fluorine attach to glucose. Intravenous FDG and PET/CT scan images identify BAT spots through the anatomic localization of radiotracer uptake (Holstila et al., 2013; Hu, Perkins, Chia, & Gilsanz, 2013; J. W. Park et al., 2015).

The amount of active BAT in adult humans is associated with temperature, stress, age, and obesity (Cereijo, Giralt, & Villarroya, 2015; De Matteis et al., 2013; Saely et al., 2012; Virtanen, van Marken Lichtenbelt, & Nuutila, 2013; Vosselman et al., 2013; Zafrir, 2013). Catecholamine secreted in response to stress is also correlated with BAT activity. Pheochromocytoma patients have six times higher plasma metanephrine than normal patients and more BAT measured by 18^{F}-FDG PET/CT, while their body weight, cholesterol, blood glucose, triglyceride, and WAT show no significant difference (Q. Wang et al., 2011). BAT is more activated when exposed to cold temperature (16°C) compared to warm temperature (22°C) in lean male adults (body mass index (BMI) of 23 or lower). In addition, more BAT is detected in lean male adults in PET/CT scan images than obese adult males when exposed to cold temperature (van Marken Lichtenbelt et al., 2009). This also extends to in vivo studies that show lean mice have more BAT in 18^{F}-FDG PET images than obese imprinting control region (ICR) mice fed a high-fat diet (70% fat) and streptozocin-induced diabetic mice (C. Wu et al., 2014).

1.1.3 Functions of adipose tissue: WAT and BAT

The main functions of WAT are lipid synthesis and energy storage (Pavelka, Roth, Pavelka, & Roth, 2010). Excess energy in the form of triglycerides stored in WAT is hydrolyzed to free fatty acids and then released into the body's circulation to be used as energy for the organs (Giralt & Villarroya, 2013; Saely et al., 2012). This process of lipolysis plays important roles in energy metabolism, such as energy homeostasis in the human body. Besides energy storage and release, WAT also acts as an important endocrine organ as it expresses and secretes several polypeptide hormones known as adipokines, including leptin and adiponectin (Trayhurn & Beattle, 2001).

Increased serum leptin levels and decreased serum adiponectin levels are associated with higher obesity rates (Ricci & Bevilacqua, 2012). A higher ratio of leptin to adiponectin is observed in Italian young adults with severe obesity and metabolic phenotypes (insulin resistance and higher plasma lipid levels) than normal obese Italian young adults (Labruna et al., 2011). Leptin was first identified as an adipocyte hormone and plays an important role in controlling appetite, leading to the regulation of energy homeostasis in the body (Siegrist-Kaiser et al., 1997). Serum leptin level and body weight are increased in C57BL/6 mice fed a high-fat diet (60% fat) compared to regular chow-fed lean mice (Rhodes et al., 2013). Leptin (10 nM) significantly increases glycerol release, leading to lipolysis, in the WAT fat pad of Sprague-Dawley rats (Siegrist-Kaiser et al., 1997). Leptin-deficient ob/ob mice (C57BL/6J) have higher body weight and blood glucose level than lean mice (C57BL/6) (Drel et al., 2006). Acute physiological leptin (50-200 ng/h implanted tube by surgery) in leptin-deficient ob/ob mice dose-dependently reduces body weight and significantly increases plasma leptin level (Morton et al., 2011). Adiponectin, known as adipoQ, is also a key regulator of energy metabolism (Bjursell et al., 2007; Fang & Sweeney, 2006; Lafontan & Viguerie, 2006). Adiponectin is responsible for insulin sensitivity (Kadowaki et al., 2006; Maeda et al., 2002) and fatty acid oxidation (Yamauchi et al., 2002; Yoon et al., 2006). The levels of adiponectin and insulin resistance are significantly decreased in humans with obesity (Abdelgadir, Karlsson, Berglund, & Berne, 2013; Yadav, Kataria, Saini, & Yadav, 2013). Adiponectin macrophage-specific transgenic mice encoding human adiponectin gene and fed a high-fat diet have less tumor necrosis factor (TNF)-α and monocyte chemotactic protein (MCP)-1 mRNA expression in macrophage, skeletal muscle, and adipose tissue. In

addition, glucose tolerance and insulin tolerance are decreased in transgenic mice fed a high-fat diet compared to lean mice (Luo et al., 2010).

In contrast, the key function of BAT is to promote energy expenditure (Y. H. Lee et al., 2014). BAT is primarily responsible for energy oxidation to produce heat via uncoupling respiration to maintain the body's temperature (McMillan & White, 2015; Saely et al., 2012; van Marken Lichtenbelt & Schrauwen, 2011; Virtanen et al., 2013). In WAT, once the sympathetic nervous system (SNS) is activated, a neurotransmitter such as noradrenaline is released. The neurotransmitter then binds to beta-adrenergic receptors (β-AR) on the plasma membrane of adipocytes, leading to adenylyl cyclase activation. This in turn promotes the conversion of adenosine triphosphate (ATP) into the second messenger cyclic adenosine monophosphate (cyclic AMP or cAMP), activates protein kinase A (PKA), and subsequently releases free fatty acid through the lipolysis process. Free fatty acid released from lipid droplets is oxidized through the Krebs cycle in the mitochondria, and the intermediated electrons from the Krebs cycle flow through the electron transport chain (ETC) and produce a proton gradient to generate energy through ATP synthesis (Azzu & Brand, 2010; Brondani et al., 2012). In BAT, however, proton leak is produced from uncoupling protein-1 (UCP-1) on the mitochondrial inner membrane to generate heat instead of cellular respiration ATP synthesis (Azzu & Brand, 2010; Brondani et al., 2012; Cohen & Spiegelman, 2015; Harms & Seale, 2013). Saturated purine nucleotides (GDP) inhibit UCP-1 activation and fatty acids (palmitate) reactivate UCP-1. Heat generation via UCP-1 protein in BAT uncouples the respiratory chain, allowing fatty acid to be oxidized with low ATP production. The function of UCP-1 in BAT is discussed further in a later section.

Understanding the physiological and pathological mechanisms for reducing WAT functions and developing BAT functions can be important for preventing obesity. The key regulators of BAT development are discussed in a later section.

1.2 Chronic inflammation in obesity

1.2.1 Adipose inflammation in obesity

Inflammation in adipose tissue has been generally recognized as a primary cause of obesity and obesity-associated diseases (Balistreri, Caruso, & Candore, 2010). Adipose tissue comprises many kinds of cell types, including adipocytes, vascular cells, fibroblasts, and macrophages (Eto et al., 2009). Research has detected the infiltration of macrophages in adipose tissue of obese mice (Nishimura, Manabe, Nagasaki, et al., 2009). Infiltration of F4/80+ cluster of differentiation (CD)11b+ macrophages has also been demonstrated to be significantly higher in obese C57BL/6J mice fed a high-fat diet high fat diet and leptin-deficient ob/ob mice compared to regular chow-fed counterparts (Nishimura, Manabe, Nagasaki, et al., 2009). Macrophages in adipose tissue are responsible for inflammatory-specific gene expression, such as interleukin (IL)-6, TNF-α, transforming growth factor (TGF)-β, MCP-1, and chemotactic cytokine ligand 5 (CCL5 or RANTES) (Balistreri et al., 2010; Braunersreuther, Viviani, Mach, & Montecucco, 2012; Fantuzzi, 2005; Gilbert & Slingerland, 2013). Mice intraperitoneally injected with serum free macrophage-derived condition medium (0.1 mL/10 g) have significantly higher mRNA expression of TNF-α, IL-6, and MCP-1 in adipose tissue compared to saline-injected mice (Jiang et al., 2014). Ponies with metabolic diseases have 10-fold higher resting insulin level, serum TNF-α and IL-6 concentration, and body weight with

increased macrophage infiltration and TNF-α and IL-6 expression in adipose tissue compared to healthy ponies (Basinska, Marycz, Śmieszek, & Nicpoń, 2015).

TNF-α is secreted from adipocytes through activation of the mitogen-activated protein kinase (MAPK) and nuclear factor kappa B (NF-κB) signaling pathways, leading to the enhanced expression of inflammatory-related genes (X. Chen, Xun, Chen, & Wang, 2009; Gountopoulou, Leondaritis, Galanopoulou, & Mavri-Vavayanni, 2008). TNF-α is an especially important factor for adipose tissue because it regulates insulin resistance through insulin receptor signaling, and its upregulation leads to obesity and diabetes. A clinical study has indicated that serum TNF-α is upregulated in overweight/obese humans (13 males and 15 females with BMI of 27 or more) compared to lean humans (7 males and 8 females with BMI of 25 or less). In addition, expression of TNF-α in both subcutaneous and visceral adipose tissues is significantly increased (3 folds) in obese humans compared to lean humans (Winkler et al., 2003). TNF-α-infused male Syrian golden hamsters (0.5 μg/kg/h for 4 hours) have lower phosphorylation of insulin receptor (IR)-β and IR substrate-1 (IRS-1) in primary hepatocytes compared to control hamsters (Qin, Anderson, & Adeli, 2008), indicating TNF-α-induced hepatic insulin resistance.

As with TNF-α, IL-6 also plays an important role in inflammation in adipose tissue (Carlsen et al., 2009; Eder, Baffy, Falus, & Fulop, 2009). It has been shown that higher adiposity, body fat mass, waist circumference, and fatty acid levels increase serum IL-6 level in human studies (Morisset, Huot, Légaré, & Tchernof, 2008; Rexrode, Pradhan, Manson, Buring, & Ridker, 2003). Women (773 aged 50s) who have higher weight, BMI, body fat mass, and abdominal adipose tissue have higher circulating IL-6 level

(Morisset et al., 2008). A randomized double-blind study has also shown that higher serum IL-6 levels are detected in women who have higher BMI and waist/hip ratio among a total of 48 women (aged 39.6-61.7 and BMI of 17.2-41.3) (Rexrode et al., 2003).

MCP-1, a chemotactic factor, is significantly enhanced in the plasma of obese mice and humans (C. Kim et al., 2006; Takahashi et al., 2003). MCP-1 expression in epididymal WAT and circulating MCP-1 protein level are remarkably increased in C57BL/6N mice fed a high-fat diet (32.6% fat for 6 months) compared to regular chow-fed mice (Takahashi et al., 2003). A clinical study by Kim and associates has demonstrated that obese subjects (BMI of 30 or above) have higher triglyceride, total cholesterol, MCP-1, and IL-6 in serum compared to non-obese counterparts (BMI of 20 or less) (C. Kim et al., 2006). The expression of MCP-1 mRNA in WAT and plasma MCP-1 levels are significantly increased in C57BL/6J obese mice fed a high-fat diet, but not increased in regular chow-fed mice (Kanda et al., 2006). In addition, macrophage infiltration and expression of macrophage-related genes, TNF-α, CD68, and F4/80, are reduced in adipose tissue of MCP-1 knockout C57BL/6J mice (Kanda et al., 2006).

Evidence of the relationship between adipose tissue inflammation and obesity has been shown in animal and human studies (Nishimura, Manabe, & Nagai, 2009; Vieira et al., 2009; Wentworth et al., 2010). Humans with obesity or with both obesity and metabolic diseases have more macrophage infiltration in subcutaneous adipose tissue compared to lean humans. More macrophage infiltration leads to higher expression of proinflammatory cytokines, IL-1β, IL-6, and TNF-α (Wentworth et al., 2010). Furthermore, abnormal adipose function and lipid metabolism in obesity lead to

inflammation in adipose tissue (Ichimura et al., 2012; Iyer, Fairlie, Prins, Hammock, & Brown, 2010; Lumeng & Saltiel, 2011). High-fat diet-fed G-protein coupled receptor (GPR)120 knockout mice have 10% increased body weight compared to high-fat diet-fed wild-type mice. Lacking of GPR120 also leads to insulin resistance, resulting in decreased insulin signaling and increased inflammation in adipose tissue. High-fat diet-fed GPR120 knockout mice show impaired glucose metabolism, which is revealed by increased levels of fasting glucose and blood glucose. Moreover, adipocyte size and macrophage marker genes, CD11b, CD68 and F4/80, in adipose tissue are increased in high-fat diet-fed GPR120 knockout mice (Ichimura et al., 2012).

1.2.2 Role of the pattern recognition receptor in adipose inflammation

Lumeng has reviewed the importance of the innate immune response in obesity (Lumeng, 2013). Adipocytes attacked by foreign microbes recruit inflammatory macrophages around the damage site of the adipocytes, which secrete inflammatory cytokine, resulting in insulin resistance (Lumeng, 2013). The innate immune system recognizes pathogen-associated molecular patterns (PAMPs) via pattern recognition receptors (PRRs) that play an important role in inflammation and immune response (Miller et al., 2011; Takeuchi & Akira, 2010; Tang et al., 2011). There are two families of PPRs: membrane-bound toll-like receptors (TLRs) and cytoplasmic nucleotide oligomerization domain-like receptors (NLRs) in response to the inflammation of adipose tissue (J. Y. Lee, Zhao, & Hwang, 2010; Watanabe, Nagai, & Takatsu, 2013).

TLRs are composed of the extracellular leucine-rich repeat (LRR) and the cytoplasmic toll/interleukin-1 receptor (TIR) domain. There are 10 TLRs identified in humans, and each TLR recognizes a different ligand. For example, TLR2 and TLR4

recognize lipoprotein and lipopolysaccharide (LPS), respectively (Barton & Medzhitov, 2002; S.-J. Kim, Choi, Choi, & Park, 2012; Takeuchi & Akira, 2010). It has been widely shown that TLR2 and TLR4 are involved in metabolic functions and the inflammatory response in obesity (Ahmad et al., 2012; Fusaru et al., 2012). Immunohistochemical reaction results have shown that in lean subjects, TLR2 and TLR4 are expressed only in CD68 positive immunocompetent cells (which could be lymphocytes and myeloblasts). However, in obese subjects with BMI of 30 and over, TLRs 2 and 4 are expressed in three cell types: immunocompetent cells, vessels, and adipose cells. Subjects with diabesity (obesity and diabetes) have higher TLR2 and TLR4 expression in all three types of cells than obese subjects (Fusaru et al., 2012). The activation of TLR2 and TLR4 is mediated by MyD88, which comprises the death domain and TIR domain. Ahmad et al. have shown that TLR2 and TLR4 mRNA expression in peripheral blood mononuclear cells is positively correlated with BMI in human subjects (obese>overweight>lean). TLR2 and TLR4 expression in adipose tissue also increases in obese subjects (also obese>overweight>lean) (Ahmad et al., 2012).

MyD88 is more highly expressed in peripheral blood mononuclear cells and the adipose tissue of obese subjects than in lean subjects (Ahmad et al., 2012). MyD88 activates the MAPK and NF-κB pathways that are responsible for inflammatory response (Kawai & Akira, 2007). LPS (0.25-5 μg/mL for 12-48 hours) increases expression of TLR4 and proinflammatory cytokines, IL-6 and TNF-α, in primary bone marrow mesenchymal stem cells isolated from C57BL/6J mice (R.-L. Huang et al., 2013). Phosphorylation of NF-κB p65 and NF-κB are significantly increased in the LPS-treated bone marrow mesenchymal stem cells of wild type mice (C57BL/10 and

C57BL/6J), but are reduced in TLR4 knockout mice (C57BL/10ScNJ) and MyD88 knockout mice (R.-L. Huang et al., 2013). Fatty acid induces inflammatory response through TLR4 in adipose tissue in obese mice (Jung & Choi, 2014; Shi et al., 2006; Song, Kim, Yoon, & Kim, 2006). Free fatty acid induces TNF-α mRNA and IL-6 expression in macrophages and adipocytes isolated from wild-type mice but not in macrophages isolated from TLR4 knockout mice (C57BL6/J strain). Obese C57BL6/J mice fed a high fat diet (D12331 from Research Diets Inc. for 16 weeks) and leptin-deficient ob/ob mice have higher TLR4 mRNA expression in adipose tissue than regular chow-fed control mice and wild-type mice, respectively (Shi et al., 2006). 3T3-L1 adipocytes treated with free fatty acid (750 μM for 3 hours), LPS (5 μg/mL for 1 hour), and TNF-α (5 ng/mL for 1 hour) increase NF-κB activities by 2, 2, and 4-fold, respectively (Song et al., 2006). Male TLR4 knockout mice fed a high-fat diet (45% fat) have less body weight, subcutaneous adipose tissue, and visceral adipose tissue than C57BL/6J wild-type mice (Pierre et al., 2013). Both TLR4 and TLR2 mRNA are highly expressed in mature 3T3-L1 adipocytes and adipose tissue of high-fat diet-fed C57BL/6J mice and leptin-deficient ob/ob mice (Purohit et al., 2013; Zhao, Hu, Zhou, Purohit, & Hwang, 2011). Furthermore, TLR2 is responsible for insulin resistance in adipocytes. A previous study has shown that expression of IL-6, MCP-1, TLR2, and TLR4 is increased in 3T3-L1 adipocytes treated either palmitate (0.5 mM) or LPS (10 μg/mL) compared to non-treated cells. 3T3-L1 adipocytes treated with palmitate and LPS for 48 hours reduce insulin-stimulated 2-deoxyglucose uptake compared to non-treated control cells. Palmitate and LPS also increase NF-κB activation and IL-6, MCP-1, TLR2, and TLR4 mRNA expression through JNK pathways in 3T3-L1 adipocytes

(Davis, Gabler, Walker-Daniels, & Spurlock, 2009). Unlike TLR4 knockout mice, TLR2 knockout mice (C57BL/6J strain) are heavier than wild-type mice. MyD88 and IRS-1 expression is also increased, but insulin sensitivity is decreased in the muscle, liver, and adipose tissue of TLR2 knockout mice compared to wild-type mice (Caricilli et al., 2011). On the other hand, Ehses has reported that female TLR2 knockout mice (C57BL/6J strain) fed a high-fat diet for 20 weeks have improved peripheral insulin sensitivity than wild-type mice fed a high fat diet, indicating that the lack of TLR2 may lead to metabolic phenotype. Female TLR2 knockout mice fed a high-fat diet have less fat weight and MCP-1 mRNA expression in the liver, with no changes of other inflammatory cytokines in the liver, including IL-6 and TNF-α (Ehses et al., 2010). This suggests that mice without TLR2 may be protected from insulin resistance when fed a high fat diet. The different results from Caricilli and Ehses may be explained by the gender difference (male vs. female) or diet (regular chow vs. high-fat diet).

The NLR family is composed of the central nucleotide binding domain and the C-terminal LRR domain. There are two prominent members in the NLR family: nucleotide binding oligomerization domain (NOD)1 and NOD2. NOD1 recognizes γ-D-glutamyl-meso-diaminopimelic acid (iE-DAP, found in the peptidoglycan of gram-negative bacteria), and NOD2 recognizes MurNAc-L-Ala-D-isoGln (MDP, found in all bacteria) in the cytoplasm (Takeuchi & Akira, 2010). It has been shown that activated NOD1 and NOD2 intermediate inflammation in the adipocytes and adipose tissue of high-fat diet-induced obese mice and obese humans (Zhao et al., 2011; Zhou, Zhou, Li, & Song, 2012). NOD1 and NOD2 mRNA expression is positively correlated with the differentiation rate of primary adipocytes isolated from the subcutaneous abdominal

WAT of obese women. Primary human adipocytes treated with NOD1 ligand (iE-DAP, 100 μg/mL) induce NF-κB expression as well as IL-6, IL-8, and MCP-1 production, but no change is observed in primary human adipocytes treated with MDP (10 μg/mL) (Zhou et al., 2012).

Similar to TLRs, NLRs are also responsible for inflammatory reactions through the activation of MAPK and NF-κB pathways, leading to the production of proinflammatory cytokines. Studies have shown that mRNA expression of NOD1 and NOD2 is significantly increased in mature murine adipocytes, and NOD1, but not NOD2, is highly expressed in epididymal and subcutaneous adipose tissue of high-fat diet (60% fat for 20 weeks)-induced obese mice (C57BL/6J) (Zhao et al., 2011). MCP-1, CCL5, TNF-α, and IL-6 expression through the MAPK/NF-κB pathway is significantly increased in NOD1 ligand Tri-DAP (10-50 μg/mL for 15 hours)-induced 3T3-L1 adipocytes (Zhao et al., 2011). NOD1/2 double knockout male mice (C57BL/6 strain) fed a high-fat diet for 16 weeks have less adipose tissue, decreased liver weight, and reduced blood glucose level in insulin-tolerance compared to wild-type male C57BL/6 mice. NOD1 activation by NOD1 ligand FK156 (100 μg) induces insulin intolerance in NOD1 knockout mice, which is revealed by no change in blood glucose level. However, the glucose level is increased in wild-type and NOD2 knockout mice (Schertzer et al., 2011). On the other hand, NOD2 activation by NOD2 ligand MDP (5-10 μg/mL) significantly decreases 2-deoxyglucose uptake in L6-GLUT4 muscle cells. Phosphorylation of MAPK and IRS-1 are increased in L6-GLUT4 muscle cells treated with 10 μg/mL of MDP (Tamrakar et al., 2010).

Inflammation in adipose tissue, a hallmark of obesity, interferes with insulin resistance in WAT and energy expenditure in BAT, potentially leading to adipose tissue dysfunction. Inflammation also inhibits white and brown adipocyte differentiation, which disrupts energy storage in WAT and reduces BAT activation. Therefore, better understanding of the adipose tissue inflammation mechanism can help in the prevention of adipose dysfunction.

1.3 Novel targets for obesity treatment and prevention: Brown and beige adipocytes

1.3.1 Browning and beige

The main cells in both types of adipose tissue are called adipocytes (Rosenwald & Wolfrum, 2014). Interscapular BAT contains classic brown adipocytes, whereas epididymal and subcutaneous adipose tissues contain classic white adipocytes (Sanchez-Gurmaches & Guertin, 2014). White adipocytes have a single lipid droplet consisting of triglycerides and a small number of mitochondria. In contrast, brown adipocytes have multiple small lipid droplets and enriched amounts of mitochondria that are closer to those of skeletal muscle cells rather than white adipocytes (Algire, Medrikova, & Herzig, 2013; Giralt & Villarroya, 2013; Nakagami, 2013; A. Park, Kim, & Bae, 2014; Rosenwald & Wolfrum, 2014). Besides white and brown adipocytes, a third type has recently been discovered called beige adipocytes (Beranger et al., 2013; Giralt & Villarroya, 2013), which is identified in WAT. They differ in that they have few mitochondria and lower UCP-1 expression without stimuli. However, upon activation by exposure to physiological, pharmacological, or hormonal stimuli, the cells demonstrate

BAT-like phenotype with increased number of mitochondria, UCP-1 expression, and cellular respiration, a process referred to as the “browning” of WAT (Barneda, Frontini, Cinti, & Christian, 2013; Bartelt & Heeren, 2014; Bi & Li, 2013; Bonet, Oliver, & Palou, 2013; Elsen, Raschke, & Eckel, 2014; Giralt & Villarroya, 2013). Although certain cells in WAT show the BAT phenotype, the cells are not exactly the same as the classic brown fat cells, which is why the brown-like cells located in WAT have been called “beige” or “brite (brown in white)” cells (Harms & Seale, 2013; Keipert & Jastroch, 2014; P. Lee, Werner, Kebebew, & Celi, 2014; McMillan & White, 2015; A. Park et al., 2014; J. Wu et al., 2012; J. Wu, Cohen, & Spiegelman, 2013).

Human beige cells have been detected in PET/CT scan images in the neck and chest upon cold exposure (Bartelt & Heeren, 2014; J. W. Park et al., 2015). The number of white adipocytes in WAT is decreased while BAT is increased when adult female Sv129 mice are exposed to cold temperature for 10 days (Cinti, 2009). Obese patients have fewer beige cells compared to lean patients (Fernández-Galilea et al., 2015; P. Lee et al., 2014; Vijgen et al., 2011). Beige cells have also been detected in the WAT deposits of lean rodents but not in obese rodents (Rachid et al., 2015; J. Wu et al., 2012). Carey and colleagues have detected UCP-1 expression in differentiated primary white adipocytes isolated from the abdominal subcutaneous adipose tissue of healthy young adults but not in that of obese young adults (Carey et al., 2014). Expression of genes representing general adipogenesis, browning, and beige adipogenesis is higher in differentiated primary adipocytes than precursor cells (Carey et al., 2014). Although genes for classic brown adipogenesis have not been sufficiently detected, precursor cells in WAT have the potential to become brown-like adipocytes or beige adipocytes

since genes related to browning and beige adipogenesis are highly expressed in the primary adipocytes of WAT.

After beige cells are discovered, transdifferentiation, which is the transformation of white cells into brown-like cells, has been used for research on preventing obesity. Although white fat cells and brown fat cells have different characteristics, functions, and morphology, they share pluripotent mesenchymal stem cell as a common precursor. Hence, pluripotent mesenchymal stem cells are widely used for the browning process in in vitro studies (Algire et al., 2013; Birerdinc, Jarrar, Stotish, Randhawa, & Baranova, 2013; Giralt & Villarroya, 2013; Nakagami, 2013; A. Park et al., 2014; Rosenwald & Wolfrum, 2014). The regulators of the browning process are discussed in more detail in a later section.

1.3.2 Origins of brown and beige adipocytes

The difference of preadipocytes among brown adipocytes, white adipocytes, and beige adipocytes is the expression of myogenic regulatory factor (Myf)5, which is essential for skeletal muscle function (Ott, Bober, Lyons, Arnold, & Buckingham, 1991). Reduced muscle mass and delayed skeletal muscle regeneration are observed in Myf5 knockout mice (129Sv/C57BL/6 background) compared to wild-type mice (Ustanina, Carvajal, Rigby, & Braun, 2007). BAT contains 95% Myf5-positive and 5% Myf5-negative preadipocytes, while subcutaneous WAT contains 49% Myf5-positive and 51% Myf5-negative cells, and visceral WAT contains 70% Myf5-positive and 30% Myf5-negative preadipocytes (Sanchez-Gurmaches & Guertin, 2014). Brown adipocytes derived are exclusively from Myf5-positive myogenic lineages that can also be muscle cells, while white adipocytes are derived from Myf5-negative adipogenic lineages

(Sanchez-Gurmaches & Guertin, 2014). Beige adipocytes, however, have not been clearly defined. Reviewers have suggested that beige adipocytes can be derived from both Myf5-positive and -negative lineages, which exist in BAT and WAT, respectively (Gilsanz, Hu, & Kajimura, 2012; Giralt & Villarroya, 2013). Hence, the Myf5 expression of beige adipocytes is still questionable. In addition, the origin of beige adipocytes is reversible in that beige adipocytes are derived from either white adipocyte precursor cells or are converted from mature white adipocytes (Cinti, 2009; Q. A. Wang, Tao, Gupta, & Scherer, 2013; J. Wu et al., 2012).

There are several phases in between pluripotent mesenchymal stem cells and mature adipocytes, including the commitment and differentiation phases (Rosen & MacDougald, 2006). Key regulators covert the pluripotent mesenchymal stem cells to undifferentiated pre-cells such as osteoblasts, preadipocytes, and myoblasts (DiMarino, Caplan, & Bonfield, 2013). When stem cells complete the commitment phase, the pre-cells are differentiated by the regulation of specific transcriptional factors and become bone cells, fat cells, or muscle cells with their specific properties (Alonso, Claros, Becerra, & Andrades, 2008; Andrades et al., 2011; DiMarino et al., 2013).

1.3.3 Regulation of BAT development and function

Adipogenesis is a multi-step process, that includes growth arrest, clonal expansion, and differentiation from preadipocytes to become mature adipocytes (Carobbio, Rosen, & Vidal-Puig, 2013). Murine 3T3-L1 and 3T3-F442A white preadipocytes are widely used in white adipogenesis studies, and immortalized brown fat cell lines are available for brown adipogenesis studies (Moreno-Navarrete & Fernández-Real, 2012). Furthermore, transgenic mice models are used for studies

regarding adipose tissue function and development. A review paper (Harms & Seale, 2013) published in 2013 indicates enhanced beige fat activity in five types of transgenic mouse models with overexpression of prostaglandin-endoperoxide synthase (PTGS)2, forkhead box protein c (Foxc)2, PR domain containing (PRDM)16, phosphatase and tensin homolog (Pten), and UCP-1. Several transcriptional factors have been identified as regulating adipogenesis and adipose tissue development (Siersbæk, Nielsen, & Mandrup, 2012). Many studies on WAT and white adipocytes have already been conducted for the prevention of obesity, from benchside to human studies (Cummins et al., 2014; E. Y. Kim et al., 2015; Vázquez-Vela, Torres, & Tovar, 2008). Over the past decade, however, there has been increasing interest in the function and development of BAT and brown adipocytes for obesity prevention (Beranger et al., 2013; Bi & Li, 2013; Elattar & Satyanarayana, 2015; Harms & Seale, 2013; Lo & Sun, 2013; Saely et al., 2012; Seale, Kajimura, & Spiegelman, 2009; Virtanen et al., 2013; Vosselman et al., 2013; Whittle, Relat-Pardo, & Vidal-Puig, 2013). Therefore, in this section discusses three key regulators for BAT function and development: UCP-1, PGC1α, and PPARγ.

UCP-1 is a key brown marker gene for adaptive non-shivering thermogenesis in BAT (Cypess et al., 2009; Kozak, Koza, & Anunciado-Koza, 2010; Richard & Picard, 2011). UCP-1 is located in the inner mitochondrial membrane and produces heat in the ETC (Symonds, 2013). The expression of UCP-1 is regulated by several factors, including chronic cold exposure (van der Lans et al., 2013), activated hormone receptors (Martinez de Mena, Scanlan, & Obregon, 2010), the activation of the SNS (Mottillo et al., 2014), and other transcriptional factors (Symonds, 2013). Mice exposed to cold temperature have a greater UCP-1 expression in BAT than mice exposed to

warm temperature (Dong et al., 2013). UCP-1 knockout mice (C57BL/6J strain) have more cold-sensitive characteristics and a lesser ability to produce heat than wild-type mice (C57BL/6J) (Stier et al., 2014). The UCP-1 mRNA level is much lower in leptin-deficient obese mice than in wild-type mice (Ricciardi et al., 2014), and UCP-1 knockout mice are more likely to become obese when fed a high fat diet (Feldmann, Golozoubova, Cannon, & Nedergaard, 2009). In addition, UCP-1 is also regulated by the activation of cAMP, the thyroid hormone, and PPAR response elements (Martinez de Mena et al., 2010; Sears, MacGinnitie, Kovacs, & Graves, 1996). Mice with a reduced triiodothyronine (T3) level have lesser UCP-1 expression and lesser thermogenic resistance when exposed to cold temperature (Marrif et al., 2005). Moreover, the activation of the β-adrenergic receptor also induces UCP-1 expression (Mattsson et al., 2011). The activation of the β-adrenergic receptor activates cAMP and PKA activation and then activates downstream pathways, such as p38 MAPK, increasing UCP-1 expression (Cao, Medvedev, Daniel, & Collins, 2001; Chernogubova, Cannon, & Bengtsson, 2004; Collins, 2011; Hutchinson, Chernogubova, Dallner, Cannon, & Bengtsson, 2005). Therefore, UCP-1 is essential for BAT function in thermogenesis in a cold environment.

Peroxisome proliferator-activated receptor (PPAR) coactivator 1α (PGC1α), a transcriptional factor, is well known as a coactivator of PPAR (Medina-Gomez, Gray, & Vidal-Puig, 2007). PGC1α plays a critical role in tissue-specific sites that have a high number of mitochondria (Huss & Kelly, 2005). PGC1α induces hepatic gluconeogenesis against fasting, leading to the maintenance of blood glucose homeostasis in the liver (Rodgers et al., 2005; Y. Wang et al., 2012). PGC1α also regulates glucose uptake and

energy metabolism upon physical activities in the skeletal muscle (Baar et al., 2002; Bonen, 2009; Ehrenborg & Krook, 2009; C. Kang & Li Ji, 2012; Y.-X. Wang, 2010). Furthermore, it plays a more important role in mitochondria biogenesis in BAT than WAT, and it is responsible for the UCP-1 expression leading to heat production (Bostrom et al., 2012; H. Y. Chen, Liu, Salter, & Lomax, 2013). Therefore, like UCP-1, PGC1α is also significantly induced in cold temperatures and by β-adrenergic stimulation (Jan Nedergaard, Bengtsson, & Cannon, 2007). PCG1α expression is increased by the activation of cAMP-PKA signaling upon β-adrenergic stimulation (Cao et al., 2004; Singh, Simpson, & Bennett, 2015). Previous animal studies have shown that PGC1α knockout mice have significantly reduced thermogenic function with the exhibition of cold intolerance in response to cold exposure (Lin et al., 2004). In addition, PGC1α plays a major role in mitochondria biogenesis and the oxidative pathway in BAT with PPARγ and PPARα (Hondares et al., 2011). Overexpression of PGC1α in BAT increases the number of mitochondria and thermogenic-associated genes, including UCP-1 (Bostrom et al., 2012; Valle, Álvarez-Barrientos, Arza, Lamas, & Monsalve, 2005). Therefore, PGC1α is essential for BAT development and UCP-1 expression.

PPARγ plays a critical role in regulating adipogenesis in adipose tissue, as well as in adipocytes (Chawla, Schwarz, Dimaculangan, & Lazar, 1994; Lowell et al., 1999; Spiegelman, 1998). Studies have shown that PPARγ is required for BAT development (S. Kajimura, Seale, & Spiegelman, 2010; J. Nedergaard, Petrovic, Lindgren, Jacobsson, & Cannon, 2005; N. Petrovic et al., 2010), and PPARγ knockout mice reduce BAT development and thermogenic function (Jones et al., 2005). The activation of PPARγ induced by ligands promotes adipose tissue function and increases

adipocytes, leading to the increased expression of lipogenic genes such as fatty acid binding protein 4 (FABP4) (Benvenuti et al., 2007; Mallon et al., 2008; Tzeng, Chang, & Liu, 2014). Knocking out the PPARγ gene in the adipose tissue of mice leads to loss of fat and degeneration of adipose tissue function (Jones et al., 2005; F. Wang, Mullican, DiSpirito, Peed, & Lazar, 2013). In vitro, PPARγ is a master regulator of adipocyte differentiation from preadipocytes to mature adipocytes, and it increases the adipogenic gene expression (Chawla et al., 1994; J. Nedergaard et al., 2005; Spiegelman, 1998). Likewise, UCP-1 expression is regulated by PPARγ activation in brown adipocytes. It has been shown that rosiglitazone, a PPARγ agonist, induces UCP-1 expression in brown adipocytes (Pardo et al., 2011; Natasa Petrovic et al., 2010; Teruel, Hernandez, Benito, & Lorenzo, 2003).

1.3.4 Regulation of the browning process

As discussed in a previous section, browning is the process of transdifferentiation from white adipocytes to brown-like adipocytes or beige adipocytes (Beranger et al., 2013; Bi & Li, 2013; Cinti, 2009). In vivo, browning of WAT is when WAT takes BAT phenotype upon certain stimuli (Barneda et al., 2013; Bi & Li, 2013; Lo & Sun, 2013), such as exposure to cold, PPARγ agonist, or β-adrenergic receptor activator, which lead to thermogenesis, adipogenesis, and/or mitochondria biogenesis (Mineo et al., 2012; Nguyen et al., 2011; Teulier et al., 2010; van der Lans et al., 2013; van Marken Lichtenbelt & Schrauwen, 2011). Therefore, brown-specific markers and regulators- i.e. UCP-1, PGC1α, PPARγ and several newly discovered regulators- are key regulators for the browning process (Lo & Sun, 2013).

PRDM16 is major factor for brown adipogenesis in WAT and it works with other regulators for BAT development, including UCP-1, PGC1α, and PPARγ (Bartelt & Heeren, 2014; Lo & Sun, 2013; Seale et al., 2008). PRDM16 is essential for conversion from pluripotent mesenchymal stem cells to brown-like cells (Algire et al., 2013; Beranger et al., 2013; J. Wu et al., 2012). It has been shown that PRDM16 has higher expression in primary adipocytes isolated from subcutaneous WAT but not visceral WAT. UCP-1 expression is also enriched in primary adipocytes. Primary subcutaneous adipocytes isolated from PRDM16 knockout C57BL/6 mice significantly reduce total and uncoupled respiration compared to wild-type mice (Cohen et al., 2014). The role of PRDM16 for browning has also been determined in some animal studies. PRDM16, UCP-1, and PGC1α mRNA expression in subcutaneous WAT is reduced in PRDM16 knockout C57BL/6 mice fed a high-fat diet when the mice are exposed to cold temperature (Cohen et al., 2014). In contrast, PRDM16 transgenic mice (C57BL/6 strain) have greater energy expenditure and increased brown adipose-specific markers, UCP-1 and PGC1α mRNA levels in WAT. PRDM16 transgenic mice show reduced body weight and blood glucose in response to a high-fat diet (Ohno, Shinoda, Spiegelman, & Kajimura, 2012; Seale et al., 2011).

Bone morphogenetic proteins (BMPs), transforming growth factor beta (TGF-β) family, are multi-functional growth factors and are initially discovered to induce bone formation. A comprehensive analysis study has shown that five BMPs are commonly used for both osteogenic and adipogenic differentiation. It has been confirmed that BMP2,4,6,7, and 9 induce osteogenic differentiation and adipogenic differentiation,

which is revealed by alkaline phosphatase activity at day 7 and oil red O staining at day 20, respectively, in C3H10T1/2 mesenchymal stem cell (Q. Kang et al., 2008).

BMP2, BMP4, and BMP7 are mainly used and involved in adipogenic differentiation. BMP2 and BMP4 are responsible for conversion of mesenchymal stem cells to white adipocytes, whereas BMP7 is responsible for brown adipogenesis (Tseng et al., 2008). Recently, it has been discovered that BMP is an essential factor for commitment of mesenchymal stem cells to adipocyte lineage (H. Huang et al., 2009). During the commitment phase, mesenchymal stem cells treated with 10 ng/mL of BMP2 and 4, followed by induction of differentiation media resulted in increased lipid accumulation, which is assessed by oil red O staining (H. Huang et al., 2009). BMP7 (3.3 nM for 8 days) induces differentiation of primary brown preadipocytes derived from newborn wild-type mice to adipocytes, but 3T3-L1 preadipocytes are not differentiated into adipocytes by BMP7 (Tseng et al., 2008). In addition, gene expression of PPARγ, C/EBPα, FABP4, PGC1α, PRDM16, nuclear respiratory factor (NRF)-1, and transcription factor A (TFAM) are significantly increased in BMP7-treated brown adipocytes (Tseng et al., 2008). BMP7 treatment in the commitment phase also induces UCP-1 expression in C3H10T1/2 cells (Tseng et al., 2008). In contrast, Xue has shown that C3H10T1/2 cells treated with either BMP4 (20 ng/mL) or 7 (100 ng/mL) during the commitment phase significantly induce lipid accumulation and increase brown fat specific markers, including UCP-1 and PGC1α expression, as well as mitochondrial components (Xue et al., 2014). The same results have been shown in 3T3-L1 adipocytes (Xue et al., 2014).

BMP signaling also plays an important role in browning of WAT. Recently, it has been shown that BMP4 also promotes a white-to-brown transition in primary human adipose stem cells with the induction of BAT-specific markers, including UCP-1 and BAT development regulators, such as PRDM16 (Elsen, Raschke, Tennagels, et al., 2014; Gustafson et al., 2015). UCP-1, PGC1α, and PRDM16 are increased in BMP4-treated 3T3-L1 adipocytes (Qian et al., 2013). A large number of multilocular brown adipocytes and a small number of unilocular white adipocytes are found in BALB/C nude mice injected with stem cells treated with either BMP4 or 7 (Xue et al., 2014). BMP is also responsible for thermogenesis to maintain body temperature. It has confirmed that newborn BMP receptor (BmprIB) knockout mice (C57BL/6J strain) take more time to return to normal temperature after cold exposure compared to wild-type newborn mice (11 days vs. 48 hours) (Schulz et al., 2013).

Irisin, first reported in 2012, is well known as the ‘exercise hormone’, because it is produced during exercise and leads to energy expenditure in both mice and humans (Bostrom et al., 2012). Also called myokine, irisin was initially discovered in muscle cells after exercise. Irisin production from primary human skeletal muscle cells is significantly different between healthy adults and diabetic adults, but not obese adults [220]. The concentration of irisin is in the same range of that of insulin and leptin in human blood (Jedrychowski et al., 2015). Serum irisin levels are higher in exercised B6 mice (12 weeks) and non-diabetic obese male adults aged 50 days (free wheel running for 3 weeks and endurance exercise for 10 weeks, respectively). Another study, however, has shown that plasma irisin levels after 26 weeks of training are not significantly different between sedentary, aerobic endurance training, and strength endurance

training groups among healthy humans (age 50s, females and males, not obese and diabetic) (Hecksteden et al., 2013). These differences may be due to the different samples sizes, health conditions (healthy vs. obese vs. diabetic), age (20s vs. 50s), and gender (male only vs. male/female mix) used in different studies.

Recently, plasma irisin is detected by mass spectrometry in young healthy subjects. A high-intensity aerobic training group at over 70% aerobic capacity (3 days/week cycle ergometer and 2 days/week walking on a treadmill for 12 weeks) has more plasma irisin than a sedentary group (Jedrychowski et al., 2015). Purified r-irisin (0.5 μg/g/d for 14 days using intraperitoneal injection) increases UCP-1 and PGC1α gene expression and UCP-1-positive adipocytes in subcutaneous WAT of C57BL/6 mice fed a high-fat diet (60% fat) (Zhang et al., 2014). After 14 days, the body weight is decreased in irisin-injected mice compared to saline-injected mice fed a high-fat diet (Zhang et al., 2014). In addition, it has been shown that irisin increases UCP-1 and the thermogenic-related gene expression in the 3T3-L1 mature adipocytes (C. Wang et al., 2015) and WAT of mice (Bostrom et al., 2012). Irisin could be a potential target to prevent obesity through the browning of WAT. More studies are still needed to determine the underlying mechanism of the browning effect of irisin.

1.3.5 Nutritional intervention of BAT development and browning

It has been shown that both BAT and the browning of WAT are responsible for energy expenditure in many ways, including thermogenesis, mitochondria biogenesis, and fatty acid oxidation (Bartelt & Heeren, 2014; Cereijo et al., 2015; Cohen & Spiegelman, 2015; P. Lee & Greenfield, 2015; Lidell, Betz, & Enerback, 2014; McMillan & White, 2015; Roman et al., 2015; Symonds, 2013; Virtanen et al., 2013; Vosselman et

al., 2013; Zafrir, 2013). Thus, several nutritional compounds have been experimentally established to increase BAT function and energy expenditure to prevent obesity (Bonet et al., 2013; S. Wang et al., 2014).

Resveratrol is a type of natural polyphenolic compound found widely in the skins of grapes, red wine, and berries, and is well known as a protective agent against metabolic diseases (Lagouge et al., 2006). Numerous animal studies have supported the beneficial effects of resveratrol on obesity. Resveratrol reduces body weight and insulin resistance in high-fat diet-fed obese mice (C57BL6J) in the short term (400 mg/kg/day in commercial high fat diet purchased from Research diet for 15 weeks), as well as in the long term (25 mg/kg/day in 54.35% fat diet for 20 months) (Lagouge et al., 2006; Montero, de la Fuente, Fonteriz, Moreno, & Alvarez, 2014). Recently, resveratrol has been shown to promote cAMP-AMPK-PGC1α signaling, leading to the upregulating of mitochondria biogenesis and function (S. Wang et al., 2015). Lipid accumulation is significantly decreased in stromal vascular cells, isolated from inguinal WAT that are treated with 20 μM resveratrol.

Differentiated stromal vascular cells treated with 10 μM resveratrol significantly increase BAT-specific genes, UCP-1, PGC1α, and PRDM16; beige adipocyte selective genes, CD137 and transmembrane protein (TMEM)26; and AMPK phosphorylation (S. Wang et al., 2015). An animal study has supported that feeding a high-fat diet (45% fat) containing 0.1% resveratrol to CD1 female mice results in reduced body weight, increased AMPK phosphorylation, and increased UCP-1 and PRDM16 expression, but not PPARγ expression, in contrast to control mice fed a high-fat diet only (S. Wang et al., 2015). The thermogenic gene and the BAT-specific marker, the UCP-1 gene, is also

upregulated in BAT of male mice fed a resveratrol containing diet (4g/kg) (Andrade et al., 2014). Resveratrol also has novel browning properties in cell models and affects the number of mitochondria and fatty acid oxidation and UCP-1 expression in 3T3-L1 adipocytes (Mercader, Palou, & Bonet, 2011; Rayalam, Yang, Ambati, Della-Fera, & Baile, 2008). Resveratrol (20 μM) increases palmitate oxidation in both primary mouse embryonic fibroblast-derived adipocytes and 3T3-L1 adipocytes. In addition, resveratrol significantly increases UCP-1 expression in primary mouse embryonic fibroblast-derived adipocytes, but not in 3T3-L1 adipocytes (Mercader et al., 2011). Another study, however, has shown that resveratrol (25 μM) significantly decreases lipid accumulation and increases UCP-1 expression in 3T3-L1 adipocytes (Rayalam et al., 2008).

Polyunsaturated fatty acid (PUFA) contains two or more double bonds and includes the essential fatty acids, α-linolenic acid (ω-3) and linoleic acid (ω-6), which are known as anti-oxidant reagents (Buckley & Howe, 2010). Linoleic acid has provided browning effects in animal models. A diet containing linoleic acid (20% linoleic acid applied in 6.5% total lipid) increases UCP-1 and PGC1α gene expression in the epididymal WAT of leptin-deficient ob/ob mice (Wendel, Purushotham, Liu, & Belury, 2009). In addition, the omega-3 PUFA, eicosapentaenoic acid (EPA, 20:5) and docosahexaenoic acid (DHA, 22:6) found in fish oil, diminish obesity in animals (Buckley & Howe, 2010). Wistar rats fed a standard diet supplemented with either EPA or DHA show significantly decreased body weight gain (-27.4 and -22.1%, respectively) compared to standard diet only (10.8%). In addition, high-fat diet supplemented with either EPA or DHA also reduces body weight gain (8.8 and 5.5%, respectively) compared to a high-fat diet alone (15.3%) in wistar rats (Poudyal, Panchal, Ward, &

Brown, 2013). Omega-3 PUFA-supplemented high-fat diet (44% of lipids are replaced by EPA and DHA) increases fatty acid oxidation and mitochondria biogenesis by increasing the PGC1α and NRF-1 gene expressions in the epididymal WAT of male C57BL/6J mice (Flachs et al., 2005). Moreover, EPA and DHA enhance BAT weight with higher mitochondrial protein in high-fat diet-fed male wistar rats (Oudart et al., 1997).

Capsaicin has also been studied in regard to its role in BAT function and browning effects (Yoneshiro, Aita, Kawai, Iwanaga, & Saito, 2012). Capsaicin can be found in peppers and spicy food ingredients (Hayman & Kam, 2008). Capsaicin has been confirmed as an anti-obesity reagent targeting WAT and weight control in numerous previous studies, from in vitro to clinical human studies (Hwang et al., 2005; Joo, Kim, Choi, & Yun, 2010; J.-H. Kang et al., 2011; J. H. Kang et al., 2010; M. S. Lee, Kim, Kim, & Kim, 2011; Lejeune, Kovacs, & Westerterp-Plantenga, 2003). Recently, several studies have shown that capsaicin promotes BAT thermogenesis and energy expenditure in animal and human studies (Okamatsu-Ogura et al., 2015; Saito & Yoneshiro, 2013; Yoneshiro et al., 2012). Capsaicin administration (0.3% w/w for 8 weeks) together with exercise (free access to a running wheel) significantly increases BAT functions and lipolysis through cAMP-PKA pathways in high-fat diet-induced obese C57BL/6J mice (Ohyama et al., 2015). In addition, capsaicin (2 mg/kg BW dissolved in 0.9% saline for 12 weeks) upregulates brown adipocyte-specific markers, including UCP-1, PGC1α, and cell death-inducing DNA fragmentation factor alpha-like effector A (CIDEA) in subcutaneous WAT of regular chow-fed LACA mice (Baboota et al., 2014). A low dose of capsaicin at 1μM inhibits lipid accumulation and induces browning

through enhanced beige adipocytes and brown adipocyte-specific markers in 3T3-L1 adipocytes. In contrast, high dose of capsaicin at 100 μM increases lipid accumulation and decreases brown adipocytes-specific markers (Baboota et al., 2014).

Ginsenoid Rb1 is a major component found in ginseng (Leung & Wong, 2010). A previous study has shown that ginsenoid Rb1 significantly enhances glucose tolerance and increases insulin sensitivity via AMPK activation in male rats (Shen et al., 2015). Very recently, it has been found that ginsenoid Rb1 (10 μM) promotes browning effects through the amplified expression of UCP-1, PGC1α, and PRDM16, increased mitochondria respiration measured by oxygen consumption rate (OCR), and PPARγ activation in 3T3-L1 adipocytes (Mu et al., 2015).

In summary, various studies have shown evidence that BAT has properties related to energy expenditure while WAT is responsible for energy storage. Although BAT is detected in human adults, the amount of BAT is very low compared to infants. Instead, WAT increases with age, and human adults have plenty. Thus, the development of BAT as well as brown-like cells in WAT could have beneficial effects for the prevention of obesity. Understanding the mechanism of BAT function and the browning of WAT would be advantageous. The specific aims of this dissertation are to investigate whether 1) activation of PRRs induces inflammation and reduces UCP-1 and mitochondrial respiration in classic brown adipocytes; 2) activation of PRRs suppresses brown-like adipogenesis in C3H10T1/2 mesenchymal stem cells and brown preadipocytes; and 3) whether nutritional compound boosts brown adipocytes phenotypes in β-AR activation-induced 3T3-L1 white adipocytes.

1.4 References

Abdelgadir, M., Karlsson, A. F., Berglund, L., & Berne, C. (2013). Low serum adiponectin concentrations are associated with insulin sensitivity independent of obesity in Sudanese subjects with type 2 diabetes mellitus. *Diabetol Metab Syndr, 5*(1), 15.

Ahmad, R., Al-Mass, A., Atizado, V., Al-Hubail, A., Al-Ghimlas, F., Al-Arouj, M., . . . Behbehani, K. (2012). Elevated expression of the toll like receptors 2 and 4 in obese individuals: its significance for obesity-induced inflammation. *J Inflamm (Lond), 9*(1), 48.

Algire, C., Medrikova, D., & Herzig, S. (2013). White and brown adipose stem cells: from signaling to clinical implications. *Biochim Biophys Acta, 1831*(5), 896-904. doi:10.1016/j.bbalip.2012.10.001

Alonso, M., Claros, S., Becerra, J., & Andrades, J. (2008). The effect of type I collagen on osteochondrogenic differentiation in adipose-derived stromal cells in vivo. *Cytotherapy, 10*(6), 597-610.

Andrade, J. M. O., Frade, A. C. M., Guimarães, J. B., Freitas, K. M., Lopes, M. T. P., Guimarães, A. L. S., . . . Santos, S. H. S. (2014). Resveratrol increases brown adipose tissue thermogenesis markers by increasing SIRT1 and energy expenditure and decreasing fat accumulation in adipose tissue of mice fed a standard diet. *European journal of nutrition, 53*(7), 1503-1510.

Andrades, J. A., Guerado, E., Becerra, J., López-Puertas, J. M., Monleón, M., Araque, M. C., . . . Claros, S. (2011). *Skeletal Regeneration by Mesenchymal Stem Cells: What Else?* : INTECH Open Access Publisher.

Apovian, C. M., & Gokce, N. (2012). Obesity and cardiovascular disease. *Circulation, 125*(9), 1178-1182. doi:10.1161/CIRCULATIONAHA.111.022541

Azzu, V., & Brand, M. D. (2010). The on-off switches of the mitochondrial uncoupling proteins. *Trends Biochem Sci, 35*(5), 298-307. doi:10.1016/j.tibs.2009.11.001

Baar, K., Wende, A. R., Jones, T. E., Marison, M., Nolte, L. A., Chen, M., . . . Holloszy, J. O. (2002). Adaptations of skeletal muscle to exercise: rapid increase in the transcriptional coactivator PGC-1. *The FASEB Journal, 16*(14), 1879-1886.

Baboota, R. K., Singh, D. P., Sarma, S. M., Kaur, J., Sandhir, R., Boparai, R. K., . . . Bishnoi, M. (2014). Capsaicin induces "brite" phenotype in differentiating 3T3-L1 preadipocytes. *PLoS One, 9*(7), e103093. doi:10.1371/journal.pone.0103093

Balistreri, C. R., Caruso, C., & Candore, G. (2010). The role of adipose tissue and adipokines in obesity-related inflammatory diseases. *Mediators Inflamm, 2010*, 802078. doi:10.1155/2010/802078

Barneda, D., Frontini, A., Cinti, S., & Christian, M. (2013). Dynamic changes in lipid droplet-associated proteins in the "browning" of white adipose tissues. *Biochim Biophys Acta, 1831*(5), 924-933. doi:10.1016/j.bbalip.2013.01.015

Bartelt, A., & Heeren, J. (2014). Adipose tissue browning and metabolic health. *Nat Rev Endocrinol, 10*(1), 24-36. doi:10.1038/nrendo.2013.204

Barton, G., & Medzhitov, R. (2002). Toll-like receptors and their ligands *Toll-Like Receptor Family Members and Their Ligands* (pp. 81-92): Springer.

Basen-Engquist, K., & Chang, M. (2011). Obesity and cancer risk: recent review and evidence. *Curr Oncol Rep, 13*(1), 71-76. doi:10.1007/s11912-010-0139-7

Basinska, K., Marycz, K., Śmieszek, A., & Nicpoń, J. (2015). The production and distribution of IL-6 and TNF-α in subcutaneous adipose tissue and their correlation with serum concentrations in Welsh ponies with equine metabolic syndrome. *Journal of veterinary science, 16*(1), 113-120.

Benvenuti, S., Cellai, I., Luciani, P., Deledda, C., Baglioni, S., Giuliani, C., . . . Mannucci, E. (2007). Rosiglitazone stimulates adipogenesis and decreases osteoblastogenesis in human mesenchymal stem cells. *Journal of endocrinological investigation, 30*(9), RC26-RC30.

Beranger, G. E., Karbiener, M., Barquissau, V., Pisani, D. F., Scheideler, M., Langin, D., & Amri, E. Z. (2013). In vitro brown and "brite"/"beige" adipogenesis: human cellular models and molecular aspects. *Biochim Biophys Acta, 1831*(5), 905-914. doi:10.1016/j.bbalip.2012.11.001

Bi, S., & Li, L. (2013). Browning of white adipose tissue: role of hypothalamic signaling. *Ann N Y Acad Sci, 1302*, 30-34. doi:10.1111/nyas.12258

Birerdinc, A., Jarrar, M., Stotish, T., Randhawa, M., & Baranova, A. (2013). Manipulating molecular switches in brown adipocytes and their precursors: a therapeutic potential. *Prog Lipid Res, 52*(1), 51-61. doi:10.1016/j.plipres.2012.08.001

Bjørndal, B., Burri, L., Staalesen, V., Skorve, J., & Berge, R. K. (2011). Different adipose depots: their role in the development of metabolic syndrome and mitochondrial response to hypolipidemic agents. *Journal of obesity, 2011*.

Bjursell, M., Ahnmark, A., Bohlooly-Y, M., William-Olsson, L., Rhedin, M., Peng, X.-R., . . . Elmgren, A. (2007). Opposing effects of adiponectin receptors 1 and 2 on energy metabolism. *Diabetes, 56*(3), 583-593.

Bonen, A. (2009). PGC-1α-induced improvements in skeletal muscle metabolism and insulin sensitivity This paper is one of a selection of papers published in this Special Issue, entitled 14th International Biochemistry of Exercise Conference-Muscles as Molecular and Metabolic Machines, and has undergone the Journal's usual peer review process. *Applied Physiology, Nutrition, and Metabolism, 34*(3), 307-314.

Bonet, M. L., Oliver, P., & Palou, A. (2013). Pharmacological and nutritional agents promoting browning of white adipose tissue. *Biochim Biophys Acta, 1831*(5), 969-985. doi:10.1016/j.bbalip.2012.12.002

Bostrom, P., Wu, J., Jedrychowski, M. P., Korde, A., Ye, L., Lo, J. C., . . . Spiegelman, B. M. (2012). A PGC1-alpha-dependent myokine that drives brown-fat-like development of white fat and thermogenesis. *Nature, 481*(7382), 463-468. doi:10.1038/nature10777

Braunersreuther, V., Viviani, G. L., Mach, F., & Montecucco, F. (2012). Role of cytokines and chemokines in non-alcoholic fatty liver disease. *World journal of gastroenterology: WJG, 18*(8), 727.

Brondani, L. d. A., Assmann, T. S., Duarte, G. C. K., Gross, J. L., Canani, L. H., & Crispim, D. (2012). The role of the uncoupling protein 1 (UCP1) on the development of obesity and type 2 diabetes mellitus. *Arquivos Brasileiros de Endocrinologia & Metabologia, 56*(4), 215-225.

Buckley, J. D., & Howe, P. R. (2010). Long-chain omega-3 polyunsaturated fatty acids may be beneficial for reducing obesity—a review. *Nutrients, 2*(12), 1212-1230.

Cannon, B., & Nedergaard, J. (2011). Nonshivering thermogenesis and its adequate measurement in metabolic studies. *The Journal of experimental biology, 214*(2), 242-253.

Cao, W., Daniel, K. W., Robidoux, J., Puigserver, P., Medvedev, A. V., Bai, X., . . . Collins, S. (2004). p38 mitogen-activated protein kinase is the central regulator of cyclic AMP-dependent transcription of the brown fat uncoupling protein 1 gene. *Molecular and cellular biology, 24*(7), 3057-3067.

Cao, W., Medvedev, A. V., Daniel, K. W., & Collins, S. (2001). β-adrenergic activation of p38 MAP kinase in adipocytes cAMP induction of the uncoupling protein 1 (UCP1) gene requires p38 map kinase. *Journal of Biological Chemistry, 276*(29), 27077-27082.

Carey, A. L., Vorlander, C., Reddy-Luthmoodoo, M., Natoli, A. K., Formosa, M. F., Bertovic, D. A., . . . Kingwell, B. A. (2014). Reduced UCP-1 content in in vitro differentiated beige/brite adipocytes derived from preadipocytes of human subcutaneous white adipose tissues in obesity. *PLoS One, 9*(3), e91997.

Caricilli, A. M., Picardi, P. K., de Abreu, L. L., Ueno, M., Prada, P. O., Ropelle, E. R., . . . Camara, N. O. (2011). Gut microbiota is a key modulator of insulin resistance in TLR 2 knockout mice. *PLoS-Biology, 9*(12), 2567.

Carlsen, H., Haugen, F., Zadelaar, S., Kleemann, R., Kooistra, T., Drevon, C. A., & Blomhoff, R. (2009). Diet-induced obesity increases NF-κB signaling in reporter mice. *Genes & nutrition, 4*(3), 215-222.

Carobbio, S., Rosen, B., & Vidal-Puig, A. (2013). Adipogenesis: new insights into brown adipose tissue differentiation. *J Mol Endocrinol, 51*(3), T75-85.

Cereijo, R., Giralt, M., & Villarroya, F. (2015). Thermogenic brown and beige/brite adipogenesis in humans. *Ann Med, 47*(2), 169-177.

Chawla, A., Schwarz, E. J., Dimaculangan, D. D., & Lazar, M. A. (1994). Peroxisome proliferator-activated receptor (PPAR) gamma: adipose-predominant expression and induction early in adipocyte differentiation. *Endocrinology, 135*(2), 798-800.

Chen, H. Y., Liu, Q., Salter, A. M., & Lomax, M. A. (2013). Synergism between cAMP and PPARgamma Signalling in the Initiation of UCP1 Gene Expression in HIB1B Brown Adipocytes. *PPAR Res, 2013*, 476049. doi:10.1155/2013/476049

Chen, X., Xun, K., Chen, L., & Wang, Y. (2009). TNF-α, a potent lipid metabolism regulator. *Cell biochemistry and function, 27*(7), 407-416.

Chernogubova, E., Cannon, B., & Bengtsson, T. (2004). Norepinephrine increases glucose transport in brown adipocytes via β3-adrenoceptors through a cAMP, PKA, and PI3-kinase-dependent pathway stimulating conventional and novel PKCs. *Endocrinology, 145*(1), 269-280.

Church, T. S., Thomas, D. M., Tudor-Locke, C., Katzmarzyk, P. T., Earnest, C. P., Rodarte, R. Q., . . . Bouchard, C. (2011). Trends over 5 decades in US occupation-related physical activity and their associations with obesity. *PLoS One, 6*(5), e19657.

Cinti, S. (2001). The adipose organ: morphological perspectives of adipose tissues. *Proceedings of the Nutrition Society, 60*(03), 319-328.

Cinti, S. (2007). The adipose organ *Adipose tissue and adipokines in health and disease* (pp. 3-19): Springer.

Cinti, S. (2009). Transdifferentiation properties of adipocytes in the adipose organ. *American Journal of Physiology-Endocrinology and Metabolism, 297*(5), E977-E986.

Cohen, P., Levy, J. D., Zhang, Y., Frontini, A., Kolodin, D. P., Svensson, K. J., . . . Khandekar, M. J. (2014). Ablation of PRDM16 and beige adipose causes metabolic dysfunction and a subcutaneous to visceral fat switch. *Cell, 156*(1), 304-316.

Cohen, P., & Spiegelman, B. M. (2015). Brown and Beige Fat: Molecular Parts of a Thermogenic Machine. *Diabetes, 64*(7), 2346-2351.

Collins, S. (2011). β-Adrenoceptor signaling networks in adipocytes for recruiting stored fat and energy expenditure. *Frontiers in endocrinology, 2*.

Cummins, T. D., Holden, C. R., Sansbury, B. E., Gibb, A. A., Shah, J., Zafar, N., . . . Spite, M. (2014). Metabolic remodeling of white adipose tissue in obesity. *American Journal of Physiology-Endocrinology and Metabolism, 307*(3), E262-E277.

Cypess, A. M., Lehman, S., Williams, G., Tal, I., Rodman, D., Goldfine, A. B., . . . Doria, A. (2009). Identification and importance of brown adipose tissue in adult humans. *New England Journal of Medicine, 360*(15), 1509-1517.

Davis, J., Gabler, N., Walker-Daniels, J., & Spurlock, M. (2009). The c-Jun N-terminal kinase mediates the induction of oxidative stress and insulin resistance by palmitate and toll-like receptor 2 and 4 ligands in 3T3-L1 adipocytes. *Hormone and metabolic research= Hormon-und Stoffwechselforschung= Hormones et métabolisme, 41*(7), 523-530.

De Matteis, R., Lucertini, F., Guescini, M., Polidori, E., Zeppa, S., Stocchi, V., . . . Cuppini, R. (2013). Exercise as a new physiological stimulus for brown adipose tissue activity. *Nutr Metab Cardiovasc Dis, 23*(6), 582-590. doi:10.1016/j.numecd.2012.01.013

Devlin, M. J. (2015). The "Skinny" on brown fat, obesity, and bone. *Am J Phys Anthropol, 156 Suppl 59*, 98-115. doi:10.1002/ajpa.22661

DiMarino, A. M., Caplan, A. I., & Bonfield, T. L. (2013). Mesenchymal stem cells in tissue repair. *Frontiers in immunology, 4*.

Dong, M., Yang, X., Lim, S., Cao, Z., Honek, J., Lu, H., . . . Wahlberg, E. (2013). Cold exposure promotes atherosclerotic plaque growth and instability via UCP1-dependent lipolysis. *Cell metabolism, 18*(1), 118-129.

Drel, V. R., Mashtalir, N., Ilnytska, O., Shin, J., Li, F., Lyzogubov, V. V., & Obrosova, I. G. (2006). The leptin-deficient (ob/ob) mouse a new animal model of peripheral neuropathy of type 2 diabetes and obesity. *Diabetes, 55*(12), 3335-3343.

Eder, K., Baffy, N., Falus, A., & Fulop, A. K. (2009). The major inflammatory mediator interleukin-6 and obesity. *Inflammation Research, 58*(11), 727-736.

Ehrenborg, E., & Krook, A. (2009). Regulation of skeletal muscle physiology and metabolism by peroxisome proliferator-activated receptor δ. *Pharmacological Reviews, 61*(3), 373-393.

Ehses, J., Meier, D., Wueest, S., Rytka, J., Boller, S., Wielinga, P., . . . Van Lommel, L. (2010). Toll-like receptor 2-deficient mice are protected from insulin resistance and beta cell dysfunction induced by a high-fat diet. *Diabetologia, 53*(8), 1795-1806.

Elattar, S., & Satyanarayana, A. (2015). Can Brown Fat Win the Battle Against White Fat? *J Cell Physiol, 230*(10), 2311-2317. doi:10.1002/jcp.24986

Elsen, M., Raschke, S., & Eckel, J. (2014). Browning of white fat: does irisin play a role in humans? *J Endocrinol, 222*(1), R25-38. doi:10.1530/JOE-14-0189

Elsen, M., Raschke, S., Tennagels, N., Schwahn, U., Jelenik, T., Roden, M., . . . Eckel, J. (2014). BMP4 and BMP7 induce the white-to-brown transition of primary human adipose stem cells. *Am J Physiol Cell Physiol, 306*(5), C431-440. doi:10.1152/ajpcell.00290.2013

Eto, H., Suga, H., Matsumoto, D., Inoue, K., Aoi, N., Kato, H., . . . Yoshimura, K. (2009). Characterization of structure and cellular components of aspirated and excised adipose tissue. *Plastic and reconstructive surgery, 124*(4), 1087-1097.

Ezzati, M., Martin, H., Skjold, S., Vander Hoorn, S., & Murray, C. (2006). Trends in national and state-level obesity in the USA after correction for self-report bias: analysis of health surveys. *J R Soc Med, 99*, 250-257.

Fang, X., & Sweeney, G. (2006). Mechanisms regulating energy metabolism by adiponectin in obesity and diabetes. *Biochemical Society Transactions, 34*(Pt 5), 798-801.

Fantuzzi, G. (2005). Adipose tissue, adipokines, and inflammation. *J Allergy Clin Immunol, 115*(5), 911-919; quiz 920. doi:10.1016/j.jaci.2005.02.023

Feldmann, H. M., Golozoubova, V., Cannon, B., & Nedergaard, J. (2009). UCP1 ablation induces obesity and abolishes diet-induced thermogenesis in mice exempt from thermal stress by living at thermoneutrality. *Cell metabolism, 9*(2), 203-209.

Fernández-Galilea, M., Pérez-Matute, P., Prieto-Hontoria, P. L., Houssier, M., Burrell, M. A., Langin, D., . . . Moreno-Aliaga, M. J. (2015). α-Lipoic acid treatment increases mitochondrial biogenesis and promotes beige adipose features in subcutaneous adipocytes from overweight/obese subjects. *Biochimica et Biophysica Acta (BBA)-Molecular and Cell Biology of Lipids, 1851*(3), 273-281.

Flachs, P., Horakova, O., Brauner, P., Rossmeisl, M., Pecina, P., Franssen-van Hal, N., . . . Vlcek, C. (2005). Polyunsaturated fatty acids of marine origin upregulate mitochondrial biogenesis and induce β-oxidation in white fat. *Diabetologia, 48*(11), 2365-2375.

Fusaru, A., Stanciulescu, C., Surlin, V., Taisescu, C., Bold, A., Pop, O., . . . Pisoschi, C. (2012). Role of innate immune receptors TLR2 and TLR4 as mediators of the inflammatory reaction in human visceral adipose tissue. *Rom J Morphol Embryol, 53*(3 Suppl), 693-701.

Gesta, S., Tseng, Y. H., & Kahn, C. R. (2007). Developmental origin of fat: tracking obesity to its source. *Cell, 131*(2), 242-256. doi:10.1016/j.cell.2007.10.004

Gilbert, C. A., & Slingerland, J. M. (2013). Cytokines, obesity, and cancer: new insights on mechanisms linking obesity to cancer risk and progression. *Annual review of medicine, 64*, 45-57.

Gilsanz, V., Hu, H. H., & Kajimura, S. (2012). Relevance of brown adipose tissue in infancy and adolescence. *Pediatric research, 73*(1), 3-9.

Giralt, M., & Villarroya, F. (2013). White, brown, beige/brite: different adipose cells for different functions? *Endocrinology, 154*(9), 2992-3000. doi:10.1210/en.2013-1403

Gountopoulou, A., Leondaritis, G., Galanopoulou, D., & Mavri-Vavayanni, M. (2008). TNFα is a potent inducer of platelet-activating factor synthesis in adipocytes but not in preadipocytes. Differential regulation by PI3K. *Cytokine, 41*(2), 174-181.

Gustafson, B., Hammarstedt, A., Hedjazifar, S., Hoffmann, J. M., Svensson, P.-A., Grimsby, J., . . . Smith, U. (2015). BMP4 and BMP antagonists regulate human white and beige adipogenesis. *Diabetes, 64*(5), 1670-1681.

Harms, M., & Seale, P. (2013). Brown and beige fat: development, function and therapeutic potential. *Nat Med, 19*(10), 1252-1263. doi:10.1038/nm.3361

Hayman, M., & Kam, P. C. (2008). Capsaicin: a review of its pharmacology and clinical applications. *Current Anaesthesia & Critical Care, 19*(5), 338-343.

Hecksteden, A., Wegmann, M., Steffen, A., Kraushaar, J., Morsch, A., Ruppenthal, S., . . . Meyer, T. (2013). Irisin and exercise training in humans–results from a randomized controlled training trial. *BMC medicine, 11*(1), 235.

Hill, J. O., Wyatt, H. R., & Peters, J. C. (2012). Energy balance and obesity. *Circulation, 126*(1), 126-132.

Holstila, M., Virtanen, K. A., Gronroos, T. J., Laine, J., Lepomaki, V., Saunavaara, J., . . . Borra, R. J. (2013). Measurement of brown adipose tissue mass using a novel dual-echo magnetic resonance imaging approach: a validation study. *Metabolism, 62*(8), 1189-1198. doi:10.1016/j.metabol.2013.03.002

Hondares, E., Rosell, M., Díaz-Delfín, J., Olmos, Y., Monsalve, M., Iglesias, R., . . . Giralt, M. (2011). Peroxisome Proliferator-activated Receptor α (PPARα) Induces PPARγ Coactivator 1α (PGC-1α) Gene Expression and Contributes to Thermogenic Activation of Brown Fat INVOLVEMENT OF PRDM16. *Journal of Biological Chemistry, 286*(50), 43112-43122.

Hu, H. H., Perkins, T. G., Chia, J. M., & Gilsanz, V. (2013). Characterization of human brown adipose tissue by chemical-shift water-fat MRI. *AJR Am J Roentgenol, 200*(1), 177-183. doi:10.2214/AJR.12.8996

Hu, H. H., Yin, L., Aggabao, P. C., Perkins, T. G., Chia, J. M., & Gilsanz, V. (2013). Comparison of brown and white adipose tissues in infants and children with chemical-shift-encoded water-fat MRI. *J Magn Reson Imaging, 38*(4), 885-896. doi:10.1002/jmri.24053

Huang, H., Song, T. J., Li, X., Hu, L., He, Q., Liu, M., . . . Tang, Q. Q. (2009). BMP signaling pathway is required for commitment of C3H10T1/2 pluripotent stem cells to the adipocyte lineage. *Proc Natl Acad Sci U S A, 106*(31), 12670-12675. doi:10.1073/pnas.0906266106

Huang, R.-L., Yuan, Y., Zou, G.-M., Liu, G., Tu, J., & Li, Q. (2013). LPS-stimulated inflammatory environment inhibits BMP-2-induced osteoblastic differentiation through crosstalk between TLR4/MyD88/NF-κB and BMP/Smad signaling. *Stem cells and development, 23*(3), 277-289.

Huss, J. M., & Kelly, D. P. (2005). Mitochondrial energy metabolism in heart failure: a question of balance. *The Journal of clinical investigation, 115*(115 (3)), 547-555.

Hutchinson, D., Chernogubova, E., Dallner, O., Cannon, B., & Bengtsson, T. (2005). β-Adrenoceptors, but not α-adrenoceptors, stimulate AMP-activated protein kinase in brown adipocytes independently of uncoupling protein-1. *Diabetologia, 48*(11), 2386-2395.

Hwang, J.-T., Park, I.-J., Shin, J.-I., Lee, Y. K., Lee, S. K., Baik, H. W., . . . Park, O. J. (2005). Genistein, EGCG, and capsaicin inhibit adipocyte differentiation process via activating AMP-activated protein kinase. *Biochemical and biophysical research communications, 338*(2), 694-699.

Ichimura, A., Hirasawa, A., Poulain-Godefroy, O., Bonnefond, A., Hara, T., Yengo, L., . . . Iida, K. (2012). Dysfunction of lipid sensor GPR120 leads to obesity in both mouse and human. *Nature, 483*(7389), 350-354.

Iyer, A., Fairlie, D. P., Prins, J. B., Hammock, B. D., & Brown, L. (2010). Inflammatory lipid mediators in adipocyte function and obesity. *Nature Reviews Endocrinology, 6*(2), 71-82.

Jedrychowski, M. P., Wrann, C. D., Paulo, J. A., Gerber, K. K., Szpyt, J., Robinson, M. M., . . . Spiegelman, B. M. (2015). Detection and quantitation of circulating human irisin by tandem mass spectrometry. *Cell metabolism*.

Jiang, C., Yao, N., Wang, Q., Zhang, J., Sun, Y., Xiao, N., . . . Shang, X. (2014). Cyclocarya paliurus extract modulates adipokine expression and improves insulin sensitivity by inhibition of inflammation in mice. *Journal of ethnopharmacology, 153*(2), 344-351.

Jin, C., Henao-Mejia, J. and Flavell, R. A. (2013). Innate immune receptors: key regulators of metabolic disease progression. *Cell Metabolism*, 17(6), 873-882.

Jones, J. R., Barrick, C., Kim, K.-A., Lindner, J., Blondeau, B., Fujimoto, Y., . . . Magnuson, M. A. (2005). Deletion of PPARγ in adipose tissues of mice protects against high fat diet-induced obesity and insulin resistance. *Proceedings of the National Academy of Sciences, 102*(17), 6207-6212.

Joo, J. I., Kim, D. H., Choi, J.-W., & Yun, J. W. (2010). Proteomic analysis for antiobesity potential of capsaicin on white adipose tissue in rats fed with a high fat diet. *Journal of proteome research, 9*(6), 2977-2987.

Joosen, A., & Westerterp, K. R. (2006). Energy expenditure during overfeeding. *Nutr Metab (Lond), 3*, 25.

Jung, U. J., & Choi, M.-S. (2014). Obesity and its metabolic complications: the role of adipokines and the relationship between obesity, inflammation, insulin resistance, dyslipidemia and nonalcoholic fatty liver disease. *International journal of molecular sciences, 15*(4), 6184-6223.

Kadowaki, T., Yamauchi, T., Kubota, N., Hara, K., Ueki, K., & Tobe, K. (2006). Adiponectin and adiponectin receptors in insulin resistance, diabetes, and the metabolic syndrome. *Journal of Clinical Investigation, 116*(7), 1784.

Kajimura, S., & Saito, M. (2014). A new era in brown adipose tissue biology: molecular control of brown fat development and energy homeostasis. *Annual review of physiology, 76*, 225.

Kajimura, S., Seale, P., & Spiegelman, B. M. (2010). Transcriptional control of brown fat development. *Cell Metab, 11*(4), 257-262. doi:10.1016/j.cmet.2010.03.005

Kanda, H., Tateya, S., Tamori, Y., Kotani, K., Hiasa, K.-i., Kitazawa, R., . . . Egashira, K. (2006). MCP-1 contributes to macrophage infiltration into adipose tissue, insulin resistance, and hepatic steatosis in obesity. *Journal of Clinical Investigation, 116*(6), 1494.

Kang, C., & Li Ji, L. (2012). Role of PGC-1α signaling in skeletal muscle health and disease. *Annals of the New York Academy of Sciences, 1271*(1), 110-117.

Kang, J.-H., Tsuyoshi, G., Le Ngoc, H., Kim, H.-M., Tu, T. H., Noh, H.-J., . . . Yoo, H. (2011). Dietary capsaicin attenuates metabolic dysregulation in genetically obese diabetic mice. *Journal of medicinal food, 14*(3), 310-315.

Kang, J. H., Tsuyoshi, G., Han, I. S., Kawada, T., Kim, Y. M., & Yu, R. (2010). Dietary capsaicin reduces obesity-induced insulin resistance and hepatic steatosis in obese mice fed a high-fat diet. *Obesity, 18*(4), 780-787.

Kang, Q., Song, W.-X., Luo, Q., Tang, N., Luo, J., Luo, X., . . . Park, J. K. (2008). A comprehensive analysis of the dual roles of BMPs in regulating adipogenic and osteogenic differentiation of mesenchymal progenitor cells. *Stem cells and development, 18*(4), 545-558.

Kawai, T., & Akira, S. (2007). Signaling to NF-κB by Toll-like receptors. *Trends in molecular medicine, 13*(11), 460-469.

Keating, C., Backholer, K., & Peeters, A. (2014). Prevalence of overweight and obesity in children and adults. *The Lancet, 384*(9960), 2107-2108. doi:10.1016/s0140-6736(14)62367-9

Keipert, S., & Jastroch, M. (2014). Brite/beige fat and UCP1 - is it thermogenesis? *Biochim Biophys Acta, 1837*(7), 1075-1082. doi:10.1016/j.bbabio.2014.02.008

Kim, C., Park, H., Kawada, T., Kim, J., Lim, D., Hubbard, N., . . . Yu, R. (2006). Circulating levels of MCP-1 and IL-8 are elevated in human obese subjects and associated with obesity-related parameters. *International journal of Obesity, 30*(9), 1347-1355.

Kim, E. Y., Kim, W. K., Oh, K.-J., Han, B. S., Lee, S. C., & Bae, K.-H. (2015). Recent Advances in Proteomic Studies of Adipose Tissues and Adipocytes. *International journal of molecular sciences, 16*(3), 4581-4599.

Kim, S.-J., Choi, Y., Choi, Y.-H., & Park, T. (2012). Obesity activates toll-like receptor-mediated proinflammatory signaling cascades in the adipose tissue of mice. *The Journal of nutritional biochemistry, 23*(2), 113-122.

Kozak, L., Koza, R., & Anunciado-Koza, R. (2010). Brown fat thermogenesis and body weight regulation in mice: relevance to humans. *International journal of Obesity, 34*, S23-S27.

Labruna, G., Pasanisi, F., Nardelli, C., Caso, R., Vitale, D. F., Contaldo, F., & Sacchetti, L. (2011). High Leptin/Adiponectin Ratio and Serum Triglycerides Are Associated With an “At-Risk” Phenotype in Young Severely Obese Patients. *Obesity, 19*(7), 1492-1496.

Lafontan, M., & Viguerie, N. (2006). Role of adipokines in the control of energy metabolism: focus on adiponectin. *Current opinion in pharmacology, 6*(6), 580-585.

Lagouge, M., Argmann, C., Gerhart-Hines, Z., Meziane, H., Lerin, C., Daussin, F., . . . Elliott, P. (2006). Resveratrol improves mitochondrial function and protects against metabolic disease by activating SIRT1 and PGC-1α. *Cell, 127*(6), 1109-1122.

Lanthier, N., & Leclercq, I. A. (2014). Adipose tissues as endocrine target organs. *Best Pract Res Clin Gastroenterol, 28*(4), 545-558. doi:10.1016/j.bpg.2014.07.002

Lee, J. Y., Zhao, L., & Hwang, D. H. (2010). Modulation of pattern recognition receptor-mediated inflammation and risk of chronic diseases by dietary fatty acids. *Nutrition reviews, 68*(1), 38-61.

Lee, M. S., Kim, C. T., Kim, I. H., & Kim, Y. (2011). Effects of Capsaicin on Lipid Catabolism in 3T3-L1 Adipocytes. *Phytotherapy Research, 25*(6), 935-939.
Lee, P., & Greenfield, J. R. (2015). Non-pharmacological and pharmacological strategies of brown adipose tissue recruitment in humans. *Mol Cell Endocrinol*. doi:10.1016/j.mce.2015.05.025
Lee, P., Werner, C. D., Kebebew, E., & Celi, F. S. (2014). Functional thermogenic beige adipogenesis is inducible in human neck fat. *Int J Obes (Lond), 38*(2), 170-176. doi:10.1038/ijo.2013.82
Lee, Y. H., Mottillo, E. P., & Granneman, J. G. (2014). Adipose tissue plasticity from WAT to BAT and in between. *Biochim Biophys Acta, 1842*(3), 358-369. doi:10.1016/j.bbadis.2013.05.011
Lejeune, M. P., Kovacs, E. M., & Westerterp-Plantenga, M. S. (2003). Effect of capsaicin on substrate oxidation and weight maintenance after modest body-weight loss in human subjects. *British Journal of Nutrition, 90*(03), 651-659.
Leung, K. W., & Wong, A. S. (2010). Pharmacology of ginsenosides: a literature review. *Chinese Medicine, 5*(1), 20.
Lidell, M. E., Betz, M. J., & Enerback, S. (2014). Two types of brown adipose tissue in humans. *Adipocyte, 3*(1), 63-66. doi:10.4161/adip.26896
Lin, J., Wu, P.-H., Tarr, P. T., Lindenberg, K. S., St-Pierre, J., Zhang, C.-y., . . . Reznick, R. M. (2004). Defects in adaptive energy metabolism with CNS-linked hyperactivity in PGC-1α null mice. *Cell, 119*(1), 121-135.
Lo, K. A., & Sun, L. (2013). Turning WAT into BAT: a review on regulators controlling the browning of white adipocytes. *Biosci Rep, 33*(5). doi:10.1042/BSR20130046
Lowell, B. B., Sodroski, J. G., Okano, M., Bell, D. W., Haber, D. A., & Li, E. (1999). An essential regulator of adipogenesis and modulator of fat cell function: PPAR [gamma]. *Cell, 99*(3), 239-242.
Lumeng, C. N. (2013). Innate immune activation in obesity. *Molecular aspects of medicine, 34*(1), 12-29.
Lumeng, C. N., & Saltiel, A. R. (2011). Inflammatory links between obesity and metabolic disease. *The Journal of clinical investigation, 121*(6), 2111.
Luo, N., Liu, J., Chung, B. H., Yang, Q., Klein, R. L., Garvey, W. T., & Fu, Y. (2010). Macrophage adiponectin expression improves insulin sensitivity and protects against inflammation and atherosclerosis. *Diabetes, 59*(4), 791-799.
Maeda, N., Shimomura, I., Kishida, K., Nishizawa, H., Matsuda, M., Nagaretani, H., . . . Arita, Y. (2002). Diet-induced insulin resistance in mice lacking adiponectin/ACRP30. *Nature medicine, 8*(7), 731-737.
Mallon, P. W., Sedwell, R., Rogers, G., Nolan, D., Unemori, P., Hoy, J., . . . Cooper, D. A. (2008). Effect of rosiglitazone on peroxisome proliferator-activated receptor γ gene expression in human adipose tissue is limited by antiretroviral drug-induced mitochondrial dysfunction. *Journal of Infectious Diseases, 198*(12), 1794-1803.
Marrif, H., Schifman, A., Stepanyan, Z., Gillis, M.-A., Calderone, A., Weiss, R. E., . . . Silva, J. E. (2005). Temperature homeostasis in transgenic mice lacking thyroid hormone receptor-α gene products. *Endocrinology, 146*(7), 2872-2884.
Martinez de Mena, R., Scanlan, T. S., & Obregon, M.-J. (2010). The T3 receptor β1 isoform regulates UCP1 and D2 deiodinase in rat brown adipocytes. *Endocrinology, 151*(10), 5074-5083.

Mattsson, C. L., Csikasz, R. I., Chernogubova, E., Yamamoto, D. L., Hogberg, H. T., Amri, E.-Z., . . . Bengtsson, T. (2011). β1-Adrenergic receptors increase UCP1 in human MADS brown adipocytes and rescue cold-acclimated β3-adrenergic receptor-knockout mice via nonshivering thermogenesis. *American Journal of Physiology-Endocrinology and Metabolism, 301*(6), E1108-E1118.

McMillan, A. C., & White, M. D. (2015). Induction of thermogenesis in brown and beige adipose tissues: molecular markers, mild cold exposure and novel therapies. *Curr Opin Endocrinol Diabetes Obes, 22*(5), 347-352. doi:10.1097/MED.0000000000000191

Medina-Gomez, G., Gray, S., & Vidal-Puig, A. (2007). Adipogenesis and lipotoxicity: role of peroxisome proliferator-activated receptor gamma (PPARgamma) and PPARgammacoactivator-1 (PGC1). *Public Health Nutr, 10*(10A), 1132-1137. doi:10.1017/S1368980007000614

Mercader, J., Palou, A., & Bonet, M. L. (2011). Resveratrol enhances fatty acid oxidation capacity and reduces resistin and Retinol-Binding Protein 4 expression in white adipocytes. *The Journal of nutritional biochemistry, 22*(9), 828-834.

Miller, Y. I., Choi, S.-H., Wiesner, P., Fang, L., Harkewicz, R., Hartvigsen, K., . . . Que, X. (2011). Oxidation-specific epitopes are danger-associated molecular patterns recognized by pattern recognition receptors of innate immunity. *Circulation research, 108*(2), 235-248.

Mineo, P., Cassell, E., Roberts, M., & Schaeffer, P. (2012). Chronic cold acclimation increases thermogenic capacity, non-shivering thermogenesis and muscle citrate synthase activity in both wild-type and brown adipose tissue deficient mice. *Comparative Biochemistry and Physiology Part A: Molecular & Integrative Physiology, 161*(4), 395-400.

Montero, M., de la Fuente, S., Fonteriz, R. I., Moreno, A., & Alvarez, J. (2014). Effects of Long-Term Feeding of the Polyphenols Resveratrol and Kaempferol in Obese Mice.

Moreno-Navarrete, J. M., & Fernández-Real, J. M. (2012). Adipocyte differentiation *Adipose tissue biology* (pp. 17-38): Springer.

Morisset, A. S., Huot, C., Légaré, D., & Tchernof, A. (2008). Circulating IL-6 Concentrations and Abdominal Adipocyte Isoproterenol-stimulated Lipolysis in Women. *Obesity, 16*(7), 1487-1492.

Morton, G. J., Kaiyala, K. J., Fisher, J. D., Ogimoto, K., Schwartz, M. W., & Wisse, B. E. (2011). Identification of a physiological role for leptin in the regulation of ambulatory activity and wheel running in mice. *American Journal of Physiology-Endocrinology and Metabolism, 300*(2), E392-E401.

Mottillo, E. P., Balasubramanian, P., Lee, Y.-H., Weng, C., Kershaw, E. E., & Granneman, J. G. (2014). Coupling of lipolysis and de novo lipogenesis in brown, beige, and white adipose tissues during chronic β3-adrenergic receptor activation. *Journal of lipid research, 55*(11), 2276-2286.

Mu, Q., Fang, X., Li, X., Zhao, D., Mo, F., Jiang, G., . . . Fu, M. (2015). Ginsenoside Rb1 promotes browning through regulation of PPARγ in 3T3-L1 adipocytes. *Biochemical and biophysical research communications*.

Nakagami, H. (2013). The mechanism of white and brown adipocyte differentiation. *Diabetes Metab J, 37*(2), 85-90. doi:10.4093/dmj.2013.37.2.85

National Institutes of Health. (2011). What is metabolic syndrome? Retrieved from http://www.nhlbi.nih.gov/health/health-topics/topics/ms

Nedergaard, J., Bengtsson, T., & Cannon, B. (2007). Unexpected evidence for active brown adipose tissue in adult humans. *American Journal of Physiology-Endocrinology and Metabolism, 293*(2), E444-E452.

Nedergaard, J., Petrovic, N., Lindgren, E. M., Jacobsson, A., & Cannon, B. (2005). PPARgamma in the control of brown adipocyte differentiation. *Biochim Biophys Acta, 1740*(2), 293-304. doi:10.1016/j.bbadis.2005.02.003

Ng, M., Fleming, T., Robinson, M., Thomson, B., Graetz, N., Margono, C., . . . Gakidou, E. (2014). Global, regional, and national prevalence of overweight and obesity in children and adults during 1980–2013: a systematic analysis for the Global Burden of Disease Study 2013. *The Lancet, 384*(9945), 766-781. doi:10.1016/s0140-6736(14)60460-8

Nguyen, K. D., Qiu, Y., Cui, X., Goh, Y. S., Mwangi, J., David, T., . . . Chawla, A. (2011). Alternatively activated macrophages produce catecholamines to sustain adaptive thermogenesis. *Nature, 480*(7375), 104-108.

Nishimura, S., Manabe, I., & Nagai, R. (2009). Adipose tissue inflammation in obesity and metabolic syndrome. *Discovery medicine, 8*(41), 55.

Nishimura, S., Manabe, I., Nagasaki, M., Eto, K., Yamashita, H., Ohsugi, M., . . . Sugiura, S. (2009). CD8+ effector T cells contribute to macrophage recruitment and adipose tissue inflammation in obesity. *Nature medicine, 15*(8), 914-920.

Ohno, H., Shinoda, K., Spiegelman, B. M., & Kajimura, S. (2012). PPARγ agonists induce a white-to-brown fat conversion through stabilization of PRDM16 protein. *Cell metabolism, 15*(3), 395-404.

Ohyama, K., Nogusa, Y., Suzuki, K., Shinoda, K., Kajimura, S., & Bannai, M. (2015). A combination of exercise and capsinoid supplementation additively suppresses diet-induced obesity by increasing energy expenditure in mice. *American Journal of Physiology-Endocrinology and Metabolism, 308*(4), E315-E323.

Okamatsu-Ogura, Y., Tsubota, A., Ohyama, K., Nogusa, Y., Saito, M., & Kimura, K. (2015). Capsinoids suppress diet-induced obesity through uncoupling protein 1-dependent mechanism in mice. *Journal of Functional Foods, 19*, 1-9.

Ott, M.-O., Bober, E., Lyons, G., Arnold, H., & Buckingham, M. (1991). Early expression of the myogenic regulatory gene, myf-5, in precursor cells of skeletal muscle in the mouse embryo. *Development, 111*(4), 1097-1107.

Oudart, H., Groscolas, R., Calgari, C., Nibbelink, M., Leray, C., Le Maho, Y., & Malan, A. (1997). Brown fat thermogenesis in rats fed high-fat diets enriched with n-3 polyunsaturated fatty acids. *International journal of Obesity, 21*(11), 955-962.

Pardo, R., Enguix, N., Lasheras, J., Feliu, J. E., Kralli, A., & Villena, J. A. (2011). Rosiglitazone-induced mitochondrial biogenesis in white adipose tissue is independent of peroxisome proliferator-activated receptor gamma coactivator-1alpha. *PLoS One, 6*(11), e26989.

Park, A., Kim, W. K., & Bae, K. H. (2014). Distinction of white, beige and brown adipocytes derived from mesenchymal stem cells. *World J Stem Cells, 6*(1), 33-42. doi:10.4252/wjsc.v6.i1.33

Park, J. W., Jung, K. H., Lee, J. H., Quach, C. H., Moon, S. H., Cho, Y. S., & Lee, K. H. (2015). 18F-FDG PET/CT monitoring of beta3 agonist-stimulated brown

adipocyte recruitment in white adipose tissue. *J Nucl Med, 56*(1), 153-158. doi:10.2967/jnumed.114.147603
Pavelka, M., Roth, J., Pavelka, M., & Roth, J. (2010). White Adipose Tissue. *Functional Ultrastructure: Atlas of Tissue Biology and Pathology*, 290-291.
Petrovic, N., Walden, T. B., Shabalina, I. G., Timmons, J. A., Cannon, B., & Nedergaard, J. (2010). Chronic peroxisome proliferator-activated receptor gamma (PPARgamma) activation of epididymally derived white adipocyte cultures reveals a population of thermogenically competent, UCP1-containing adipocytes molecularly distinct from classic brown adipocytes. *J Biol Chem, 285*(10), 7153-7164. doi:10.1074/jbc.M109.053942
Petrovic, N., Walden, T. B., Shabalina, I. G., Timmons, J. A., Cannon, B., & Nedergaard, J. (2010). Chronic peroxisome proliferator-activated receptor γ (PPARγ) activation of epididymally derived white adipocyte cultures reveals a population of thermogenically competent, UCP1-containing adipocytes molecularly distinct from classic brown adipocytes. *Journal of Biological Chemistry, 285*(10), 7153-7164.
Pierre, N., Deldicque, L., Barbe, C., Naslain, D., Cani, P. D., & Francaux, M. (2013). Toll-like receptor 4 knockout mice are protected against endoplasmic reticulum stress induced by a high-fat diet. *PLoS One, 8*(5), e65061. doi:10.1371/journal.pone.0065061
Poudyal, H., Panchal, S. K., Ward, L. C., & Brown, L. (2013). Effects of ALA, EPA and DHA in high-carbohydrate, high-fat diet-induced metabolic syndrome in rats. *The Journal of nutritional biochemistry, 24*(6), 1041-1052.
Purohit, J. S., Hu, P., Chen, G., Whelan, J., Moustaid-Moussa, N., & Zhao, L. (2013). Activation of nucleotide oligomerization domain containing protein 1 induces lipolysis through NF-kappaB and the lipolytic PKA activation in 3T3-L1 adipocytes. *Biochem Cell Biol, 91*(6), 428-434. doi:10.1139/bcb-2013-0049
Qian, S.-W., Tang, Y., Li, X., Liu, Y., Zhang, Y.-Y., Huang, H.-Y., . . . Gao, H.-D. (2013). BMP4-mediated brown fat-like changes in white adipose tissue alter glucose and energy homeostasis. *Proceedings of the National Academy of Sciences, 110*(9), E798-E807.
Qin, B., Anderson, R. A., & Adeli, K. (2008). Tumor necrosis factor-α directly stimulates the overproduction of hepatic apolipoprotein B100-containing VLDL via impairment of hepatic insulin signaling. *American Journal of Physiology-Gastrointestinal and Liver Physiology, 294*(5), G1120-G1129.
Rachid, T. L., Penna-de-Carvalho, A., Bringhenti, I., Aguila, M. B., Mandarim-de-Lacerda, C. A., & Souza-Mello, V. (2015). Fenofibrate (PPARalpha agonist) induces beige cell formation in subcutaneous white adipose tissue from diet-induced male obese mice. *Molecular and cellular endocrinology, 402*, 86-94.
Rayalam, S., Yang, J. Y., Ambati, S., Della-Fera, M. A., & Baile, C. A. (2008). Resveratrol induces apoptosis and inhibits adipogenesis in 3T3-L1 adipocytes. *Phytotherapy Research, 22*(10), 1367-1371.
Re, R. N. (2009). Obesity-related hypertension. *The Ochsner Journal, 9*(3), 133-136.
Rexrode, K. M., Pradhan, A., Manson, J. E., Buring, J. E., & Ridker, P. M. (2003). Relationship of total and abdominal adiposity with CRP and IL-6 in women. *Annals of epidemiology, 13*(10), 674-682.

Rhodes, D. H., Pini, M., Castellanos, K. J., Montero-Melendez, T., Cooper, D., Perretti, M., & Fantuzzi, G. (2013). Adipose tissue-specific modulation of galectin expression in lean and obese mice: Evidence for regulatory function. *Obesity, 21*(2), 310-319.

Ricci, R., & Bevilacqua, F. (2012). The potential role of leptin and adiponectin in obesity: A comparative review. *The Veterinary Journal, 191*(3), 292-298.

Ricciardi, C. J., Bae, J., Esposito, D., Komarnytsky, S., Hu, P., Chen, J., & Zhao, L. (2014). 1, 25-Dihydroxyvitamin D3/vitamin D receptor suppresses brown adipocyte differentiation and mitochondrial respiration. *European journal of nutrition*, 1-12.

Richard, D., & Picard, F. (2011). Brown fat biology and thermogenesis. *Front Biosci, 16*, 1233-1260.

Rodgers, J. T., Lerin, C., Haas, W., Gygi, S. P., Spiegelman, B. M., & Puigserver, P. (2005). Nutrient control of glucose homeostasis through a complex of PGC-1α and SIRT1. *Nature, 434*(7029), 113-118.

Roman, S., Agil, A., Peran, M., Alvaro-Galue, E., Ruiz-Ojeda, F. J., Fernandez-Vazquez, G., & Marchal, J. A. (2015). Brown adipose tissue and novel therapeutic approaches to treat metabolic disorders. *Transl Res, 165*(4), 464-479. doi:10.1016/j.trsl.2014.11.002

Rosen, E. D., & MacDougald, O. A. (2006). Adipocyte differentiation from the inside out. *Nature reviews Molecular cell biology, 7*(12), 885-896.

Rosenwald, M., & Wolfrum, C. (2014). The origin and definition of brite versus white and classical brown adipocytes. *Adipocyte, 3*(1), 4-9. doi:10.4161/adip.26232

Saely, C. H., Geiger, K., & Drexel, H. (2012). Brown versus white adipose tissue: a mini-review. *Gerontology, 58*(1), 15-23. doi:10.1159/000321319

Saito, M., & Yoneshiro, T. (2013). Capsinoids and related food ingredients activating brown fat thermogenesis and reducing body fat in humans. *Current opinion in lipidology, 24*(1), 71-77.

Sammons, M. F., & Price, D. A. (2014). Modulation of adipose tissue thermogenesis as a method for increasing energy expenditure. *Bioorg Med Chem Lett, 24*(2), 425-429. doi:10.1016/j.bmcl.2013.12.016

Sanchez-Gurmaches, J., & Guertin, D. A. (2014). Adipocyte lineages: tracing back the origins of fat. *Biochimica et Biophysica Acta (BBA)-Molecular Basis of Disease, 1842*(3), 340-351.

Schertzer, J. D., Tamrakar, A. K., Magalhães, J. G., Pereira, S., Bilan, P. J., Fullerton, M. D., . . . Philpott, D. J. (2011). NOD1 activators link innate immunity to insulin resistance. *Diabetes, 60*(9), 2206-2215.

Schulz, T. J., Huang, P., Huang, T. L., Xue, R., McDougall, L. E., Townsend, K. L., . . . Tseng, Y.-H. (2013). Brown-fat paucity due to impaired BMP signalling induces compensatory browning of white fat. *Nature, 495*(7441), 379-383.

Seale, P., Bjork, B., Yang, W., Kajimura, S., Chin, S., Kuang, S., . . . Erdjument-Bromage, H. (2008). PRDM16 controls a brown fat/skeletal muscle switch. *Nature, 454*(7207), 961-967.

Seale, P., Conroe, H. M., Estall, J., Kajimura, S., Frontini, A., Ishibashi, J., . . . Spiegelman, B. M. (2011). Prdm16 determines the thermogenic program of

subcutaneous white adipose tissue in mice. *The Journal of clinical investigation, 121*(1), 96.
Seale, P., Kajimura, S., & Spiegelman, B. M. (2009). Transcriptional control of brown adipocyte development and physiological function—of mice and men. *Genes & development, 23*(7), 788-797.
Sears, I. B., MacGinnitie, M. A., Kovacs, L. G., & Graves, R. A. (1996). Differentiation-dependent expression of the brown adipocyte uncoupling protein gene: regulation by peroxisome proliferator-activated receptor gamma. *Molecular and cellular biology, 16*(7), 3410-3419.
Seidell, J. C., & Halberstadt, J. (2015). The global burden of obesity and the challenges of prevention. *Ann Nutr Metab, 66 Suppl 2*, 7-12. doi:10.1159/000375143
Shen, L., Haas, M., Wang, D. Q. H., May, A., Lo, C. C., Obici, S., . . . Liu, M. (2015). Ginsenoside Rb1 increases insulin sensitivity by activating AMP-activated protein kinase in male rats. *Physiological Reports, 3*(9), e12543.
Shi, H., Kokoeva, M. V., Inouye, K., Tzameli, I., Yin, H., & Flier, J. S. (2006). TLR4 links innate immunity and fatty acid–induced insulin resistance. *Journal of Clinical Investigation, 116*(11), 3015.
Shigetoh, Y., Adachi, H., Yamagishi, S.-i., Enomoto, M., Fukami, A., Otsuka, M., . . . Imaizumi, T. (2009). Higher heart rate may predispose to obesity and diabetes mellitus: 20-year prospective study in a general population. *American journal of hypertension, 22*(2), 151-155.
Siegrist-Kaiser, C. A., Pauli, V., Juge-Aubry, C. E., Boss, O., Pernin, A., Chin, W. W., . . . Zapf, J. (1997). Direct effects of leptin on brown and white adipose tissue. *Journal of Clinical Investigation, 100*(11), 2858.
Siersbæk, R., Nielsen, R., & Mandrup, S. (2012). Transcriptional networks and chromatin remodeling controlling adipogenesis. *Trends in Endocrinology & Metabolism, 23*(2), 56-64.
Singh, S., Simpson, R. L., & Bennett, R. G. (2015). Relaxin Activates Peroxisome Proliferator-Activated Receptor γ (PPARγ) Through a Pathway Involving PPARγ Coactivator 1α (PGC1α). *Journal of Biological Chemistry, 290*(2), 950-959.
Song, M. J., Kim, K. H., Yoon, J. M., & Kim, J. B. (2006). Activation of Toll-like receptor 4 is associated with insulin resistance in adipocytes. *Biochemical and biophysical research communications, 346*(3), 739-745.
Spiegelman, B. (1998). PPAR-gamma: adipogenic regulator and thiazolidinedione receptor. *Diabetes, 47*(4), 507-514.
Stier, A., Bize, P., Habold, C., Bouillaud, F., Massemin, S., & Criscuolo, F. (2014). Mitochondrial uncoupling prevents cold-induced oxidative stress: a case study using UCP1 knockout mice. *The Journal of experimental biology, 217*(4), 624-630.
Symonds, M. E. (2013). Brown adipose tissue growth and development. *Scientifica, 2013*.
Takahashi, K., Mizuarai, S., Araki, H., Mashiko, S., Ishihara, A., Kanatani, A., . . . Kotani, H. (2003). Adiposity elevates plasma MCP-1 levels leading to the increased CD11b-positive monocytes in mice. *Journal of Biological Chemistry, 278*(47), 46654-46660.

Takeuchi, O., & Akira, S. (2010). Pattern recognition receptors and inflammation. *Cell, 140*(6), 805-820. doi:10.1016/j.cell.2010.01.022

Tamrakar, A. K., Schertzer, J. D., Chiu, T. T., Foley, K. P., Bilan, P. J., Philpott, D. J., & Klip, A. (2010). NOD2 activation induces muscle cell-autonomous innate immune responses and insulin resistance. *Endocrinology, 151*(12), 5624-5637.

Tang, L., Zhou, X. D., Wang, Q., Zhang, L., Wang, Y., Li, X. Y., & Huang, D. M. (2011). Expression of TRAF6 and pro-inflammatory cytokines through activation of TLR2, TLR4, NOD1, and NOD2 in human periodontal ligament fibroblasts. *Arch Oral Biol, 56*(10), 1064-1072. doi:10.1016/j.archoralbio.2011.02.020

Teruel, T., Hernandez, R., Benito, M., & Lorenzo, M. (2003). Rosiglitazone and retinoic acid induce uncoupling protein-1 (UCP-1) in a p38 mitogen-activated protein kinase-dependent manner in fetal primary brown adipocytes. *Journal of Biological Chemistry, 278*(1), 263-269.

Teulier, L., Rouanet, J.-L., Letexier, D., Romestaing, C., Belouze, M., Rey, B., . . . Roussel, D. (2010). Cold-acclimation-induced non-shivering thermogenesis in birds is associated with upregulation of avian UCP but not with innate uncoupling or altered ATP efficiency. *The Journal of experimental biology, 213*(14), 2476-2482.

Trayhurn, P., & Beattle, J. (2001). Physiological role of adipose tissue: white adipose tissue as an endocrine and secretory organ. *Proc Nutr Soc, 60*(3), 329-339.

Tseng, Y.-H., Cypess, A. M., & Kahn, C. R. (2010). Cellular bioenergetics as a target for obesity therapy. *Nature reviews Drug discovery, 9*(6), 465-482.

Tseng, Y.-H., Kokkotou, E., Schulz, T. J., Huang, T. L., Winnay, J. N., Taniguchi, C. M., . . . Yamamoto, Y. (2008). New role of bone morphogenetic protein 7 in brown adipogenesis and energy expenditure. *Nature, 454*(7207), 1000-1004.

Tzeng, T. F., Chang, C. J., & Liu, I. M. (2014). 6-Gingerol Inhibits Rosiglitazone-Induced Adipogenesis in 3T3-L1 Adipocytes. *Phytotherapy Research, 28*(2), 187-192.

Ustanina, S., Carvajal, J., Rigby, P., & Braun, T. (2007). The myogenic factor Myf5 supports efficient skeletal muscle regeneration by enabling transient myoblast amplification. *Stem Cells, 25*(8), 2006-2016.

Valle, I., Álvarez-Barrientos, A., Arza, E., Lamas, S., & Monsalve, M. (2005). PGC-1α regulates the mitochondrial antioxidant defense system in vascular endothelial cells. *Cardiovascular research, 66*(3), 562-573.

van den Berg, S. A., van Marken Lichtenbelt, W., van Dijk, K. W., & Schrauwen, P. (2011). Skeletal muscle mitochondrial uncoupling, adaptive thermogenesis and energy expenditure. *Current Opinion in Clinical Nutrition & Metabolic Care, 14*(3), 243-249.

van der Lans, A. A., Hoeks, J., Brans, B., Vijgen, G. H., Visser, M. G., Vosselman, M. J., . . . Mottaghy, F. M. (2013). Cold acclimation recruits human brown fat and increases nonshivering thermogenesis. *The Journal of clinical investigation, 123*(123 (8)), 3395-3403.

van Marken Lichtenbelt, W. D., & Schrauwen, P. (2011). Implications of nonshivering thermogenesis for energy balance regulation in humans. *American Journal of Physiology-Regulatory, Integrative and Comparative Physiology, 301*(2), R285-R296.

van Marken Lichtenbelt, W. D., Vanhommerig, J. W., Smulders, N. M., Drossaerts, J. M., Kemerink, G. J., Bouvy, N. D., . . . Teule, G. J. (2009). Cold-activated brown adipose tissue in healthy men. *New England Journal of Medicine, 360*(15), 1500-1508.

Vandevijvere, S., Chow, C. C., Hall, K. D., Umali, E., & Swinburn, B. A. (2015). Increased food energy supply as a major driver of the obesity epidemic: a global analysis. *Bull World Health Organ, 93*(7), 446-456. doi:10.2471/BLT.14.150565

Vázquez-Vela, M. E. F., Torres, N., & Tovar, A. R. (2008). White adipose tissue as endocrine organ and its role in obesity. *Archives of medical research, 39*(8), 715-728.

Vieira, V. J., Valentine, R. J., Wilund, K. R., Antao, N., Baynard, T., & Woods, J. A. (2009). Effects of exercise and low-fat diet on adipose tissue inflammation and metabolic complications in obese mice. *American Journal of Physiology-Endocrinology and Metabolism, 296*(5), E1164-E1171.

Vijgen, G., Bouvy, N. D., Teule, G., Brans, B., Schrauwen, P., & van Marken Lichtenbelt, W. D. (2011). Brown adipose tissue in morbidly obese subjects. *PLoS One, 6*(2), e17247.

Virtanen, K. A., van Marken Lichtenbelt, W. D., & Nuutila, P. (2013). Brown adipose tissue functions in humans. *Biochim Biophys Acta, 1831*(5), 1004-1008. doi:10.1016/j.bbalip.2012.12.011

Vosselman, M. J., van Marken Lichtenbelt, W. D., & Schrauwen, P. (2013). Energy dissipation in brown adipose tissue: from mice to men. *Mol Cell Endocrinol, 379*(1-2), 43-50. doi:10.1016/j.mce.2013.04.017

Wang, C., Wang, L., Li, W., Yan, F., Tian, M., Wu, C., . . . Hou, X. (2015). Irisin has no effect on lipolysis in 3T3-L1 adipocytes or fatty acid metabolism in HepG2 hepatocytes. *Endocrine, 49*(1), 90-96.

Wang, F., Mullican, S. E., DiSpirito, J. R., Peed, L. C., & Lazar, M. A. (2013). Lipoatrophy and severe metabolic disturbance in mice with fat-specific deletion of PPARγ. *Proceedings of the National Academy of Sciences, 110*(46), 18656-18661.

Wang, Q., Zhang, M., Ning, G., Gu, W., Su, T., Xu, M., . . . Wang, W. (2011). Brown adipose tissue in humans is activated by elevated plasma catecholamines levels and is inversely related to central obesity. *PLoS One, 6*(6), e21006.

Wang, Q. A., Tao, C., Gupta, R. K., & Scherer, P. E. (2013). Tracking adipogenesis during white adipose tissue development, expansion and regeneration. *Nature medicine, 19*(10), 1338-1344.

Wang, S., Liang, X., Yang, Q., Fu, X., Rogers, C., Zhu, M., . . . Du, M. (2015). Resveratrol induces brown-like adipocyte formation in white fat through activation of AMP-activated protein kinase (AMPK) α1. *International journal of Obesity*.

Wang, S., Moustaid-Moussa, N., Chen, L., Mo, H., Shastri, A., Su, R., . . . Shen, C. L. (2014). Novel insights of dietary polyphenols and obesity. *J Nutr Biochem, 25*(1), 1-18. doi:10.1016/j.jnutbio.2013.09.001

Wang, Y., Li, G., Goode, J., Paz, J. C., Ouyang, K., Screaton, R., . . . Montminy, M. (2012). Inositol-1, 4, 5-trisphosphate receptor regulates hepatic gluconeogenesis in fasting and diabetes. *Nature, 485*(7396), 128-132.

Wang, Y.-X. (2010). PPARs: diverse regulators in energy metabolism and metabolic diseases. *Cell research, 20*(2), 124-137.

Watanabe, Y., Nagai, Y., & Takatsu, K. (2013). Activation and regulation of the pattern recognition receptors in obesity-induced adipose tissue inflammation and insulin resistance. *Nutrients, 5*(9), 3757-3778.

Wendel, A. A., Purushotham, A., Liu, L.-F., & Belury, M. A. (2009). Conjugated linoleic acid induces uncoupling protein 1 in white adipose tissue of ob/ob mice. *Lipids, 44*(11), 975-982.

Wentworth, J. M., Naselli, G., Brown, W. A., Doyle, L., Phipson, B., Smyth, G. K., . . . Harrison, L. C. (2010). Pro-inflammatory CD11c+ CD206+ adipose tissue macrophages are associated with insulin resistance in human obesity. *Diabetes, 59*(7), 1648-1656.

Whittle, A., Relat-Pardo, J., & Vidal-Puig, A. (2013). Pharmacological strategies for targeting BAT thermogenesis. *Trends Pharmacol Sci, 34*(6), 347-355. doi:10.1016/j.tips.2013.04.004

Winkler, G., Kiss, S., Keszthelyi, L., Sápi, Z., Ory, I., Salamon, F., . . . Speer, G. (2003). Expression of tumor necrosis factor (TNF)-alpha protein in the subcutaneous and visceral adipose tissue in correlation with adipocyte cell volume, serum TNF-alpha, soluble serum TNF-receptor-2 concentrations and C-peptide level. *European Journal of Endocrinology, 149*(2), 129-135.

Wu, C., Cheng, W., Sun, Y., Dang, Y., Gong, F., Zhu, H., . . . Zhu, Z. (2014). Activating brown adipose tissue for weight loss and lowering of blood glucose levels: A microPET study using obese and diabetic model mice. *PLoS One, 9*(12), e113742.

Wu, J., Bostrom, P., Sparks, L. M., Ye, L., Choi, J. H., Giang, A. H., . . . Spiegelman, B. M. (2012). Beige adipocytes are a distinct type of thermogenic fat cell in mouse and human. *Cell, 150*(2), 366-376. doi:10.1016/j.cell.2012.05.016

Wu, J., Cohen, P., & Spiegelman, B. M. (2013). Adaptive thermogenesis in adipocytes: is beige the new brown? *Genes Dev, 27*(3), 234-250. doi:10.1101/gad.211649.112

Xue, R., Wan, Y., Zhang, S., Zhang, Q., Ye, H., & Li, Y. (2014). Role of bone morphogenetic protein 4 in the differentiation of brown fat-like adipocytes. *Am J Physiol Endocrinol Metab, 306*(4), E363-372. doi:10.1152/ajpendo.00119.2013

Yadav, A., Kataria, M. A., Saini, V., & Yadav, A. (2013). Role of leptin and adiponectin in insulin resistance. *Clinica Chimica Acta, 417*, 80-84.

Yamauchi, T., Kamon, J., Minokoshi, Y. a., Ito, Y., Waki, H., Uchida, S., . . . Ueki, K. (2002). Adiponectin stimulates glucose utilization and fatty-acid oxidation by activating AMP-activated protein kinase. *Nature medicine, 8*(11), 1288-1295.

Yoneshiro, T., Aita, S., Kawai, Y., Iwanaga, T., & Saito, M. (2012). Nonpungent capsaicin analogs (capsinoids) increase energy expenditure through the activation of brown adipose tissue in humans. *The American journal of clinical nutrition, 95*(4), 845-850.

Yoon, M. J., Lee, G. Y., Chung, J.-J., Ahn, Y. H., Hong, S. H., & Kim, J. B. (2006). Adiponectin increases fatty acid oxidation in skeletal muscle cells by sequential activation of AMP-activated protein kinase, p38 mitogen-activated protein kinase, and peroxisome proliferator–activated receptor α. *Diabetes, 55*(9), 2562-2570.

Zafrir, B. (2013). Brown adipose tissue: research milestones of a potential player in human energy balance and obesity. *Horm Metab Res, 45*(11), 774-785. doi:10.1055/s-0033-1348264

Zhang, Y., Li, R., Meng, Y., Li, S., Donelan, W., Zhao, Y., . . . Tang, D. (2014). Irisin stimulates browning of white adipocytes through mitogen-activated protein kinase p38 MAP kinase and ERK MAP kinase signaling. *Diabetes, 63*(2), 514-525. doi:10.2337/db13-1106/-/DC1

Zhao, L., Hu, P., Zhou, Y., Purohit, J., & Hwang, D. (2011). NOD1 activation induces proinflammatory gene expression and insulin resistance in 3T3-L1 adipocytes. *Am J Physiol Endocrinol Metab, 301*(4), E587-598. doi:10.1152/ajpendo.00709.2010

Zhou, Y.-J., Zhou, H., Li, Y., & Song, Y.-L. (2012). NOD1 activation induces innate immune responses and insulin resistance in human adipocytes. *Diabetes & metabolism, 38*(6), 538-543.

CHAPTER II

ACTIVATION OF PATTERN RECOGNITION RECEPTORS IN BROWN ADIPOCYTES INDUCES INFLAMMATION AND SUPPRESSES UNCOUPLING PROTEIN 1 EXPRESSION AND MITOCHONDRIAL RESPIRATION

A version of this chapter was originally published by Jiyoung Bae, Carolyn J. Ricciardi, Debora Esposito, Slavko Komarnytsky, Pan Hu, Benjamin J. Curry, Patricia L. Brown, Zhanguo Gao, John P. Biggerstaff, Jiangang Chen, Ling Zhao entitled "Activation of pattern recognition receptors in brown adipocytes induces inflammation and suppresses uncoupling protein 1 expression and mitochondrial respiration" *American Journal of Physiology-Cell Physiology* 306(10): C918-930 (2014).

2.1 Abstract

Pattern recognition receptors (PRR), Toll-like receptors (TLR), and nucleotide-oligomerization domain-containing proteins (NOD) play critical roles in mediating inflammation and modulating functions in white adipocytes in obesity. However, the role of PRR activation in brown adipocytes, which are recently found to be present in adult humans, has not been studied. Here, we report that mRNA of TLR4, TLR2, NOD1, and NOD2 is upregulated, paralleled with upregulated mRNA of inflammatory cytokines and chemokines in the brown adipose tissue (BAT) of the obese mice. During brown adipocyte differentiation, mRNA and protein expression of NOD1 and TLR4, but not TLR2 and NOD2, is also increased. Activation of TLR4, TLR2, or NOD1 in brown adipocytes induces activation of NF-κB and MAPK signaling pathways, leading to inflammatory cytokine/chemokine mRNA expression and/or protein secretion. Moreover, activation of TLR4, TLR2, or NOD1 attenuates both basal and isoproterenol-induced uncoupling protein 1 (UCP-1) expression without affecting mitochondrial biogenesis and lipid accumulation in brown adipocytes. Cellular bioenergetics measurements confirm that attenuation of UCP-1 expression by PRR activation is accompanied by suppression of both basal and isoproterenol-stimulated oxygen consumption rates and isoproterenol-induced uncoupled respiration from proton leak; however, maximal respiration and ATP-coupled respiration are not changed. Further, the attenuation of UCP-1 by PRR activation appears to be mediated through downregulation of the UCP-1 promoter activities. Taken together, our results demonstrate the role of selected PRR activation in inducing inflammation and downregulation of UCP-1 expression and mitochondrial

respiration in brown adipocytes. Our results uncover novel targets in BAT for obesity treatment and prevention.

2.2 Introduction

Brown adipose tissue (BAT) is a specialized tissue whose function is to produce heat through nonshivering thermogenesis. BAT is found in relative abundance in small eutherian mammals, such as rat or mice, to allow the animals to live in a cold environment without utilizing shivering mechanism to produce heat (Cannon & Nedergaard, 2004). The thermogenic property of BAT is conferred to mainly by the functions of uncoupling protein 1 (UCP-1), which is uniquely expressed and localized in the inner membrane of brown adipocyte mitochondria to uncouple ATP synthesis from respiration (Nicholls & Locke, 1984; Ricquier, 2005). BAT is heavily innervated by sympathetic efferent fibers, and the release of norepinephrine by these fibers not only increases BAT thermogenic activity (i.e., heat production) but also thermogenic capacity (i.e., brown adipogenesis, mitochondrial biogenesis, and synthesis of UCP-1 and other BAT thermogenic proteins) (Richard & Picard, 2011).

It was thought until recently that humans only possess BAT when they were newborn infants and that BAT quickly regresses following birth. However, new evidence from positron emission tomography/computed tomography scanning has revealed symmetrical fat depots in the cervical, supreclavicular, and parasphinal regions in adult humans that have all the characteristics of BAT (Cypess et al., 2009; Saito et al., 2009; van Marken Lichtenbelt et al., 2009; Virtanen et al., 2009; Zingaretti et al., 2009). Recent gene expression profilings have confirmed many classical BAT features in the supraclavicular regions of adult humans (Cypess et al., 2013; Jespersen et al., 2013). Due to its energy-dissipating activity, BAT has become a novel target for obesity

treatment and prevention (Vijgen & van Marken Lichtenbelt, 2013; Vosselman, van Marken Lichtenbelt, & Schrauwen, 2013).

In contrast to white adipose tissue (WAT), whose function is to store energy, brown adipocytes are multilocular with many small lipid droplets and contain a large number of mitochondria, compared with a single large lipid droplet and few mitochondria in white adipocytes. It is now recognized that obesity is associated with chronic inflammation in WAT at both local and systemic levels. Adipose inflammation, characterized by elevated pro inflammatory cytokine/chemokine expression and secretions and infiltration of immune cells, including macrophages, is thought to contribute to obesity associated comorbidities, such as insulin resistance and diabetes (Gregor & Hotamisligil, 2011; Kwon & Pessin, 2013; Ouchi, Parker, Lugus, & Walsh, 2011; Rasouli & Kern, 2008).

The mechanisms underlying adipose inflammation in obesity have been the focus of intense research (Sun, Ji, Kersten, & Qi, 2012). Recent studies suggest that adipose inflammation is mediated through the activation of germline-encoded pattern recognition receptors (PRR) in the adipose tissue/adipocytes (Jin, Henao-Mejia, & Flavell, 2013). PRRs belong to innate immune system and are responsible for the sensing of invading microbial pathogens and activate specific signaling pathways leading to distinct inflammatory and immune responses in the host cells (Akira, Uematsu, & Takeuchi, 2006; Kawai & Akira, 2009). Toll-like receptors (TLR) and Nod-like receptors (NLR) are two prominent families of PRRs. TLRs are transmembrane receptors composed of extracellular leucine-rich repeat (LRR) motifs and a cytoplasmic Toll/interleukin-1 receptor (TIR) homology domain. So far, 10 and 12 functional TLRs

have been identified in humans and mice, respectively. The respective bacterial or viral pathogen-associated molecular patterns (PAMP) that individual TLR detects have been characterized (Akira et al., 2006). In contrast, NLRs are a family of cytosolic sensors that play important roles in innate immunity and inflammation (Inohara, Chamaillard, McDonald, & Nunez, 2005). These NLRs display a central nucleotide-binding domain, an NH_2-terminal protein interaction domain, and a COOH-terminal LRR domain. Two prominent members of NLRs are NOD1 and NOD2, and each recognizes a distinct minimal peptidoglycan structure: NOD1 recognizes a dipeptide, γ-D-Glu-meso-diaminopimelic acid (iE-DAP) (Chamaillard et al., 2003), or a tripeptide, L-Ala-γ-D-Glu-meso-diaminopimelic acid (Tri-DAP) (Girardin, Boneca, Carneiro, et al., 2003) derived mostly from Gram-negative bacteria; NOD2 recognizes the peptidoglycan muramyl dipeptide MurNAc-L-Ala-D-isoGln (MDP) from both Gram-positive and Gram-negative bacteria (Girardin, Boneca, Viala, et al., 2003; Inohara et al., 2003). Various PRRs, including TLR4, TLR2, NOD1, and NOD2, have been detected in WAT and/or white adipocytes, and activation of PRR induces a proinflammatory response (Davis, Braucher, Walker-Daniels, & Spurlock, 2011; Song, Kim, Yoon, & Kim, 2006; Zhao, Hu, Zhou, Purohit, & Hwang, 2011), resulting in adipocyte dysfunction and disturbed homeostasis of whole body metabolism (Ehses et al., 2010; Himes & Smith, 2010; Schertzer et al., 2011; Shi et al., 2006).

Here, we report the expression of NOD1, NOD2, TLR4, and TLR2 in classical BAT of mouse models of obesity and during brown adipocyte differentiation. Activation of NOD1, TLR4, and TLR2, but not NOD2, induces a proinflammatory response in brown adipocytes through NF-κB and MAPK signaling pathways. Moreover, the

activation of these selected PRRs leads to downregulation of basal and isoproterenol-induced UCP-1 mRNA and protein expression and suppresses mitochondrial respiration in brown adipocytes.

2.3 Materials and methods

Reagents

NOD1 synthetic ligand lauroyl-γ-D-Glu-meso-diaminopimelic acid (C12-iEDAP) and TLR2 ligand a synthetic triacylated lipoprotein Pam3CSK4 were from Invivogen (San Diego, CA). Ultra pure TLR4 ligand lipopolysaccharide (LPS) was from List Biological Laboratories (Campbell, CA). 3-Isobutyl-L-methylxanthine, T3, dexamethasone, insulin, indometacin, and isoproterenol were from Sigma (St. Louis, MO). The pharmacological MAPK inhibitors PD98054, SP600125, and SB203580 were from Tocris Bioscience (Ellisville, MI), and the NF-κB inhibitors QNZ and caffeic acid phenethyl ester (CAPE) were from Cayman Chemical (Ann Arbor, MI). Antibodies anti-phospho-ERK1/2(Thr202/Tyr204) (no. 4376), anti-ERK1/2 (no. 4695), anti-phospho-p38(Thr180/Tyr182) (no. 9211), anti-p38 (no. 9212), anti-phospho-JNK(Thr183/Tyr185) (no. 9251), anti-JNK (no. 9258), anti-phospho-p65(Ser536) (no. 3033), anti-p65 (no. 3034), anti-phospho-IκB(Ser32) (no. 2859), anti-proliferator-activated receptor-gamma (PPARγ; no. 2443) were from Cell Signaling Technology (Danvers, MA). Anti-UCP-1 antibody (U6382) was from Sigma-Aldrich (St. Louis, MO). Anti-peroxisome proliferator-activated receptor-gamma coactivator-1α (PGC-1α) antibody (AB3242) was from Millipore (Temecula, CA). Antibodies anti-NOD1 (ab105338), anti-TLR4 (ab13867), and anti-TLR2 (ab108998) were from Abcam (Cambridge, MA).

Animals

Diet-induced obesity (DIO) mice and ob/ob and their respective controls have been described previously (Zhao et al., 2011). The mice were purchased from the Jackson Laboratory (Bar Harbor, ME). For DIO study, male C57BL/6J mice (n=7 per

group) were fed with a high-fat diet (60% Kcal% from fat; Research Diets) or regular chow diet for 20 wk before being killed at 26 wk of age. Male ob/ob and their control mice (n=6 per group) were fed with chow diet for 8 wk before being killed at 14 wk of age. Upon death, interscapular BAT was removed and immediately snap frozen in liquid nitrogen and stored at -80°C until analysis. The mice studies were approved by the Institutional Animal Care and Use Committee at the University of Tennessee.

Brown fat cell culture and differentiation

The murine brown fat cell line was a generous gift from Dr. Johannes Klein (University of Lubeck, Lubeck, Germany), who has generated the cell line from the interscapular brown fat of 6- to 7-wk-old of C57BL mice (Klein, Fasshauer, Klein, Benito, & Kahn, 2002). Brown fat cells were maintained in DMEM supplemented with 20% fetal bovine serum (FBS; Atlas Biologicals, Fort Collins, CO) at 37°C humidified atmosphere of 5% CO_2 in air until they reached confluence [designated as *day 0* (D0)]. The cells were changed into differentiation media DMEM supplemented with 20% FBS, 1 nM T3, and 20 nM insulin for 24 h, followed by induction in DMEM supplemented with 20% FBS, 1 nM T3, 20 nM insulin, 0.125 mM indometacin, 5 μM dexamethasone, and 0.5 mM 3-isobutyl-L-methylxanthine for another 24 h. The cells were then changed back to differentiation media and subsequently changed every 2 days until fully differentiated into brown adipocytes on *day 6* (D6).

PRR stimulation

Differentiated brown adipocytes were serum starved in DMEM containing 1% FBS for 12–15 h and stimulated with vehicle control, C12-iEDAP, LPS, or Pam3CSK4 as indicated. Total RNA and media were collected for cytokine/chemokine mRNA

expression and protein secretion analysis. For the studies using the inhibitors of NF-κB or MAPK, cells were pretreated with the inhibitor for 1 h and were co-stimulated with the respective ligand for the indicated time.

Western blot analysis

Total cell lysates were prepared and protein concentrations were determined by the BCA assay kit (Thermo Scientific, Waltham, MA). Fifty micrograms of total cell lysates were subjected to 10% SDS-PAGE and transferred to polyvinylidene difluoride membrane (Bio-Rad, Hercules, CA). The membrane was blocked in 20 mM Tris·HCl, 137 mM NaCl, and 0.1% Tween 20 (pH 7.4) containing 5% nonfat milk. The membrane was immunoblotted with primary antibodies at 4°C overnight followed by secondary antibody conjugated with horseradish peroxidase (GE Healthcare). The signal was quantified by densitometry using a ChemiDocXRS+ imaging system with ImageLab software (Bio-Rad).

RNA preparation and quantitative real-time PCR analysis

Total RNA was prepared from BAT from DIO or ob/ob mice or from brown adipocytes using TRI reagent (Molecular Research Center, Cincinnati, OH) according to the manufacturer's instructions. Total RNA abundance was quantified using NanoDrop ND-1000 spectrophotometer (NanoDrop Technologies, Wilmington, DE). Reverse transcription was carried out using Fermentas first strand synthesis kit (Thermo Scientific, Pittsburgh, PA) according to the manufacturer's instructions. mRNA expression of PRRs, brown adipocyte marker genes, inflammatory cytokine/chemokine genes, and the housekeeping gene 36B4 was measured quantitatively using gene-specific TaqMan gene expression assays (Applied Biosystems) (for samples of BAT) or

Absolute Blue QPCR SYBR Green ROX mix (Thermo Fisher Scientific) and gene-specific primers (for samples of brown adipocytes). Specific primer sequences can be provided upon request. PCR reactions were run in a 96-well format using an ABI 7300HT instrument. Cycle conditions were 50°C 2 min, 95°C 15 min and then 40 cycles of 95°C for 15 s/60°C for 1 min. Relative gene expression was calculated using the $2^{-\Delta\Delta Ct}$ method, which normalizes against 36B4.

Reporter gene assays

For NF-κB-Luc experiments, brown adipocytes in 24-well plates were infected with adenovirus encoding NF-κB-Luc reporter gene for 24 h. The cells were stimulated with C12-iEDAP, LPS, Pam3CSK4, or the vehicle control for 15 h. For UCP-1-Luc experiments, brown adipocytes were subcultured and transfected with a mouse 3.1 kb UCP-1 promoter luciferase construct (UCP-1-Luc) (Rim & Kozak, 2002) and subsequently pretreated with the ligand for each PRR or the vehicle control for 1 h and then cotreated with isoproterenol for 15 h. The cell lysate was prepared and reporter luciferase activities were measured with GloMax Luminometer (Promega, Madison, WI). Relative luciferase activities were normalized by protein concentrations and expressed as fold of vehicle control.

Measurement of cytokine/chemokine

The supernatant from brown adipocytes that were stimulated with PRRs was collected and the levels of monocyte chemotactic protein 1 (MCP-1), interleukin 6 (IL-6), and regulated upon activation, normal T-cell expressed, and secreted (RANTES) were determined by ELISA using Quantikine kits (R&D Systems, Minneapolis, MN).

Oil red O staining and quantification

Differentiated brown adipocytes were serum-starved overnight and were treated with C12-iEDAP, LPS, and Pam3CSK4 for 12 h under the basal condition, or pretreated with C12-iEDAP, LPS, Pam3CSK4, or the vehicle control for 12 h, followed by co-stimulated with isoproterenol (1 μM) in the presence of the ligand for another 6 h. The cells were fixed, and lipid accumulation in brown adipocytes was stained with oil red O (ORO) and quantified by ORO absorbance at 500 nm.

Cellular bioenergetics measurements

D6 $2.5x10^4$ brown adipocytes were subcultured and seeded in 24-well XF assay plates overnight in the differentiation medium and subjected to real-time measurements of oxygen consumption rate (OCR) and extracellular acidification rate (ECAR) using XF24 Extracellular Flux Analyzer (Seahorse Biosciences, North Billerica, MA). To study the effects of PRR ligands on bioenergetics of brown adipocytes, cells were pretreated with C12-iEDAP (10 μg/ml), LPS (0.1 μg/ml), Pam3CSK4 (1 μg/ml), or the vehicle control for 12 h, rinsed once, changed to 500 μl of XF assay buffer (DMEM without $NaHCO_3$, 10 mM glucose, 2 mM pyruvate, and 2 mM GlutaMAX, pH 7.4), and equilibrated at non-CO_2 incubator and 37°C for 1 h. Following basal measurements of OCR and ECAR, all cells were injected either with the vehicle control or isoproterenol (1 μM) and the subsequent readings were taken over the 6 h period. At the end of the experiment, mitochondrial complex inhibitors were injected to all treatments sequentially in the following order: oligomycin (1 μM), carbonyl cyanide-ptrifluoromethoxyphenylhydrazone (FCCP; 0.75 μM), and antimycin A/rotenone (1 μM

each), and three readings were taken after each inhibitor. OCR and ECAR were automatically recorded by XF24 software v1.8 provided by the manufacturer.

Basal and isoproterenol-stimulated OCR and ECAR rates were determined by averaging the measurements. Calculations of maximal OCR, ATP-coupled OCR, OCR from proton leak, spare respiration capacity, and coupling efficiency were performed according to the manufacturer's instructions.

Analysis of mitochondrial content by MitoTracker green staining

Mitochondria were labeled using the mitochondria-specific dye MitoTracker Green (Life Technologies, Carlsbad, CA) according to manufacturer's protocol. Briefly, the differentiated brown adipocytes were washed and trypsinized from the cultured plate and incubated with MitoTraker green at 100 nM for 30 min at 37°C. The fluorescence intensity was measured with Accuri C6 flow cytometry (BD, Franklin Lakes, NJ). Background autofluorescence from nonstained cells was averaged and subtracted from the mean fluorescence intensity values.

Statistical analysis

All data are presented as means±SE. Measurements were performed in triplicates. Statistical analysis was performed using SigmaPlot 11.0 (Systat Software). One-way ANOVA with repeated measures followed by multiple comparisons test (Student-Newman-Keuls method) was performed to determine the differences between the treatment groups and/or time points. Student's *t*-tests were performed when appropriate. The level of significance was set at $P<0.05$.

2.4 Results

mRNA expression of selected PRRs is upregulated in brown fat tissue of DIO and ob/ob mice

We first examined selected PRRs NOD1, NOD2, TLR4, and TLR2 mRNA expression in the classical interscapular BAT from DIO and ob/ob mice, compared with their respective controls (Figure 1A and 1B). In DIO mice, NOD1 and TLR4 were two highly expressed PRRs, followed by NOD2 and TLR2, similar to those of their chow-fed controls. Moreover, NOD1, TLR4, and TLR2 mRNA was significantly upregulated ($p<0.05$) in DIO mice compared with their controls (Figure 1A). Similar relative expression patterns were observed in BAT of ob/ob mice compared with their wild-type (WT) controls (Figure 1B). Further, we examined inflammatory gene expression in BAT from DIO and ob/ob mice. mRNA of MCP-1, IL-6 and TNF-α, but not RANTES, was significantly upregulated in BAT of DIO mice compared with the chow-fed controls ($p<0.01$ for MCP-1 and TNF-α and $p<0.05$ for IL-6; Figure 1C). mRNA of all four genes were significantly upregulated in BAT of ob/ob mice compared with the WT controls ($p<0.01$ for MCP-1 and $p<0.05$ for IL-6, TNF-α, and RANTES; Figure 1D). These results demonstrate that upregulation of selected PRRs is correlated with the upregulation of mRNA of proinflammatory genes in BAT in mice models of obesity.

Expression of selected PRRs is upregulated during brown adipocyte differentiation

To study the relationships between the upregulation of PRRs and inflammatory genes in BAT, we employed an immortalized brown fat cell line generated from the classical interscapular brown fat from C57BL6 mice (Klein et al., 2002). In vitro brown

adipocyte differentiation was validated by the increasing mRNA expression of known brown adipocyte markers UCP-1, PGC-1α, and PPARγ (Figure 2A, bottom). mRNA expression of NOD1 and TLR4, but not NOD2 and TLR2, was upregulated during differentiation (Figure.2A, top). Comparing the relative PRR expression pattern, NOD1 was the highest expressed PRR examined in brown fat cells before differentiation, followed by TLR4 and TLR2, and NOD2 had the lowest expression. In contrast, both NOD1 and TLR4 were among the highest expressed PRRs, followed by TLR2 and NOD2 after differentiation (Figure 2B). Western analysis and relative quantification confirmed that NOD1 and TLR4 were increased, whereas TLR2 was decreased upon differentiation (Figure 2C). NOD2 protein expression was undetectable by Western analysis (data not shown). These results suggest NOD1, TLR4, and TLR2 may be involved in mediating inflammation and modulating functions in brown adipocytes.

PRR activation in brown adipocytes induces phosphorylation and activation of NF-κB and MAPK signaling

Activation of PRR leads to NF-κB and MAPK signaling pathways in various PRR expressing cells, including white adipocytes. Because of the relative higher expression levels of NOD1, TLR4, and TLR2 than NOD2 in brown adipocytes, we focused on the signaling pathways downstream of NOD1, TLR4, and TLR2 activation in brown adipocytes by stimulating the cells with their respective synthetic ligands. NF-κB pathway was activated as shown by the phosphorylation of p65 and IκBα when stimulated with NOD1 ligand C12-iEDAP, TLR4 ligand LPS, or TLR2 ligand Pam3CSK4 in a time-dependent manner (Figure 3A). Moreover, MAPK pathways were also

activated within 60 min after the stimulation, as shown by the phosphorylation of p38, JNK, and ERK when stimulated with C12-iEDAP, LPS, or Pam3CSK4 (Figure 3A).

We further confirmed that activation of NOD1, TLR4, and TLR2 induced NF-κB activation with NF-κB-responsive luciferase reporter assays in brown adipocytes by transiently infecting the brown adipocytes with the adenovirus encoding NF-κB-Luc receptor gene. Activation of NOD1, TLR4, and TLR2 dose-dependently induced NF-κB reporter activation (Figure 3B). In contrast, NOD2 ligand MDP induced minimal NF-κB activation even when used up to 100 μg/ml in brown adipocytes (data not shown).

PRR activation in brown adipocytes upregulates the mRNA expression and protein secretion of proinflammatory cytokines/chemokines

Consequently, we found that activation of NOD1, TLR4, and TLR2 significantly increased mRNA expression of chemokine MCP-1, cytokine IL-6, RANTES, and tumor necrosis factor alpha (TNF-α; $p<0.01$ or $p<0.05$; Figure 4A). Other than TNF- α, which was below detection limit, protein secretion in the supernatant of the brown adipocytes was confirmed for MCP-1, IL-6, and RANTES by ELISA (Figure 4B).

Inhibitory of the NF-κB or MAPK pathways differentially attenuates proinflammatory mRNA expression in brown adipocytes

To determine if NF-κB or MAPK signaling pathway underlies proinflammatory cytokine or chemokine mRNA expression, we examined the effects of the pharmacological inhibitors of these pathways on mRNA expression on the cytokines/chemokines. NF-κB inhibitor QNZ (Tobe et al., 2003) and CAPE (Natarajan, Singh, Burke, Grunberger, & Aggarwal, 1996) significantly attenuated C12-iEDAP, LPS or Pam3CSK4-induced MCP-1, IL-6, RANTES, and TNF-α in brown adipocytes (Figure

5), suggesting NF-κB pathway is involved in NOD1-, TLR4-, or TLR2-mediated inflammatory cytokine/chemokine expression.

Among the inhibitors of MAPKs, only the p38 inhibitor SB203580 significantly attenuated C12-iEDAP-induced MCP-1, IL-6, TNF-α, and RANTES mRNA expression (Figure 6). In contrast, the JNK inhibitor SP600125 significantly attenuated LPS-induced all four mRNA. The ERK inhibitor PD98054 significantly attenuated LPS-induced IL-6, TNF-α, and RANTES mRNA, but not MCP-1 mRNA, whereas the p38 inhibitor SB203580 did not affect any of the four mRNA induced by LPS. The p38 inhibitor SB203580 significantly attenuated Pam3CSK4-induced IL-6 and RANTES mRNA, and the ERK inhibitor PD98054 only attenuated Pam3CSK4-induced MCP-1 and IL-6 mRNA, whereas the JNK inhibitor SP600125 attenuated Pam3CSK4-induced MCP-1, TNF-α, RANTES, but not IL-6 (Figure 6).

PRR activation suppresses both basal and isoproterenol-inducted UCP-1 expression, but not mitochondrial biogenesis, in brown adipocytes

The main function of brown adipocytes is mediated by UCP-1 to uncouple oxidative phosphorylation from ATP synthesis to produce heat and UCP-1 is known to be predominantly regulated at transcriptional level (Richard & Picard, 2011). We next examined whether PRR activation in brown adipocytes affects UCP-1 mRNA expression. Activation of NOD1, TLR4, and TLR2 suppressed both basal and isoproterenol, a nonspecific β-adrenergic agonist, -induced UCP-1 mRNA expression (Figure 7A). We also examined other brown adipocyte markers. Similar suppression was observed for cell-death inducing DFFA-like effector a (Cidea), and distinct but different changes were observed for PGC-1α and PPARγ. PPARγ mRNA was

suppressed by activation of NOD1, TLR4, or TLR2 under basal and isoproterenol -induced conditions. In contrast, PGC-1α mRNA was only suppressed by the activation of the PRR under the basal condition. Moreover, no changes were observed for nuclear respiratory factor 1 (Nrf1) and transcription factor A (Tfam), and two nucleus encoded mitochondrial genes, cytochrome c oxidase subunit IV a (COX4a) and cytochrome b-c1complex subunit 6 (Uqcrh) (Figure 7A). Western analysis and relative quantification confirmed that UCP-1 expression was suppressed by the activation of NOD1, TLR4, and TLR2 in brown adipocytes under both conditions but more pronounced under isoproterenol-stimulated condition (Figure 7B). PPARγ protein expression was markedly suppressed by the PRR activation under both conditions, similar to that of PPARγ mRNA. In contrast, the PGC-1α protein was not affected by PRR activation under both conditions in brown adipocytes. We further examined the effects of PRR activation on brown adipocyte cell morphology and lipid accumulation. Under our experimental conditions, there were no significant changes in cell morphology (data not shown) and lipid accumulation, revealed by ORO staining, by the activation of NOD1, TLR4, or TLR2 under both conditions (Figure 7C).

To test whether suppression of UCP-1 mRNA by PRR activation is a direct effect on the UCP-1 promoter or due to the effects on mitochondrial biogenesis, we performed UCP-1 promoter-driven reporter assays and confirmed that the effects of PRR activation was via suppressing UCP-1 promoter activities (Figure 7D). Consistent with the above mRNA expression results, PRR activation did not affect mitochondrial biogenesis as revealed by the staining of mitochondrial specific fluorescence mitoTracker Green (Figure 7E). Taken together, these results suggest that PRR activation in brown

adipocytes suppresses both basal and isoproterenol-induced UCP-1 expression at least in part through downregulation of the UCP-1 promoter, but not through modulation of mitochondrial biogenesis.

PRR activation suppresses mitochondrial respiration in brown adipocytes

To further determine whether the suppression of UCP-1 by PRR activation leads to changes in mitochondrial respiration, we performed cellular bioenergetics measurements in brown adipocytes using XF24 Extracellular Flux Analyzers (Figure 8). It has been determined that the activation of NOD1, TLR4, TLR2 did not change cell viability as measured by the MTT assays (data not shown). The basal oxygen consumption rate (OCR) of brown adipocytes was 109±10.02 pM/min, which was suppressed to 93±8.4, 79.9±5.5, and 82.5±9.79 pM/min by C12-iEDAP ($p<0.05$), LPS ($p<0.01$), and Pam3CSK4 ($p<0.01$), respectively (Figure 8C). Injection of isoproterenol (1 μM) resulted in a gradual increase in OCR that peaked at 142.2±21.1 pM/min ($p<0.05$), which was significantly reduced to 99.3±10, 92±8.7, and 76.8±3.4 pM/min by C12-iEDAP ($p<0.05$), LPS ($p<0.01$), and Pam3CSK4 ($p<0.01$), respectively (Figure 8C). The ECAR, an indirect measure of glycolysis and lactate production, was measured simultaneously with OCR. Brown adipocytes treated with C12-iEDAP ($p<0.05$), LPS ($p<0.01$), and Pam3CSK4 ($p<0.05$) all showed a significant increase in basal ECAR, with LPS inducing the highest level. Injection of isoproterenol induced a modest but significant increase in ECAR over the baseline ($p<0.05$); however, both C12-iEDAP and Pam3CSK4 significantly suppressed isoproterenol-induced ECARs ($p<0.05$). LPS induced a suppressive, but not significant, trend on isoproterenol-induced ECAR (Figure 8D).

Further calculations revealed that PRR activation did not affect isoproterenol-induced maximal respiration (Figure 8E) and ATP-generating OCR (Figure 8F), but significantly suppressed isoproterenol-induced uncoupled OCR from proton leak (Figure 8G) and increased coupling efficiency (Figure 8H). Taken together, these results show that PRR activation significantly attenuates basal and isoproterenol-induced OCR and isoproterenol-induced uncoupled respiration from proton leak, but does not affect maximal respiration and ATP-coupled respiration, consistent with the suppressive effects of PRR activation on UCP-1 expression in brown adipocytes.

2.5 Discussion

It has been well recognized that obesity is associated with chronic inflammation, both systemically and locally in WAT. Here we report, for the first time, that mRNA of major PRR NOD1, TLR4, and TLR2, but not NOD2, was upregulated in BAT, which was paralleled by the mRNA expression of the inflammatory chemokine MCP-1 and cytokines IL-6 and TNF-α in both DIO and ob/ob mice compared with their respective controls (Figure 1). Using an immortalized brown cell line derived from the classical interscapular BAT, we show that both mRNA expression and protein expression of NOD1 and TLR4, but not NOD2 or TLR2, were increased upon brown adipocyte differentiation (Figure 2); the activation of NOD1, TLR4, and TLR2 induced activation of the NF-κB and MAPK signaling pathways (Figure 3), leading to upregulation of mRNA and/or protein expression of the proinflammatory gene MCP-1, IL-6, RANTES, and TNF-α, in the cultured brown adipocytes (Figure 4-6). Moreover, activation of these PRRs in the brown adipocytes suppressed basal and isoproterenol-induced UCP-1 mRNA and protein expression (Figure 7A and B), at least in part through suppressing UCP-1 promoter activities (Figure 7D). Further, PRR activation suppressed both basal and isoproterenol-induced oxygen consumption rates (Figure 8C), and isoproterenol-induced uncoupled respiration from proton leaks (Figure 8G) and increased coupling efficiency (Figure 8H), but did not affect the maximal respiration (Figure 8E) and ATP-generating respiration (Figure 8F).

BAT has emerged as a novel target for obesity treatment and prevention, due to its unique role in energy expenditure. Two sources of brown adipocytes have been identified. One is from classical BAT depots, such as interscapular region, the other one

is from UCP-1 expressing, brown-like adipocytes from WAT depots, such as subcutaneous depot. While it is still unclear about the formation of the brown-like adipocytes in typical WAT, it is less debated that classical brown adipocytes share a common progenitor with skeletal muscle, different from that of brown-like adipocytes from WAT. The findings that adult humans do have classical BAT argue for research on classical BAT depots in rodents as they also have relevance to human physiology (Nedergaard & Cannon, 2013). To our knowledge, this is the first report demonstrating that the upregulation of mRNA expression of the selected PRRs in the classical BAT in obesity and the regulation of PRR expression at both mRNA and protein levels in differentiating brown adipocytes in culture. Our report further shows that activation of selected PRRs induces the proinflammatory response and suppresses UCP-1 expression, which are accompanied by attenuated mitochondrial respiration in cultured brown adipocytes. Our results suggest that PRR-mediated inflammation in BAT may be targets for modulation of brown adipose function to combat against obesity.

It is well recognized that PRRs are capable of sensing the disturbance from not only the immune system but also metabolism, the homeostasis of both processes is important for the survival of the organisms (Hotamisligil & Erbay, 2008; Jin et al., 2013). It is believed that the disturbances in obesity, i.e., the ligands for the PRRs, are excess of nutrients [e.g., saturated fatty acids (Könner & Brüning, 2011)], production of endogenous molecules from metabolic stress and tissue injuries [e.g., ceramides (Fischer et al., 2007), and high mobility group box 1 (Li et al., 2011)], or modulation of intestinal microbiota (Cani et al., 2007; Nicholson et al., 2012). Whether these ligands activate PRR in BAT in obesity remains to be determined in the future.

Mouse models of global deficiency of the PRRs have been instrumental in determining the role of PRRs in linking inflammation and metabolic stress. The effects of global deficiency of TLR4 and TLR2 on DIO, tissue inflammation, and insulin resistance have been reported (Davis et al., 2011; Ehses et al., 2010; Himes & Smith, 2010; Shi et al., 2006; Tsukumo et al., 2007). Shi et al. (Shi et al., 2006) reported that only female mice lacking TLR4 were partially protected from high-fat DIO and insulin resistance, accompanied by less inflammation in the liver and fat (with no specification of fat type) compared with the WT control mice; however, energy expenditure was not reported. Male C3H/HeJ mice, which have a loss-of-function mutation in TLR4, were reported to be protected against the development of DIO with increased oxygen consumption (indicating the increased metabolic rate), and decreased respiratory exchange ratio (indicating the preferential use of fat as an energy source), improved insulin sensitivity, and enhanced insulin-signaling in white adipose tissue, muscle, and liver, compared with the controls. Inflammation of brown adipose was not reported in this study (Tsukumo et al., 2007). Moreover, global TLR2 deficiency protected the mice from DIO (Ehses et al., 2010; Himes & Smith, 2010; Kuo et al., 2011), liver, muscle (Ehses et al., 2010; Kuo et al., 2011), and pancreatic β-cells (Ehses et al., 2010). TLR2-deficient mice showed an increase in energy expenditure as measured by oxygen consumption (VO_2) in the dark cycle (Ehses et al., 2010; Kuo et al., 2011). In these studies, inflammation in BAT was not reported. Furthermore, mice with double knockout of NOD1 and NOD2 were shown to be protected from high-fat DIO, insulin resistance, inflammation in the white adipose and the liver (Schertzer et al., 2011). Energy expenditure and inflammation in brown adipose were not reported in this study

(Schertzer et al., 2011). Therefore, the role of PRR-mediated inflammation in BAT in diet-induced systemic inflammation, insulin resistance, and altered energy expenditure in obesity remains to be determined.

Our results show that mRNA of selected PRR (NOD1, TLR4, TLR2, and NOD2) was upregulated in BAT in obesity, which correlated with increased mRNA expression of proinflammatory cytokines/chemokines, i.e., MCP-1, IL-6, TNF-α, and RANTES (Figure 1). MCP-1 has been reported to be a critical chemotactic factor for macrophage infiltration into the adipose tissue, leading to adipose inflammation (Kamei et al., 2006; Kanda et al., 2006). TNF-α and IL-6 are known cytokines that induce insulin resistance in skeletal muscle and liver (Rasouli & Kern, 2008). RANTES has also been reported to be upregulated and is associated with T-cell accumulation in murine and human obesity (Wu et al., 2007). Activation of NOD1, TLR4, and TLR2 is capable of inducing MCP-1, IL-6, RANTES, and TNF-α mRNA as well as protein secretion (except for TNF-α, which is below detection limit) in brown adipocytes (Figure 4). The differences in patterns between protein secretion and mRNA expression downstream of PRRs may reflect the differences in posttranscriptional modulation of those cytokines/chemokines downstream of the PRR activation in brown adipocytes. Using pharmacological inhibitors of NF-κB and MAPK, we show these pathways were differentially involved in mRNA expression of MCP-1, IL-6, TNF-α, and RANTES downstream of NOD1, TLR4, and TLR2 (Figure 5 and 6). While the NF-κB pathway appeared to be involved in all four examined cytokines/chemokines induced by C12-iEDAP, LPS, or Pam3CSK4, the involvement of MAPK seemed to differ among the activation of NOD1, TLR4, and TLR2. NOD1 activation primarily induced p38 MAPK as inhibition of p38 MAPK, but not other

MAPKs, attenuated mRNA of all four cytokines/chemokines. In contrast, differential yet distinct involvements of MAPKs downstream of activation of TLR4 and TLR2 were noted in brown adipocytes. The JNK inhibitor SP600125 significantly attenuated, whereas the p38 inhibitor SB203580 did not affect the mRNA of the four proinflammatory genes induced by LPS. The ERK inhibitor PD98054 significantly attenuated LPS-induced IL-6, TNF-α, and RANTES mRNA, but not MCP-1 mRNA. On the other hand, the JNK inhibitor SP600125 attenuated Pam3CSK4-induced mRNA of MCP-1, TNF-α, RANTES, but not IL-6, whereas the p38 inhibitor SB203580 only significantly attenuated Pam3CSK4-induced IL-6 and RANTES mRNA and the ERK inhibitor PD98054 only attenuated Pam3CSK4-induced MCP-1 and IL-6 mRNA. That distinct intracellular signaling pathways downstream of various PRRs control cytokines/chemokine expression, which has been reported in other cell types (Kopp et al., 2009; Natarajan et al., 1996), make it possible to design specific strategies to target individual PRR or cytokine/chemokine for the benefits of enhancing the functions of brown adipocytes.

Moreover, our results demonstrate that PRR activation led to down-regulation of both basal and isoproterenol-stimulated UCP-1 mRNA as well as protein expression with more pronounced suppression under isoproterenol-stimulated condition (Figure 7A and B). These were accompanied by attenuated basal and isoproterenol-stimulated oxygen consumption and uncoupled respiration from proton leaks, but not maximal respiration and ATP-generated respiration (Figure 8). Initial mechanistic studies show that PRR-mediated downregulation of UCP-1 mRNA was not due to suppression of mitochondrial biogenesis as there were no changes in mRNA of two other mitochondrial

genes (COX4a and Uqcrh) (Figure 7A) and no changes of mitochondrial biogenesis by mitoTracker staining (Figure 7E). In contrast, similar degrees of suppression of UCP-1 promoter activities were observed (Figure 8D). Taken together, these results demonstrate that PRR activation suppresses UCP-1 expression, leading to attenuated mitochondrial respiration, via at least in part down regulation of UCP-1 promoter activities. One of the possible mechanisms for PRR-mediated suppression of UCP-1 promoter is through NF-κB pathway, since we have shown that PRR activation leads to NF-κB activation in brown adipocytes, and a few putative NF-κB transcriptional factor binding sites have been identified upstream of the transcription start site using bioinformatics tools. The molecular mechanisms underlying the cross talk between NF-κB pathway downstream of PRR activation and UCP-1 transcription under the basal or β-adrenergic stimulation need to be explored further.

Compared with UCP-1 expression, PRR activation at the same time also differentially affected PPARγ and PGC-1α expression, both of which are important for the expression of brown adipocyte markers, such as UCP-1. Evidence has emerged from studies that PPARγ not only controls white adipocyte differentiation but also controls brown adipocyte differentiation (Gray et al., 2006; Petrovic, Shabalina, Timmons, Cannon, & Nedergaard, 2008; Sell et al., 2004). PGC-1α coactivates transcription factor PPARγ bound to the rpomoters of target genes, such as UCP-1, to control gene transcription (Puigserver et al., 1998; Tiraby et al., 2003). The results show PRR activation suppressed both PPARγ mRNA and protein expression under the basal and isoproterenol-stimulated conditions whereas PRR activation only suppressed PGC-1α mRNA under the basal condition, but did not suppress PGC-1α protein under both

conditions (Figure 7A and B). The differences between mRNA and protein expression of PGC-1α may be due to the protein stability. Moreover, we also examined the brown adipocyte cell morphology and lipid accumulation under the same conditions. Both the cell morphology (data not shown) and lipid accumulation by ORO staining and quantification (Figure 7C) did not seem to be affected by PRR activation. Taken together, our results demonstrate that PRR activation in differentiated brown adipocytes selectively suppressed UCP-1 and some other brown adipocyte markers expression (e.g., PPARγ and Cidea) without affecting mitochondrial biogenesis and lipid accumulation, which is sufficient to lead to suppressed mitochondrial oxygen consumption and uncoupled respiration.

In summary, we have demonstrated the role of selected PRRs in mediating inflammation and downregulation of UCP-1 expression without affecting mitochondrial biogenesis and lipid accumulation, leading to suppressed mitochondrial respiration in the classical brown adipocytes. Our results suggest that PRR-mediated inflammation in brown adipocytes may be potential targets to modulate BAT function for obesity treatment and prevention.

2.6 References

Akira, S., Uematsu, S., & Takeuchi, O. (2006). Pathogen recognition and innate immunity. *Cell, 124*(4), 783-801.

Cani, P. D., Amar, J., Iglesias, M. A., Poggi, M., Knauf, C., Bastelica, D., . . . Chabo, C. (2007). Metabolic endotoxemia initiates obesity and insulin resistance. *Diabetes, 56*(7), 1761-1772.

Cannon, B., & Nedergaard, J. (2004). Brown adipose tissue: function and physiological significance. *Physiological reviews, 84*(1), 277-359.

Chamaillard, M., Hashimoto, M., Horie, Y., Masumoto, J., Qiu, S., Saab, L., . . . Kusumoto, S. (2003). An essential role for NOD1 in host recognition of bacterial peptidoglycan containing diaminopimelic acid. *Nature immunology, 4*(7), 702-707.

Cypess, A. M., Lehman, S., Williams, G., Tal, I., Rodman, D., Goldfine, A. B., . . . Doria, A. (2009). Identification and importance of brown adipose tissue in adult humans. *New England Journal of Medicine, 360*(15), 1509-1517.

Cypess, A. M., White, A. P., Vernochet, C., Schulz, T. J., Xue, R., Sass, C. A., . . . Sze, C. (2013). Anatomical localization, gene expression profiling and functional characterization of adult human neck brown fat. *Nature medicine, 19*(5), 635-639.

Davis, J. E., Braucher, D. R., Walker-Daniels, J., & Spurlock, M. E. (2011). Absence of Tlr2 protects against high-fat diet-induced inflammation and results in greater insulin-stimulated glucose transport in cultured adipocytes. *The Journal of nutritional biochemistry, 22*(2), 136-141.

Ehses, J., Meier, D., Wueest, S., Rytka, J., Boller, S., Wielinga, P., . . . Van Lommel, L. (2010). Toll-like receptor 2-deficient mice are protected from insulin resistance and beta cell dysfunction induced by a high-fat diet. *Diabetologia, 53*(8), 1795-1806.

Fischer, H., Ellström, P., Ekström, K., Gustafsson, L., Gustafsson, M., & Svanborg, C. (2007). Ceramide as a TLR4 agonist; a putative signalling intermediate between sphingolipid receptors for microbial ligands and TLR4. *Cellular microbiology, 9*(5), 1239-1251.

Girardin, S. E., Boneca, I. G., Carneiro, L. A., Antignac, A., Jéhanno, M., Viala, J., . . . Zäthringer, U. (2003). Nod1 detects a unique muropeptide from gram-negative bacterial peptidoglycan. *Science, 300*(5625), 1584-1587.

Girardin, S. E., Boneca, I. G., Viala, J., Chamaillard, M., Labigne, A., Thomas, G., . . . Sansonetti, P. J. (2003). Nod2 is a general sensor of peptidoglycan through muramyl dipeptide (MDP) detection. *Journal of Biological Chemistry, 278*(11), 8869-8872.

Gray, S. L., Dalla Nora, E., Backlund, E. C., Manieri, M., Virtue, S., Noland, R. C., . . . Cannon, B. (2006). Decreased brown adipocyte recruitment and thermogenic capacity in mice with impaired peroxisome proliferator-activated receptor (P465L PPARγ) function. *Endocrinology, 147*(12), 5708-5714.

Gregor, M. F., & Hotamisligil, G. S. (2011). Inflammatory mechanisms in obesity. *Annual review of immunology, 29*, 415-445.

Himes, R. W., & Smith, C. W. (2010). Tlr2 is critical for diet-induced metabolic syndrome in a murine model. *The FASEB Journal, 24*(3), 731-739.

Hotamisligil, G. S., & Erbay, E. (2008). Nutrient sensing and inflammation in metabolic diseases. *Nature Reviews Immunology, 8*(12), 923-934.
Inohara, N., Chamaillard, M., McDonald, C., & Nunez, G. (2005). NOD-LRR proteins: role in host-microbial interactions and inflammatory disease. *Annu. Rev. Biochem., 74*, 355-383.
Inohara, N., Ogura, Y., Fontalba, A., Gutierrez, O., Pons, F., Crespo, J., . . . Hashimoto, M. (2003). Host Recognition of Bacterial Muramyl Dipeptide Mediated through NOD2 IMPLICATIONS FOR CROHN′ S DISEASE. *Journal of Biological Chemistry, 278*(8), 5509-5512.
Jespersen, N. Z., Larsen, T. J., Peijs, L., Daugaard, S., Homøe, P., Loft, A., . . . Nedergaard, J. (2013). A classical brown adipose tissue mRNA signature partly overlaps with brite in the supraclavicular region of adult humans. *Cell metabolism, 17*(5), 798-805.
Jin, C., Henao-Mejia, J., & Flavell, R. A. (2013). Innate immune receptors: key regulators of metabolic disease progression. *Cell metabolism, 17*(6), 873-882.
Kamei, N., Tobe, K., Suzuki, R., Ohsugi, M., Watanabe, T., Kubota, N., . . . Kobayashi, M. (2006). Overexpression of monocyte chemoattractant protein-1 in adipose tissues causes macrophage recruitment and insulin resistance. *Journal of Biological Chemistry, 281*(36), 26602-26614.
Kanda, H., Tateya, S., Tamori, Y., Kotani, K., Hiasa, K.-i., Kitazawa, R., . . . Egashira, K. (2006). MCP-1 contributes to macrophage infiltration into adipose tissue, insulin resistance, and hepatic steatosis in obesity. *Journal of Clinical Investigation, 116*(6), 1494.
Kawai, T., & Akira, S. (2009). The roles of TLRs, RLRs and NLRs in pathogen recognition ARTICLE. *International immunology, 21*(4), 317-337.
Klein, J., Fasshauer, M., Klein, H. H., Benito, M., & Kahn, C. R. (2002). Novel adipocyte lines from brown fat: a model system for the study of differentiation, energy metabolism, and insulin action. *Bioessays, 24*(4), 382-388.
Könner, A. C., & Brüning, J. C. (2011). Toll-like receptors: linking inflammation to metabolism. *Trends in Endocrinology & Metabolism, 22*(1), 16-23.
Kopp, A., Buechler, C., Neumeier, M., Weigert, J., Aslanidis, C., Schölmerich, J., & Schäffler, A. (2009). Innate Immunity and Adipocyte Function: Ligand-specific Activation of Multiple Toll-like Receptors Modulates Cytokine, Adipokine, and Chemokine Secretion in Adipocytes. *Obesity, 17*(4), 648-656.
Kuo, L.-H., Tsai, P.-J., Jiang, M.-J., Chuang, Y.-L., Yu, L., Lai, K.-T., & Tsai, Y.-S. (2011). Toll-like receptor 2 deficiency improves insulin sensitivity and hepatic insulin signalling in the mouse. *Diabetologia, 54*(1), 168-179.
Kwon, H., & Pessin, J. E. (2013). Adipokines mediate inflammation and insulin resistance. *Frontiers in endocrinology, 4*.
Li, L., Chen, L., Hu, L., Liu, Y., Sun, H. Y., Tang, J., . . . Feng, G. S. (2011). Nuclear factor high-mobility group box1 mediating the activation of toll-like receptor 4 signaling in hepatocytes in the early stage of nonalcoholic fatty liver disease in mice. *Hepatology, 54*(5), 1620-1630.
Natarajan, K., Singh, S., Burke, T. R., Grunberger, D., & Aggarwal, B. B. (1996). Caffeic acid phenethyl ester is a potent and specific inhibitor of activation of nuclear

transcription factor NF-kappa B. *Proceedings of the National Academy of Sciences, 93*(17), 9090-9095.
Nedergaard, J., & Cannon, B. (2013). How brown is brown fat? It depends where you look. *Nature medicine, 19*(5), 540-541.
Nicholls, D. G., & Locke, R. M. (1984). Thermogenic mechanisms in brown fat. *Physiol Rev, 64*(1), 1-64.
Nicholson, J. K., Holmes, E., Kinross, J., Burcelin, R., Gibson, G., Jia, W., & Pettersson, S. (2012). Host-gut microbiota metabolic interactions. *Science, 336*(6086), 1262-1267.
Ouchi, N., Parker, J. L., Lugus, J. J., & Walsh, K. (2011). Adipokines in inflammation and metabolic disease. *Nature Reviews Immunology, 11*(2), 85-97.
Petrovic, N., Shabalina, I. G., Timmons, J. A., Cannon, B., & Nedergaard, J. (2008). Thermogenically competent nonadrenergic recruitment in brown preadipocytes by a PPARγ agonist. *American Journal of Physiology-Endocrinology And Metabolism, 295*(2), E287-E296.
Puigserver, P., Wu, Z., Park, C. W., Graves, R., Wright, M., & Spiegelman, B. M. (1998). A cold-inducible coactivator of nuclear receptors linked to adaptive thermogenesis. *Cell, 92*(6), 829-839.
Rasouli, N., & Kern, P. A. (2008). Adipocytokines and the metabolic complications of obesity. *The Journal of Clinical Endocrinology & Metabolism, 93*(11_supplement_1), s64-s73.
Richard, D., & Picard, F. (2011). Brown fat biology and thermogenesis. *Front Biosci, 16*, 1233-1260.
Ricquier, D. (2005). Respiration uncoupling and metabolism in the control of energy expenditure. *Proceedings of the Nutrition Society, 64*(01), 47-52.
Rim, J. S., & Kozak, L. P. (2002). Regulatory motifs for CREB-binding protein and Nfe2l2 transcription factors in the upstream enhancer of the mitochondrial uncoupling protein 1 gene. *Journal of Biological Chemistry, 277*(37), 34589-34600.
Saito, M., Okamatsu-Ogura, Y., Matsushita, M., Watanabe, K., Yoneshiro, T., Nio-Kobayashi, J., . . . Nakada, K. (2009). High incidence of metabolically active brown adipose tissue in healthy adult humans effects of cold exposure and adiposity. *Diabetes, 58*(7), 1526-1531.
Schertzer, J. D., Tamrakar, A. K., Magalhães, J. G., Pereira, S., Bilan, P. J., Fullerton, M. D., . . . Philpott, D. J. (2011). NOD1 activators link innate immunity to insulin resistance. *Diabetes, 60*(9), 2206-2215.
Sell, H., Berger, J. P., Samson, P., Castriota, G., Lalonde, J., Deshaies, Y., & Richard, D. (2004). Peroxisome proliferator-activated receptor γ agonism increases the capacity for sympathetically mediated thermogenesis in lean and ob/ob mice. *Endocrinology, 145*(8), 3925-3934.
Shi, H., Kokoeva, M. V., Inouye, K., Tzameli, I., Yin, H., & Flier, J. S. (2006). TLR4 links innate immunity and fatty acid–induced insulin resistance. *Journal of Clinical Investigation, 116*(11), 3015.
Song, M. J., Kim, K. H., Yoon, J. M., & Kim, J. B. (2006). Activation of Toll-like receptor 4 is associated with insulin resistance in adipocytes. *Biochemical and biophysical research communications, 346*(3), 739-745.

Sun, S., Ji, Y., Kersten, S., & Qi, L. (2012). Mechanisms of inflammatory responses in obese adipose tissue. *Annual review of nutrition, 32*, 261.

Tiraby, C., Tavernier, G., Lefort, C., Larrouy, D., Bouillaud, F., Ricquier, D., & Langin, D. (2003). Acquirement of brown fat cell features by human white adipocytes. *Journal of Biological Chemistry, 278*(35), 33370-33376.

Tobe, M., Isobe, Y., Tomizawa, H., Nagasaki, T., Takahashi, H., & Hayashi, H. (2003). A novel structural class of potent inhibitors of NF-κB activation: structure–activity relationships and biological effects of 6-aminoquinazoline derivatives. *Bioorganic & medicinal chemistry, 11*(18), 3869-3878.

Tsukumo, D. M., Carvalho-Filho, M. A., Carvalheira, J. B., Prada, P. O., Hirabara, S. M., Schenka, A. A., . . . Velloso, L. A. (2007). Loss-of-function mutation in Toll-like receptor 4 prevents diet-induced obesity and insulin resistance. *Diabetes, 56*(8), 1986-1998.

van Marken Lichtenbelt, W. D., Vanhommerig, J. W., Smulders, N. M., Drossaerts, J. M., Kemerink, G. J., Bouvy, N. D., . . . Teule, G. J. (2009). Cold-activated brown adipose tissue in healthy men. *New England Journal of Medicine, 360*(15), 1500-1508.

Vijgen, G., & van Marken Lichtenbelt, W. (2013). Brown adipose tissue: clinical impact of a re-discovered thermogenic organ. *Front Biosci (Elite Ed), 5*, 823-833.

Virtanen, K. A., Lidell, M. E., Orava, J., Heglind, M., Westergren, R., Niemi, T., . . . Enerbäck, S. (2009). Functional brown adipose tissue in healthy adults. *New England Journal of Medicine, 360*(15), 1518-1525.

Vosselman, M. J., van Marken Lichtenbelt, W. D., & Schrauwen, P. (2013). Energy dissipation in brown adipose tissue: From mice to men. *Molecular and cellular endocrinology, 379*(1), 43-50.

Wu, H., Ghosh, S., Dai Perrard, X., Feng, L., Garcia, G. E., Perrard, J. L., . . . Smith, C. W. (2007). T-cell accumulation and regulated on activation, normal T cell expressed and secreted upregulation in adipose tissue in obesity. *Circulation, 115*(8), 1029-1038.

Zhao, L., Hu, P., Zhou, Y., Purohit, J., & Hwang, D. (2011). NOD1 activation induces proinflammatory gene expression and insulin resistance in 3T3-L1 adipocytes. *American Journal of Physiology-Endocrinology And Metabolism, 301*(4), E587-E598.

Zingaretti, M. C., Crosta, F., Vitali, A., Guerrieri, M., Frontini, A., Cannon, B., . . . Cinti, S. (2009). The presence of UCP1 demonstrates that metabolically active adipose tissue in the neck of adult humans truly represents brown adipose tissue. *The FASEB Journal, 23*(9), 3113-3120.

2.7 Appendix

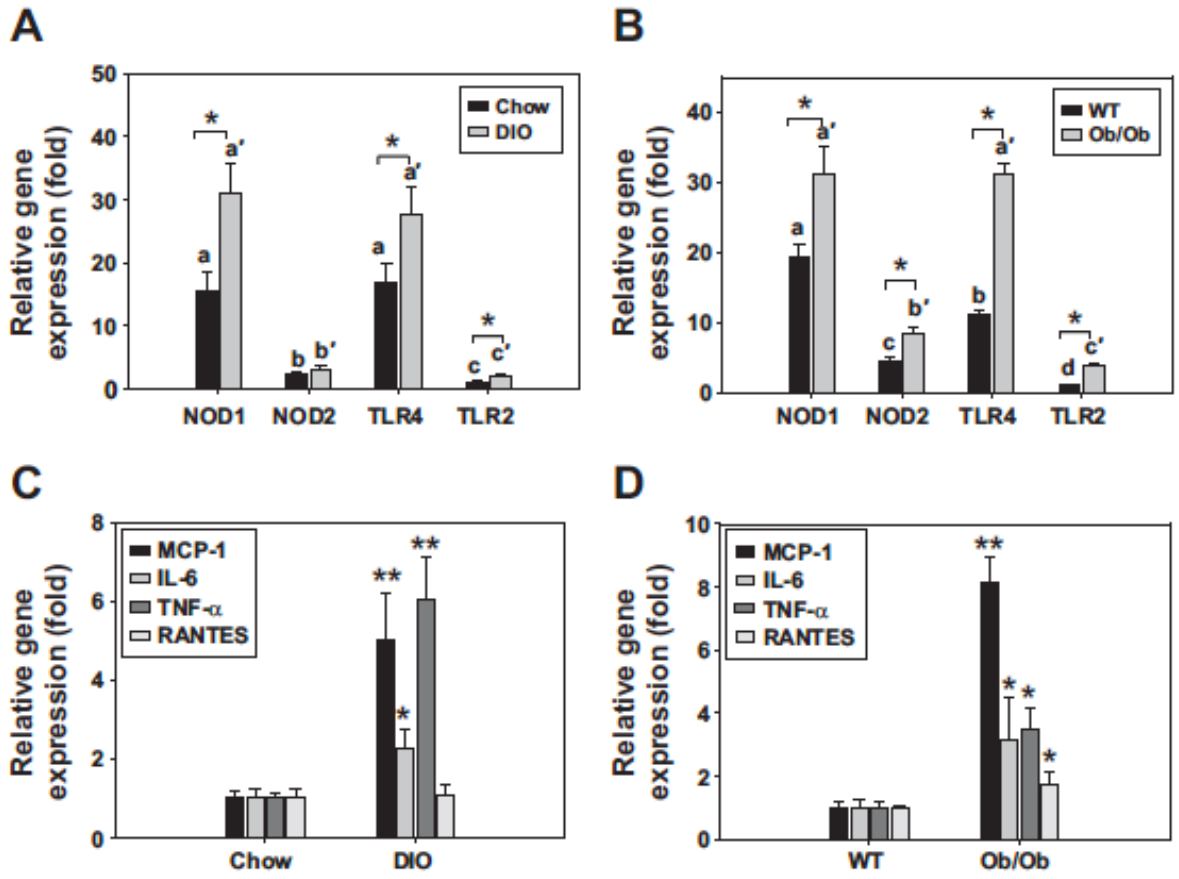

Figure 1 mRNA expression of selected PRRs are up-regulated in brown fat tissue of DIO and ob/ob mice

mRNA expression of NOD1, NOD2, TLR4 and TLR2 (A, B) and proinflammatory chemokines/cytokines (MCP-1, IL-6, RANTES, TNF-α) (C, D) in the interscapular brown fat tissue from the DIO male mice (n=7) (A, C) or ob/ob male mice (n=6), and their respective controls were evaluated by semi-quantitative RT-PCR. The relative mRNA expression was normalized to 36B4 and expressed as fold of the value of TLR2 in chow fed or wt group (set as 1). a-d are for Chow or WT groups (solid bars); a'-c' are for DIO or Ob/Ob groups (gray bars). Different letters indicate significant differences among solid or gray bars. *$p<0.05$, **$p<0.01$, significantly different from the controls.

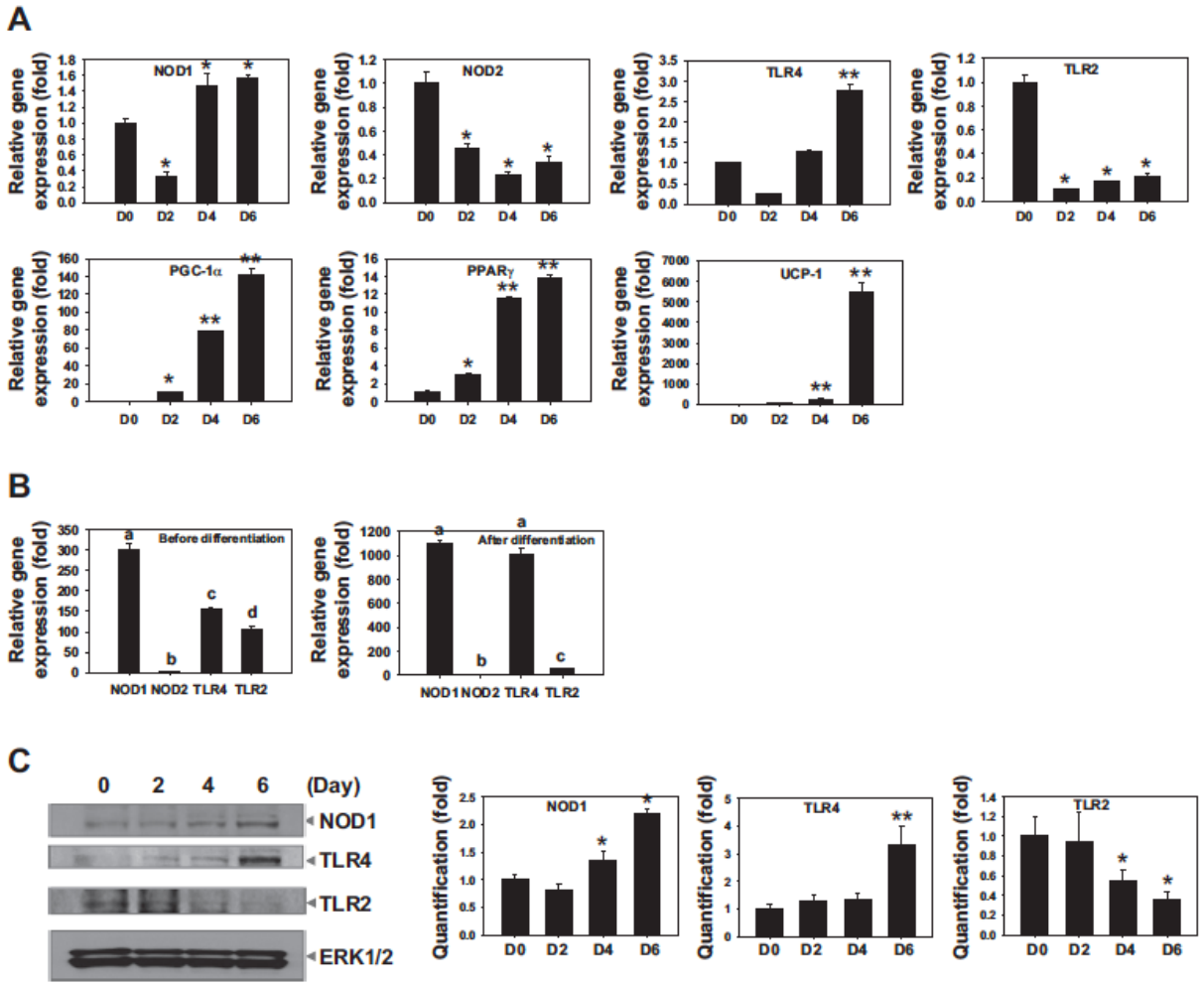

Figure 2 Expression of selected PRRs are up-regulated during brown adipocyte differentiation

Brown fat cells were differentiated as described in Materials and Methods. Total RNA was isolated at confluency (D0), 2 (D2), 4 (D4), and 6 day (D6) post initiation of differentiation. (A) mRNA expression of NOD1, NOD2, TLR4, and TLR2 and brown adipocyte markers PGC-1α, PPARγ, and UCP-1 was evaluated by semi-quantitative RT-PCR. The relative mRNA expression was normalized to 36B4 and expressed as fold of D0 value (set as 1). (B) Relative mRNA expression of NOD1, NOD2, TLR4, and TLR2 before differentiation (D0) and after differentiation (D6) was compared. The relative mRNA expression was normalized to 36B4 and expressed as fold of NOD2 value (set as 1). (C) Protein expression of NOD1, TLR4, and TLR2 was analyzed at D0, 2, 4, and 6 by western analysis with primary antibodies against NOD1, TLR4, and TLR2. ERK1/2 protein was used as a loading control. This experiment has been performed independently three times, and the representative results are shown (left). Relative quantification of western analysis was done by densitometry. The data are expressed as fold to the D0 level (set as 1) (right). Data are means±SE (n=3). Different letters indicate significant differences between bars. *$p<0.05$, **$p<0.01$, significantly different from the controls.

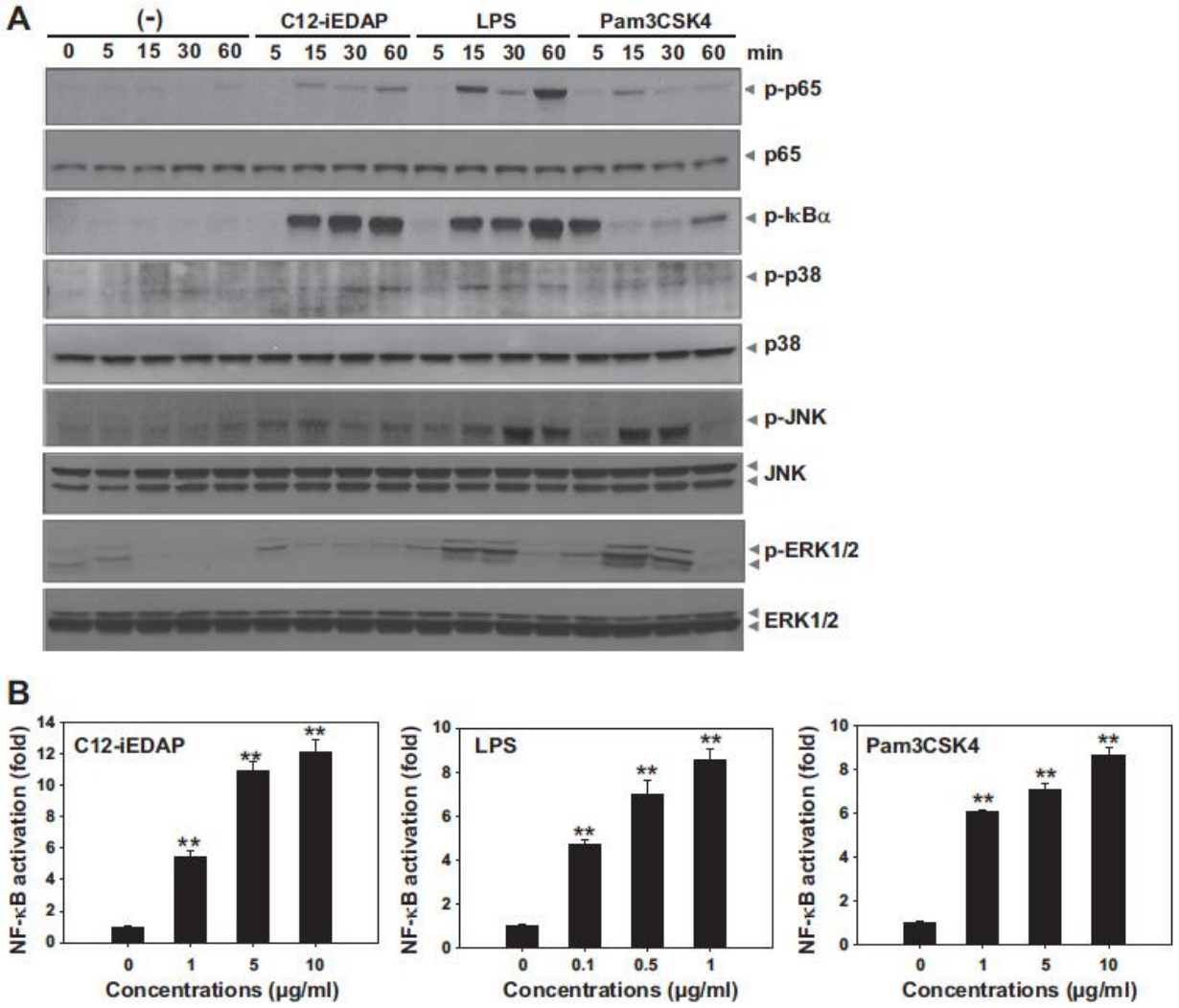

Figure 3 PRR activation in brown adipocytes induces phosphorylation and activation of NF-κB and MAPK signaling

(A) Brown adipocytes were serum starved overnight and were stimulated with C12-iEDAP (10 μg/ml), LPS (1 μg/ml), Pam3CSK4 (10 μg/ml) or the vehicle control for indicated times, and whole cell lysate was prepared and analyzed by western analysis with specific antibodies against phospho-p65, phospho-IκBα, phospho-p38, phospho-JNK, phospho-ERK, p65, p38, JNK and ERK. (B) Brown adipocytes were infected with adenovirus encoded NF-κB-Luc and β-galactosidase for 24 h and stimulated with increasing doses of C12-iEDAP, LPS, or Pam3CSK4 as indicated for 18 h. Reporter gene assays were performed. Relative luciferase activities were normalized by β-galactosidase activities for each sample and expressed as fold of the vehicle value (set as 1). Data are means±SE (n=3). **$p<0.01$, significantly different from the controls.

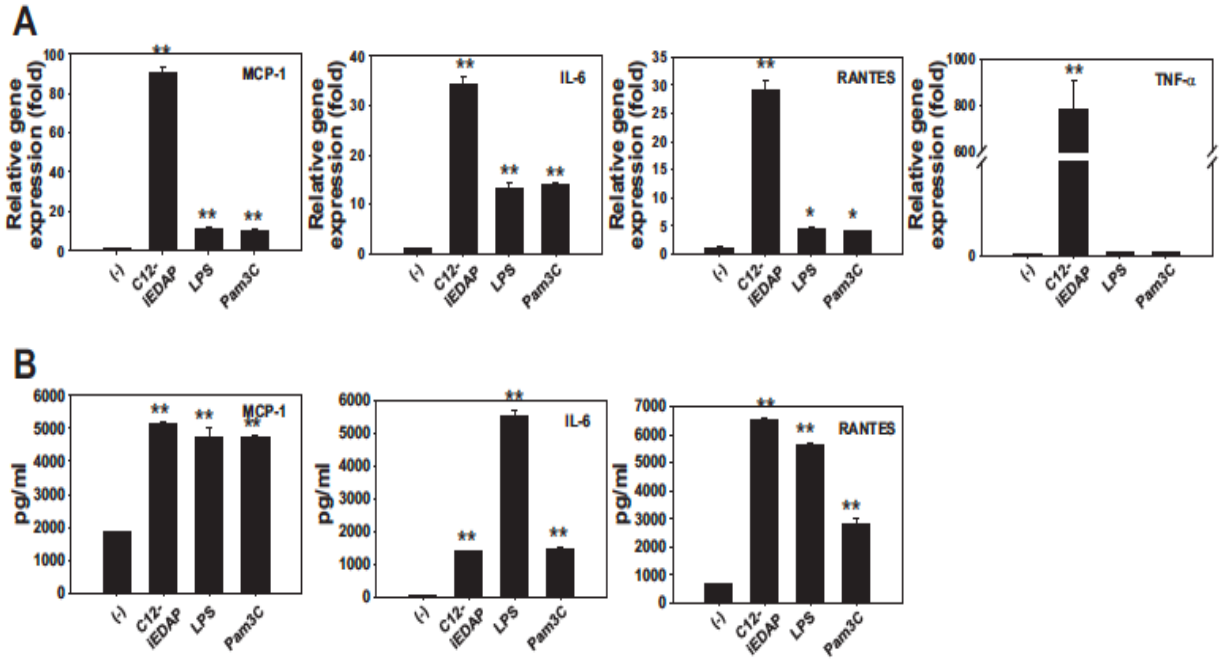

Figure 4 PRR activation in brown adipocytes up-regulates the expression and secretion of proinflammatory cytokines/chemokines
Brown adipocytes were stimulated with C12-iEDAP (10 µg/ml), LPS (0.1 µg/ml), Pam3CSK4 (1 µg/ml), or the vehicle control for 12 h. Total RNA was isolated for mRNA expression of MCP-1, IL-6, RANTES, TNF-α by semi-quantitative RT-PCR (A), and the supernatant was collected for protein measurements of MCP-1, IL-6, RANTES by ELISA (B). Data are means±SE (n=3). *p<0.05, **p<0.01, significantly different from the controls.

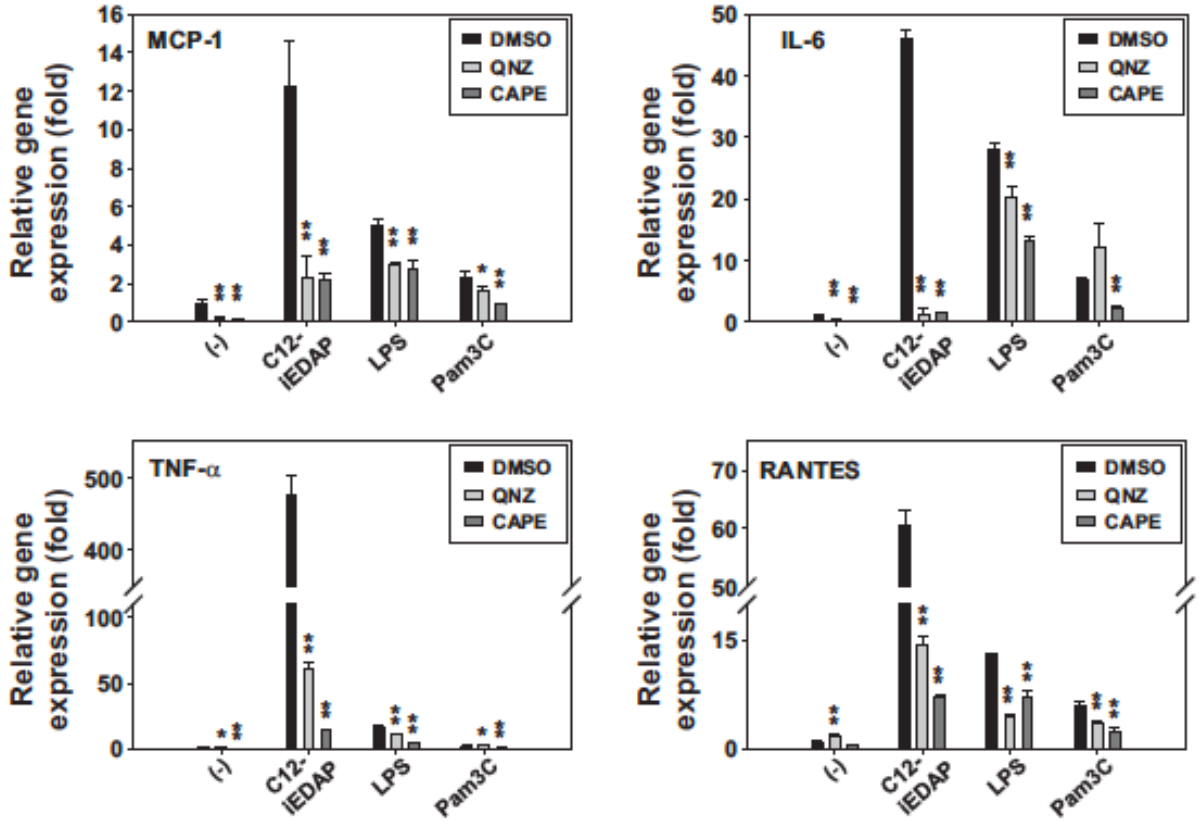

Figure 5 Inhibition of NF-κB attenuates mRNA expression of proinflammatory cytokines/chemokines induced by PRR activation

Brown adipocytes were pretreated with NF-κB inhibitor QNZ (20 nM) and CAPE (10 μM) for 1 h and costimulated with C12-iEDAP (10 μg/ml), LPS (0.1 μg/ml), Pam3CSK4 (1 μg/ml), or the vehicle control. mRNA expression of MCP-1, IL-6, RANTES, and TNF-α was evaluated by semi-quantitative RT-PCR. The relative mRNA expression was normalized to 36B4 and expressed as fold of the vehicle value (set as 1). Data are means±SE (n=3). *$p<0.05$, **$p<0.01$, significantly different from the controls.

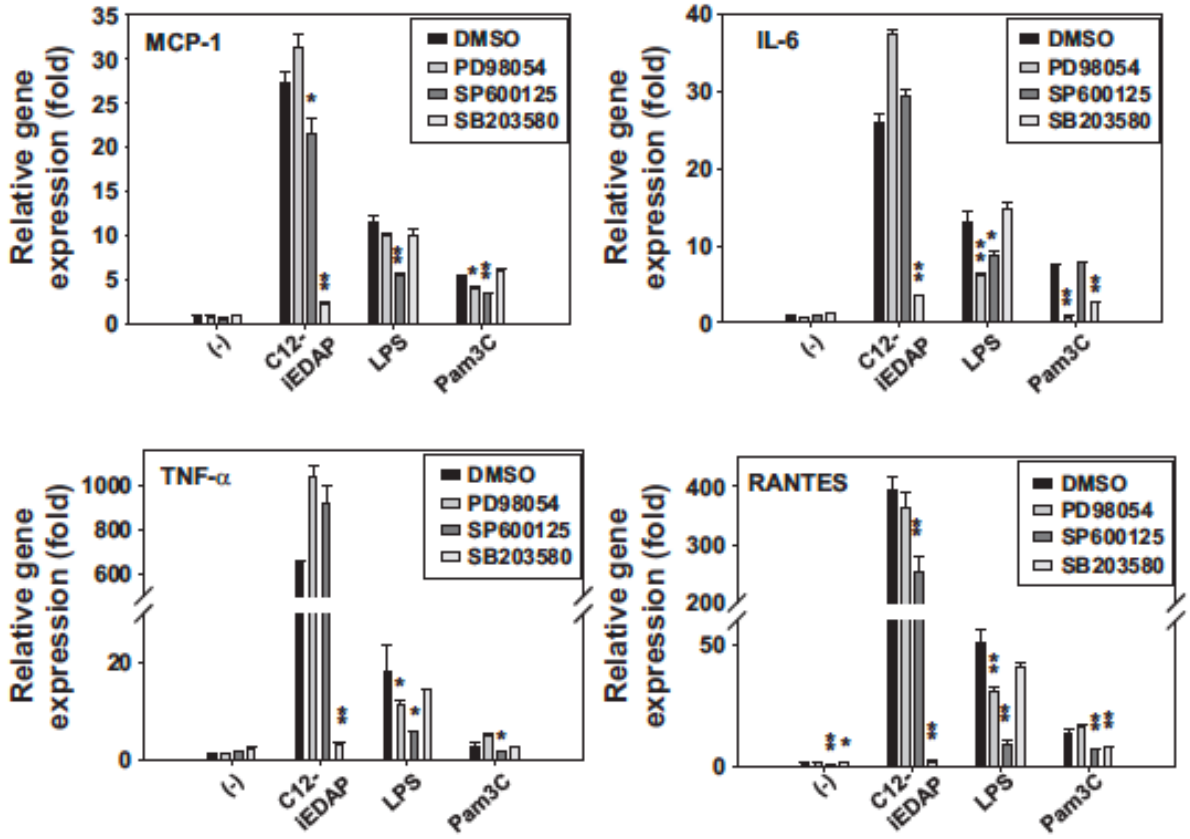

Figure 6 Inhibition of MAPK differentially attenuates mRNA expression of proinflammatory cytokines/chemokines induced by PRR activation
Brown adipocytes were pretreated with ERK inhibitor PD98054 (10 µM), JNK inhibitor SP600125 (10 µM), or p38 inhibitor SB203580 (2 µM) for 1 h and costimulated with C12-iEDAP (10 µg/ml), LPS (0.1 µg/ml), Pam3CSK4 (1 µg/ml) or the vehicle control. mRNA expression of MCP-1, IL-6, RANTES, and TNF-α was evaluated by semi-quantitative RT-PCR. The relative mRNA expression was normalized to 36B4 and expressed as fold of the vehicle value (set as 1). Data are means±SE (n=3). *$p<0.05$, **$p<0.01$, significantly different from the controls.

Figure 7 PRR activation suppresses both basal and isoproterenol-induced UCP-1 expression, but not mitochondrial biogenesis, in brown adipocytes
(A) Brown adipocytes were serum starved with 1% charcoal-dextran stripped FBS containing DMEM for overnight. The cells were pretreated with C12-iEDAP (10 µg/ml), LPS (0.1 µg/ml), Pam3CSK4 (1 µg/ml), or the vehicle control for 1 h followed by costimulated with or without isoproterenol (ISO, 1 µM) in the presence of the ligand for 6 h. mRNA of UCP-1 and other marker genes was evaluated by semi-quantitative RT-PCR. Relative gene expression was normalized to 36B4 and expressed as fold of the vehicle value (set as 1). (B, C) Brown adipocytes were serum starved overnight, and were treated with C12-iEDAP, LPS, and Pam3CSK4 for 12 h under the basal condition, or pretreated with C12-iEDAP, LPS, Pam3CSK4, or the vehicle control for 12 h, followed by costimulated with ISO in the presence of the ligand for another 6 h. Whole cell lysate was prepared from one set of cell samples and analyzed by western analysis with antibody against of UCP-1, PPARγ, and PGC-1α. ERK1/2 protein was used as a loading control. This experiment has been performed independently three times and the representative results are shown (left). Relative quantification of western analysis was done by densitometry. The data are expressed as fold to the level of the vehicle control (-) under basal condition (set as 1) (right). A duplicate set of cell samples were fixed and stained with oil red O (ORO) for lipid accumulation, and ORO absorbance at 500 nm is shown in C. (D) Brown adipocytes were subcultured and transiently transfected with mouse UCP-1-Luc together with β-galactosidase plasmid. The cells were pretreated with C12-iEDAP (10 µg/ml), LPS (0.1 µg/ml), Pam3CSK4 (1 µg/ml), or the vehicle control for 1 h followed by costimulation of the ligand with or without ISO for 15 h. Reporter gene assays were performed. Relative luciferase activities were normalized by β-galactosidase activities for each sample and expressed as fold of the vehicle value (set as 1). (E) Brown adipocytes were treated with C12-iEDAP (10 µg/ml), LPS (0.1 µg/ml), Pam3CSK4 (1 µg/ml), or the vehicle control for 12 h. The cells were washed with PBS and stained with MitoTracker green (100 nM) for 30 min at 37^0C. The fluorescence intensities were measured as described in Materials and Methods. Data are means±SE (n=3). *$p<0.05$, **$p<0.01$, significantly different from the controls.

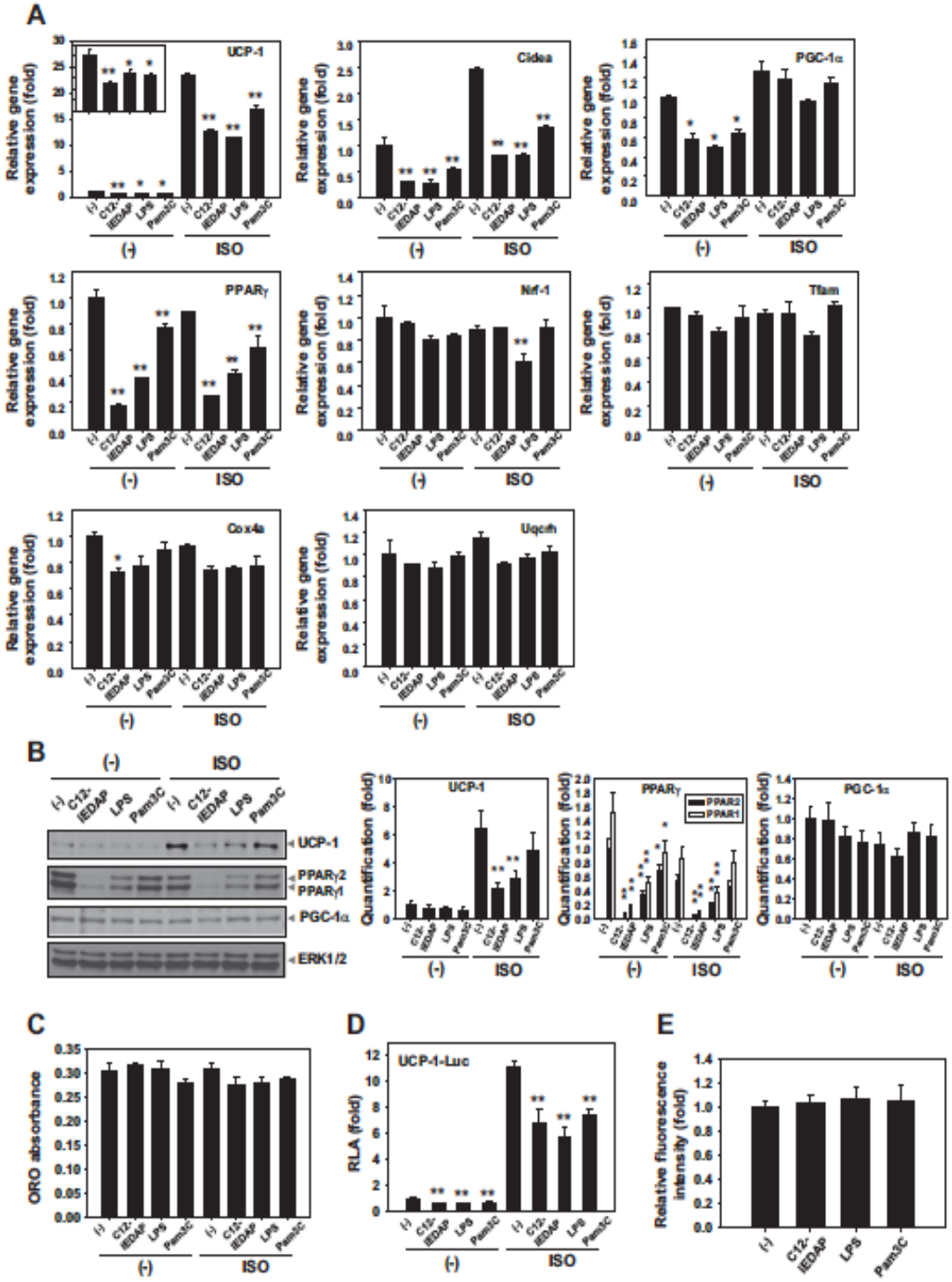
A
UCP-1
Cidea
PGC-1α
PPARγ
Nrf-1
Tfam
Cox4a
Uqcrh
Relative gene expression (fold)
(-)
C12-iEDAP
LPS
Pam3C
ISO
B
UCP-1
PPARγ2
PPARγ1
PGC-1α
ERK1/2
Quantification (fold)
PPAR2
PPAR1
C
ORO absorbance
D
UCP-1-Luc
RLA (fold)
E
Relative fluorescence intensity (fold)

Figure 8 PRR activation suppresses mitochondrial respiration in brown adipocytes

(A, B) Brown adipocytes were subcultured and seeded in 24-well XF assay plates overnight and were pretreated with LPS (0.1 μg/ml), Pam3CSK4 (1 μg/ml), C12-iEDAP (10 μg/ml), or the vehicle control for 12 h and were then subjected to real-time measurements of oxygen consumption rate (OCR) and extracellular acidification rate (ECAR). Following the basal measurements, all cells were injected either with the vehicle control or ISO (1 μM). In each experiment, mitochondrial complex inhibitors were injected to all treatments sequentially in the following order: oligomycin (1 μM), carbonyl cyanide-ptrifluoromethoxyphenylhydrazone (FCCP; 0.75 μM), antimycin A/rotenone (1 μM each), and the readings were taken after each inhibitor. The OCR (A) and ECAR (B) readings were plotted over time. Basal and ISO-induced OCR (C) and ECAR (D) is shown. ISO-induced maximal OCR (E), OCR from ATP production (F), OCR from proton leak (G), and coupling efficiency (H) are also shown. Data are means±SE (n=6-9). *$p<0.05$, **$p<0.01$, significantly different from the controls.

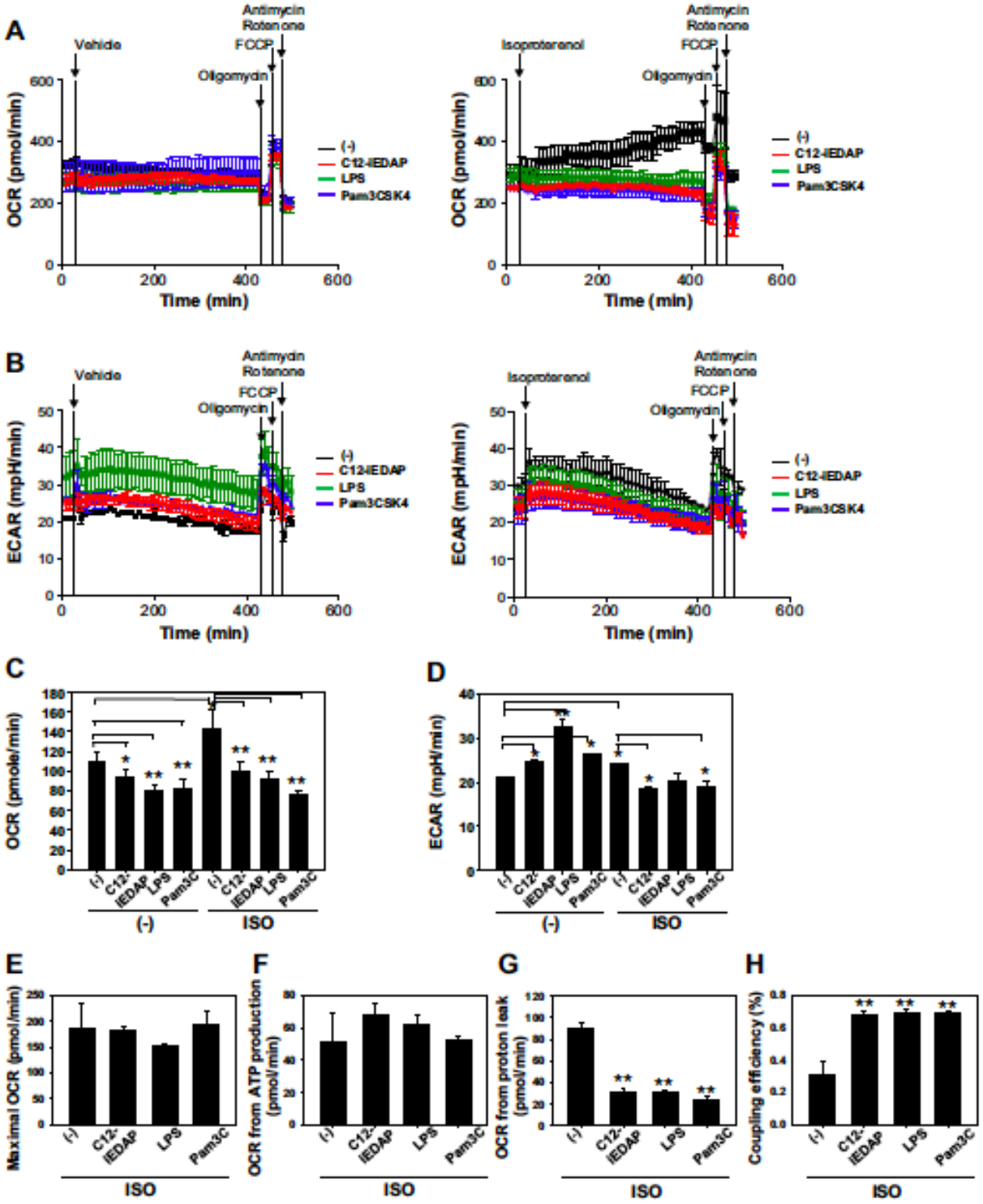
A
Vehicle
Oligomycin
FCCP
Antimycin
Rotenone
Isoproterenol
OCR (pmol/min)
Time (min)
(-)
C12-iEDAP
LPS
Pam3CSK4
B
ECAR (mpH/min)
C
OCR (pmole/min)
D
ECAR (mpH/min)
(-)
ISO
E
Maximal OCR (pmol/min)
F
OCR from ATP production (pmol/min)
G
OCR from proton leak (pmol/min)
H
Coupling efficiency (%)

CHAPTER III

CHRONIC ACTIVATION OF PATTERN RECOGNITION RECEPTORS SUPPRESSES BROWN ADIPOGENESIS OF MULTIPOTENT MESODERMAL STEM CELLS AND BROWN PRE-ADIPOCYTES

A version of this chapter was originally published by Jiyoung Bae, Jiangang Chen, Ling Zhao entitled “Chronic activation of pattern recognition receptors suppresses brown adipogenesis of multipotent mesodermal stem cells and brown pre-adipocytes” *Biochemistry and Cell Biology* 93(3): 251-261 (2015).

3.1 Abstract

Brown adipose tissue (BAT) holds promise to combat obesity through energy-spending, non-shivering thermogenesis. Understanding of regulation of BAT development can lead to novel strategies to increase BAT mass and function for obesity treatment and prevention. Here, we report the effects of chronic activation of PRR on brown adipogenesis of multipotent mesodermal stem C3H10T1/2 cells and immortalized brown pre-adipocytes from the classical interscapular BAT of mice. Activation of NOD1, TLR4, or TLR2 by their respective synthetic ligand suppressed brown marker gene expression and lipid accumulation during differentiation of brown-like adipocytes of C3H10T1/2. Activation of the PRR only during the commitment was sufficient to suppress the differentiation. PRR activation suppressed PGC-1α mRNA, but induced PRDM16 mRNA at the commitment. Consistently, PRR activation suppressed the differentiation of immortalized brown pre-adipocytes. Activation of PRR induced NF-κB activation in both cells, which correlated with their abilities to suppress PPARγ transactivation, a critical event for brown adipogenesis. Taken together, our results demonstrate that chronic PRR activation suppressed brown adipogenesis of multipotent mesodermal stem cells and brown pre-adipocytes, possibly through suppression of PPARγ transactivation. The results suggest that anti- inflammatory therapies targeting PRRs may be beneficial for the BAT development.

3.2 Introduction

Obesity is one of the main public health concerns all over the world. Obesity is associated with chronic inflammation, which is considered to be the starting point for the progression of obesity associated comorbidities, such as insulin resistance and type 2 diabetes. Evidence suggests that pattern recognition receptors (PRR) play critical roles in obesity associated inflammation (Jin et al. 2013). Toll-like receptors (TLR) and nucleotide-oligomerization domain containing protein-like receptor (NLR) are two families of PRRs that play critical roles in innate immune response and inflammation. TLRs are membrane-bound receptors, predominantly sensing microbe- or host-derived insults in the extracellular or endosomal compartments, whereas NLRs are cytosolic receptors, sensing invading intracellular pathogens and intracellular perturbations associated with stress or damage (Kawai and Akira 2009; Takeuchi and Akira 2010). TLRs are composed of extracellular leucine-rich repeat motifs and a cytoplasmic Toll/interleukin-1 receptor (TIR) homology domain. Out of the 10 and 12 functional TLRs identified in humans and mice, respectively, several TLRs, TLR4 and TLR2 in particular, have been implicated in adipose inflammation in diet-induced obesity (Shi et al. 2006; Tsukumo et al. 2007; Himes and Smith 2009; Ehses et al. 2010; Davis et al. 2011). NLRs are composed of a central nucleotide-binding domain, an N-terminal protein interaction domain, and a C-terminal leucine-rich repeat domain (Chen et al. 2009). NOD1 and NOD2 are two prominent members of NLRs. Activation of NOD1 has been shown to induce inflammation in white adipocytes (Zhao et al. 2011) and adipose inflammation and insulin resistance in mice (Schertzer et al. 2011). Activation of PRR

triggers proinflammatory signaling pathways, including NF-κB activation, leading to innate immune response in immune as well as non-immune cells.

Brown adipose tissue (BAT) has gained increasing attention due to recent findings of brown fat depots in the cervical, supraclavicular, and paraspinal regions of adult humans (Cypess et al. 2009; Saito et al. 2009; van Marken Lichtenbelt et al. 2009; Virtanen et al. 2009; Zingaretti et al. 2009). In contrast to energy-storing role for white adipocytes, brown adipocytes are responsible for energy expenditure through non-shivering thermogenesis. The thermogenic property of brown adipocytes is conferred mainly by the function of uncoupling protein 1 (UCP-1), uniquely expressed in the inner membrane of the enriched mitochondria to uncouple ATP synthesis from respiration, leading to heat production (Nicholls and Locke 1984; Ricquier 2005). Therefore, BAT has become a novel target for obesity treatment and prevention. Understanding of the regulation of BAT development by both positive and negative regulators hold great promise to lead to novel strategies to increase BAT mass and function to combat obesity (Vijgen and van Marken Lichtenbelt 2013; Vosselman et al. 2013).

We have reported that TLR4, TLR2, and NOD1 are expressed and functional in BAT of mice and/or brown adipocytes (Bae et al. 2014). Acute activation of the PRR (< 24hr) in mature brown adipocytes induces proinflammatory response, leading to suppression of UCP-1 expression and mitochondrial respiration. However, the effects of chronic activation of PRR on in vitro brown adipogenesis have not been studied. Here we report that the effects of chronic PRR activation on brown adipocyte differentiation using two well-studied cellular models of brown adipogenesis: multipotent mesodermal

stem C3H10T1/2 cells and brown pre-adipocytes derived from immortalized stromal cells from interscapular BAT of mice.

3.3 Materials and methods

Reagents

Recombinant human bone morphogenic protein 4 (BMP4) was purchased from R&D Systems (Minneapolis, MN). NOD1 synthetic ligand lauroyl-γ-D-Glu-meso-diaminopimelic acid (C12-iEDAP) and TLR2 ligand a synthetic triacylated lipoprotein Pam3CSK4 were purchased from Invivogen (San Diego, CA). Ultra pure TLR4 ligand lipopolysaccharide (LPS) was purchased from List Biological Laboratories (Campbell, CA). Fetal bovine serum (FBS) was purchased from Atlas Biologicals (Fort Collins, CO). Dulbecco's modified Eagle's medium (DMEM), 3-isobutyl-L-methylxanthine, T3, dexamethasone, insulin, indomethacin, and anti-UCP-1 antibody were purchased from Sigma-Aldrich (St. Louis, MO). Antibodies anti-ERK1/2 (#4695) and anti-PPARγ (#2443) were purchased from Cell signaling Technology (Danvers, MA). Anti-PGC-1 antibody (AB3242) was purchased from Millipore (Temecula, CA). Pharmacological inhibitor of NF-κB caffeic acid phenethyl ester (CAPE) was purchased from Tocris Bioscience (Ellisville, MI).

Cell culture and brown differentiation

Mouse multipotent mesodermal stem C3H10T1/2 cells were purchased from American Type Culture Collection (ATCC, Manassas, VA). Immortalized brown preadipocyte cell line, derived from the interscapular brown fat of 6-7 weeks old of C57BL mice, is a generous gift from Dr. Johannes Klein (University of Lubeck, Germany) (Klein et al. 2002). C3H10T1/2 cells were maintained in DMEM supplemented with 10% FBS (Atlas biological, Fort Collins, CO) and brown

preadipocytes were maintained in DMEM supplemented with 20% FBS. Both were grown at 37°C humidified atmosphere of 5% CO_2 in air.

The differentiation of brown-like adipocytes from C3H10T1/2 cells was essentially as described (Xue et al. 2014). C3H10T1/2 cells were plated into 20% confluence (day -5 or D-5). On the second day, the cells were treated with BMP4 (20 ng/mL) for 5 days until they reach confluency (day 0 or D0). On D0, the cells were changed into DMEM supplemented with 20% FBS, 1 nM/L T3, 20 nM/L insulin, 0.125 mM/L indomethacin, 5 μM/L dexamethasone, and 0.5 mM/L 3-isobutyl-L-methylxanthine for 24 h, followed by DMEM supplemented with 20% FBS, 1 nM/L T3, and 20 nM/L insulin, replenished every two days until the cells were fully differentiated at day 6 (D6). The differentiation of brown pre-adipocytes was as previously described (Bae et al. 2014). The cells were plated and grown in DMEM supplemented with 20% FBS until confluency (designed as D0). The cells were then changed into DMEM supplemented with 20% FBS, 1 nM/L T3, 20 nM/L insulin, 0.125 mM/L indomethacin, 5 μM/L dexamethasone, and 0.5 mM/L 3-isobutyl-L-methylxanthine for 24 h, followed by DMEM supplemented with 20% FBS, 1 nM/L T3, and 20 nM/L insulin, replenished every two days until the cells were fully differentiated at day 6 (D6).

The synthetic PRR ligand C12-iEDAP, LPS, Pam3CSK or the vehicle control was added to the media as indicated in the figures and figure legends. The ligands were replaced with each change of the media during the process, as indicated.

Western blot analysis

Total cell lysates were prepared and protein concentrations were determined by BCA assay kit (Thermo Scientific, Waltham, MA). Thirty micrograms of total cell lysates

were subjected to 10% SDS-PAGE and transferred to polyvinylidene difluoride membrane (Bio-Rad, Hercules, CA). The membrane was incubated with 5% nonfat milk blocking solution containing 20 mM/L Tris-HCl, 137 mM/L NaCl, and 0.1% Tween 20 (pH 7.4). The membrane was immunoblotted with primary antibodies at 4°C for overnight followed by secondary antibody conjugated with horseradish peroxidase (GE Healthcare). The signals were developed by enhanced chemiluminescence method (Thermo Scientific, Rockford, IL).

RNA preparation and quantitative real-time PCR analysis

Total RNA was prepared using TRI reagent (Molecular Research Center, Cincinnati, OH). Total RNA abundance was quantified using a NanoDrop ND-1000 Spectrophotometer (NanoDrop Technologies, Wilmington, DE). Reverse transcription was carried out using Fermentas first strand synthesis kit (Thermo Scientific, Pittsburgh, PA) according to the manufacturer's instruction. mRNA expression of indicated genes and loading control 36B4 (an uncharacterized large riobosomal protein) gene were measured quantitatively using gene-specific primers, and PCR was run in a 96-well plate using an ABI 7300HT instrument. Cycle conditions were 50 ^{0}C 2min, 95 ^{0}C 15 min, then 40 cycles of 95 ^{0}C for 15 s/60 ^{0}C for 1 min. Relative gene expression was calculated using the $2^{-\Delta\Delta Ct}$ method, which was normalized by loading control 36B4.

Reporter gene assays

Brown pre-adipocytes and C3H10T1/2 cells were transfected with PPARγ transactivation reporters, which contain a fusion of murine PPARγ ligand binding domain coupled to the Gal4 DNA binding domain (mPPARγ-Gal4), a reporter containing an upstream activating sequence (UAS)-linked luciferase (4xUAS-thymidine kinase-luc),

and β-galactosidase (β-gal) expression plasmid. PPARγ transactivation reporters were a gift from Dr. Susanne Mandrup at University of Southern Denmark, Denmark. The cells were then pre-treated with C12-iEDAP, LPS, Pam3CSK or the vehicle control for 2 h and then co-treated with or without PPARγ ligand rosiglitazone (Rosi, 0.5 μM/L) for 15 h. In some cases, the cells were pre-treated with NF-κB inhibitor CAPE or the vehicle DMSO for 2 h before the PRR ligand was added, or the cells were infected with adenovirus that encodes IκBα super-repressor (SR) or the control virus encodes β-gal for 24 h before being transfected with PPARγ transactivation reporters. For NF-κB activation experiments, C3H10T1/2 cells were infected with adenovirus encoding NF-κB-Luc reporter gene for 24 h. The cells were then stimulated with C12-iEDAP, LPS, Pam3CSK4, or the vehicle control for 15 h. The cell lysate was prepared and reporter luciferase and β-gal activities were measured with GloMax Luminometer (Promega, Madison, WI).

Oil red O staining and quantification

Differentiated brown adipocytes and C3H10T1/2 cells were fixed with 4% formaldehyde solution overnight, and lipid accumulation were stained with oil red O (ORO) and quantified by absorbance at 500 nm in a spectrophotometer.

Statistical analysis

All data were presented as means ± SE. Measurements were performed in triplicates. Data were Log transformed when appropriate. Statistical analysis was performed using SigmaPlot 12.0 (Systat Software, Inc.). One way ANOVA with repeated measures followed by multiple comparisons test (Student-Newman-Keuls Method) were performed to determine the differences between the treatment groups and/or time

points. Student's t-test was performed when appropriate. The level of significance was set at $P < 0.05$.

3.4 Results

mRNA expression and functionality of PRR during commitment and differentiation of brown-like adipocyte of multipotent mesodermal stem C3H10T1/2 cells

We examined mRNA expression of selected PRRs, NOD1, NOD2, TLR4 and TLR2 in C3H10T1/2 cells after plating (D-5), commitment (D0), and differentiation (D6) to brown-like adipocytes, as shown in Figure 9A. mRNA of all examined PRR was significantly up-regulated during commitment and then down-regulated during the differentiation phase (Figure 9A), leading to a higher mRNA expression for NOD1 and TLR4 ($p<0.05$) and no changes of mRNA expression for NOD2 and TLR2 in brown-like adipocytes (Figure 9A). Comparisons among the PRRs show that TLR4 mRNA expression was the highest, followed by NOD1 and TLR2, and NOD2 mRNA expression was the lowest after the cells were plated at D-5 (Figure 9B). Similar patterns were maintained through commitment (D0) and differentiation (D6) (Figure 9B).

We examined the functionality of the selected PRRs by NF-κB activation assays. Except for NOD2 ligand MDP (data not shown), the synthetic ligand of NOD1 (C12-iEDAP), TLR4 (LPS), and TLR2 (Pam3CSK4) induced robust NF-κB activation in C3H10T1/2 cells ($p<0.001$) (Figure 9C). Taken together, these results indicate that selected PRRs are expressed and functional in C3H10T1/2 cells.

Chronic activation of NOD1, TLR4, or TLR2 suppresses brown-like adipocyte differentiation of C3H10T1/2 cells

We next examined the effects of chronic activation of NOD1, TLR4, or TLR2 on brown-like adipocyte differentiation of C3H10T1/2 cells in the presence or absence of their respective synthetic ligand, as shown in Figure 10A. More than 95% of C3H10T1/2 cells were differentiated into brown-like adipocytes at D6 after being committed by BMP4 and differentiated as previously reported (Xue et al. 2014). The presence of the synthetic ligand of NOD1, TLR4, or TLR2 during both the commitment and differentiation phases significantly suppressed the differentiation of brown-like adipocytes, as revealed by the paucity of oil red O stained multilocular, lipid-filled brown adipocytes (Figure 10B), decreased lipid accumulation (Figure 10C), and almost completely abolished protein expression of established brown adipocyte marker PPARγ, PGC-1α, and UCP-1, compared with the controls (Figure 10D).

Analysis of mRNA further revealed that mRNA expression of PPARγ, PGC-1α, and UCP-1 was consistent with the protein expression (Figure 11A). mRNA expression of PR domain containing 16 (PRDM16), a zinc-finger binding protein recently identified as an early regulator for brown cell fate (Seale et al. 2007), was also significantly suppressed ($p<0.01$) (Figure 11A). In addition, of the two transcription factors regulating mitochondrial gene expression, mRNA expression of nuclear respiratory factor 1 (Nrf-1) ($p<0.05$ for NOD1 and TLR2, $p<0.01$ for TLR4), but not transcription factor A (Tfam), was down-regulated by the PRR activation (Figure 11B). Consequently, mRNA expression of the two nucleus-encoded mitochondrial genes, cytochrome b-c1 complex subunit 6 (Uqcrh) ($p<0.05$) and cytochrome c oxidase subunit IV a (Cox4a) ($p<0.01$)

were also down-regulated by the PRR activation (Figure 11B). Taken together, these results suggest that PRR activation suppresses brown-like differentiation, including mitochondrial biogenesis, of C3H10T1/2 cells.

Differential regulation of the novel brown and white adipocyte-specific markers by chronic PRR activation in C3H10T1/2 cells

The transcriptome analysis (Timmons et al. 2007) and a global transcription factor screen (Seale et al. 2007) have identified differences in the transcription factor profiles between brown and white adipocytes. To examine whether PRR activation could modulate brown versus white adipocyte fate, we examined the mRNA expression of novel brown transcription factor zinc finger protein of the cerebellum 1 (Zic1), LIM homeobox protein 8 (Lhx8), and mesenchyme homeobox 2 (Meox2), and white specific marker insulin-like growth factor-binding protein 3 (IGFBP3) and homeo box C9 (Hoxc9) at D6 in C3H10T1/2 cells. Activation of TLR4, but not NOD1 or TLR2, significantly suppressed novel brown marker Zic1 mRNA expression ($p<0.05$) (Figure 11C). In contrast, NOD1 activation significantly up-regulated mRNA expression of Lhx8 and Meox-2 ($p<0.01$), which were not affected by the activation of TLR4 or TLR2 (Figure 11C). Moreover, activation of NOD1 and TLR4, but not TLR2, significantly up-regulated mRNA expression of white specific IGFBP3 ($p<0.05$), whereas activation of NOD1, TLR4, or TLR2 did not alter Hoxc9 mRNA expression at D6 in C3H10T1/2 cells (Figure 11D).

PRR activation only during the commitment phase is sufficient to lead to suppression of differentiation of brown-like adipocytes of C3H10T1/2 cells

The commitment of multipotent stem cells into either white or brown adipocytes has been a focus of recent studies. The commitment of C3H10T1/2 cells into brown-like adipocytes is positively regulated by bone morphogenic proteins (BMPs) (Tseng et al. 2008; Xue et al. 2014). We examined whether activation of NOD1, TLR4, or TLR2 only during the commitment is sufficient enough to lead to suppression of differentiation of brown-like adipocytes of C3H10T1/2. C3H10T1/2 cells were committed towards brown-like adipocytes with BMP4 in the presence or absence of the PRR synthetic ligand until the cells reach confluency, followed by the induction to differentiation, as shown in Figure 12A. Activation of NOD1, TLR4, or TLR2 only during the commitment was sufficient to suppress differentiation of brown-like adipocytes of C3H10T1/2 cells, although to a lesser degree, as revealed by paucity of the oil red O stained multilocular, lipid-filled brown-like adipocytes (Figure 12B), decreased lipid accumulation (Figure 12C), and attenuated protein expression of PPARγ, PGC-1α, and UCP-1 at D6, compared with the controls (Figure 12D).

Analysis of mRNA of established brown marker PPARγ, PGC-1α, and UCP-1 was consistent with the protein expression (Figure 13A). Notably, PRDM16 mRNA was not suppressed at D6 when PRR activation only occurred during the commitment (Figure 13A). Activation of NOD1, TLR4, or TLR2 during commitment suppressed mRNA expression of Uqcrh ($p<0.01$) and Cox4a ($p<0.05$), whereas mRNA expression of Tfam and Nrf-1 was not suppressed at D6 (Figure 13B). Moreover, only Zic-1 mRNA expression was suppressed by TLR4 activation ($p<0.05$), and mRNA expression of

Lhx8 or Meox-2 was not altered at D6 (Figure 13C). Further, activation of NOD1 or TLR4, but not TLR2, during commitment induced IGFBP3 mRNA, whereas none of the activation altered Hoxc9 mRNA at D6 in C3H10T1/2 cells (Figure 13D).

Activation of PRR suppresses the commitment to brown-like adipocytes of C3H10T1/2 cells

To gain insights into the effects of PRR activation on commitment, we further examined the changes in mRNA expression by PRR activation at the commitment. C3H10T1/2 cells were committed towards brown-like adipocytes with BMP4 in the presence or absence of the PRR synthetic ligand until the cells reach confluency (D0), as shown in Figure 14A. Activation of NOD1, TLR4, or TLR2 significantly suppressed mRNA expression of PGC-1α ($p<0.01$), but not PPARγ at the commitment (Figure 14B). Surprisingly, activation of NOD1 and TLR4, but not TLR2, significantly induced up-regulation of PRDM16 ($p<0.05$) (Figure 14B). No significant change was noted for Tfam, Nrf-1, Uqcrh, and Cox4a at the commitment (data not shown). Moreover, activation of NOD1, TLR4, or TLR2 significantly suppressed mRNA expression of Zic1, Lhx8, and Meox-2 and white specific marker Hoxc9 (Figure 14C). In contrast, no changes of IGFBP3 mRNA were noted by the activation of NOD1 and TLR4, but it was induced by TLR2 activation ($p<0.05$) (Figure 14D).

Chronic activation of NOD1, TLR4, or TLR2 suppresses terminal differentiation of immortalized brown pre-adipocytes derived from BAT of mice

To validate the effects of chronic PRR activation on multipotent stem cells, we further examined the effects of PRR activation on terminal brown differentiation from immortalized brown pre-adipocytes derived from classical BAT of C57BL6 mice. We

have previously shown that NOD1, TLR4, and TLR2 were expressed and functional in these cells (Bae et al. 2014). Brown pre-adipocytes were differentiated in the presence or absence of the synthetic ligand during the differentiation, as shown in Figure 15A. Activation of NOD1, TLR4, or TLR2 suppressed brown adipocyte differentiation compared to the control, as revealed by the paucity of oil red O stained multilocular, lipid-filled brown adipocytes (Figure 15B), reduced lipid accumulation (Figure 15C), and attenuated protein expression of brown-specific marker PPARγ, PGC-1α, and UCP-1 (Figure 15D) at D6. Analysis of mRNA showed that activation of NOD1, TLR4, or TLR2 also suppressed mRNA expression of PPARγ, PGC-1α, PRDM16, and UCP-1 ($p<0.01$) (Figure 15E). Moreover, mRNA expression of nucleus-encoded mitochondrial gene Uqcrh and Cox4a was suppressed by the examined PRR ($p<0.01$); however, only TLR4 activation significantly suppressed mRNA expression of Tfam and Nrf-1 at D6 ($p<0.01$) (Figure 15F).

Activation of PRR suppresses PPARγ transactivation through NF-κB pathway

To explore molecular mechanisms by which activation of NOD1, TLR4, or TLR2 suppressed brown adipocyte differentiation, we examined whether activation of NOD1, TLR4, or TLR2 affects PPARγ transactivation, the key event for brown adipocyte differentiation, using PPARγ transactivation reporters. Activation of NOD1, TLR4, or TLR2 suppressed PPARγ ligand rosiglitazone (Rosi)-induced PPARγ transactivation in C3H10T1/2 cells, which was reversed by the specific NF-κB inhibitor CAPE (Figure 16A), and IκB super-repressor (IκB(SR)) (Figure 16B), which contains two amino acid substitutions (S32A/S36A) that prevent phosphorylation and degradation of the protein and blocks the activation of NF-κB in response to proinflammatory stimulations (Jobin et

al. 1998). Similarly, activation of NOD1, TLR4, or TLR2 also suppressed Rosi-induced PPARγ transactivation in brown pre-adipocytes, which was reversed by NF-κB inhibitor CAPE (Figure 16D) and IκB(SR) (Figure 16E). Consistently, suppression of brown-like adipocyte differentiation of C3H10T1/2 cells by PRR activation during the commitment was reversed by NF-κB inhibitor CAPE, compared to the vehicle control, as revealed by attenuation of the suppression of lipid accumulation (Figure 16C).

3.5 Discussion

PRR-mediated inflammation has been implicated in adipose inflammation and obesity. In current studies, we demonstrate, for the first time, that chronic activation of selected PRR leads to suppression of brown adipogenesis of multipotent stem cells and committed brown pre-adipocytes, suggesting that PRR activation negatively impacts BAT development. Our results have revealed a new role of PRR-mediated inflammation in the development of obesity.

The C3H10T1/2 line is the best characterized mesodermal multipotent stem cell line that faithfully mimic multipotent stem cells in vivo and can be induced to undergo commitment and differentiation to the muscle, bone, cartilage, and adipose lineage (Taylor and Jones 1979; Konieczny and Emerson 1984; Gregoire et al. 1998; Shin et al. 2000; Mikami et al. 2011; Tang and Lane 2012). The genetic mapping studies have revealed that brown adipocytes and muscle, but not white adipocytes, were derived from Myf-5 expressing precursor cells (Seale et al. 2008). The transcription factor PRDM16 was shown to act as a switch to drive differentiation of the Myf-5 expressing stem cells into brown adipocytes. Knockdown of PRDM16 in the precursor cells resulted in loss of brown fat characteristics, leading to muscle cell phenotype, while over-expression of PRDM16 in white pre-adipocytes or myoblasts resulted in brown adipocyte phenotype (Seale et al. 2008).

It has been reported that BMPs, members of transforming growth factor-β (TGFβ) superfamily, play critical roles in the commitment and differentiation of brown-like adipocytes from C3H10T1/2 cells. It has been demonstrated that pre-treatment of BMP4 at 20 ng/ml during proliferation produced clonal lines that were capable of differentiating

into brown-like adipocytes when subjected to brown differentiation inducers without exogenous BMP4 and into brown-like fat when implanted into athymic nude mice (Xue et al. 2014). BMP4 pre-treatment was shown to induce up-regulation of PRDM16, leading to the commitment of C3H10T1/2 cells into brown preadipocytes (Xue et al. 2014).

Effects of PRR activation on commitment and differentiation

We have used C3H10T1/2 line to gain insights into the effects of chronic PRR activation on commitment and differentiation of brown-like adipocytes from mesodermal stem cells. Our results demonstrate that chronic activation of selected PRR during both the commitment and differentiation suppressed the brown-like adipogenesis of C3H10T1/2 cells, as revealed by paucity of oil red O stained, multilocular brown adipocyte morphology and suppressed gene expression of brown specific markers, and lipid accumulation. It should be noted that, although to a lesser degree, compared to that of PRR activation in both the commitment and differentiation phase, PRR activation only during the commitment phase was sufficient enough to suppress brown-like differentiation of C3H10T1/2 cells. Gene expression analysis revealed that PRR activation during commitment suppressed mRNA expression of PGC-1α, but not PPARγ or PRDM16, at the commitment. In fact, there was no change of PPARγ mRNA, whereas PRDM16 mRNA was significantly up-regulated by activation of NOD1 and TLR4, but not TLR2. PPARγ, PGC-1α, and PRDM16 are considered to be the core regulators for brown differentiation (Richard and Picard 2011; Satterfield and Wu 2011; Harms and Seale 2013). Studies have shown that PRDM16 acts primarily through binding to and modulating the activities of other transcription factors, including

CCAAT/enhancer binding protein beta (C/EBPβ) (Kajimura et al. 2008), PPARγ (Seale et al. 2008), and PGC-1α (Seale et al. 2007). PPARγ is the transcription factor that not only regulates white adipocyte differentiation, but also brown adipocyte differentiation (Rosen et al. 1999; Imai et al. 2004). PGC-1α is a co-activator for PPARγ. Activation of PPARγ and PGC-1α subsequently up-regulate a number of genes involved in brown adipocyte differentiation and function, including UCP-1 (Richard and Picard 2011; Harms and Seale 2013). In addition, PGC-1α has been shown to control mitochondrial biogenesis through induction of uncoupling proteins and regulation of nuclear respiratory factors (Wu et al. 1999). Our results demonstrate that PRR activation during the commitment leads to suppression of brown-like differentiation, characterized by suppressed mRNA expression of established brown marker PPARγ, PGC-1α, and UCP-1, but not PRDM16, possibly through modulation of early events in the commitment, such as more upstream transcription factors, and epigenetic changes, which directly or indirectly suppressed the core regulators, leading to the suppression of brown-like differentiation. Further PRR activation during the differentiation leads to more robust suppression of differentiation, characterized by suppression of almost all brown specific markers, including PRDM16.

Effects of PRR activation on novel brown and white specific markers: To whiten it or not?

To our knowledge, this is the first report of PRR activation on novel brown versus white specific markers in brown-like differentiation of C3H10T1/2 cells. Identification of novel brown and white specific markers has provided molecular insights into the characterization of brown, white, and beige adipocytes. It has been reported that

chronic treatment with the PPARγ agonist rosiglitazone induced browning of epididymally derived white adipocyte cultures with norepinephrine-inducible UCP-1 gene expression and thermogenic capacity. These cells were characterized with low mRNA expression of Zic-1, Lhx8, and Meox2, novel transcription factors now associated with classic brown adipocytes (Timmons et al. 2007), decreased white adipocyte specific IGFBP3, but retained white specific Hoxc9 expression (Petrovic et al. 2008). We show that selected PRR activation during both commitment and differentiation differentially modulated novel brown specific markers. TLR4 activation suppressed Zic1 mRNA, which was not affected by the activation of NOD1 or TLR2, whereas NOD1 activation significantly induced mRNA of Lhx8 and Meox2, which were not affected by activation of TLR4 or TLR2. In contrast, activation of NOD1 and TLR4, but not TLR2, significantly induced white specific IGFBP3 mRNA and no significant changes in Hoxc9 were observed. Only the suppression of Zic1 by TLR4 activation and induction of IGFBP3 by NOD1 and TLR4 remained when the PRR activation only occurred in the commitment phase. Together, our results suggest that activation of PRR differentially modulate brown versus white marker gene expression in the stem cell differentiation. It remains to be determined whether activation of certain PRR, TLR4 in particular, induces “whitening” in brown-like adipocytes differentiated from C3H10T1/2. Further characterization of the role of each of these novel brown and white specific marker genes in controlling brown versus white cell fate will provide new insights into the impact of PRR activation on these processes.

Mechanisms of chronic PRR activation on brown differentiation

It has been shown that activation of NOD1 (Purohit et al. 2012) or TLR4 (Song et al. 2006) suppressed 3T3-L1 white adipocyte differentiation. Activation of NOD1 induced NF-κB activation in 3T3-L1 cells, which correlated with the suppression of ligand-induced PPARγ activation (Purohit et al. 2012). It has been demonstrated that NOD1, TLR4, and TLR2 are expressed and functional in brown adipocytes (Bae et al. 2014). Here, we show that these PRRs are expressed and functional in C3H10T1/2 cells. Moreover, we show that activation of NOD1, TLR4, or TLR2 suppressed PPARγ transactivation, which was reversed by the pharmacological inhibitor of NF-κB (CAPE) and IκBα super-repressor (IκB (SR)) in both cell types. Further, we show NF-κB inhibition by CAPE attenuated suppression of brown-like differentiation by PRR activation, indicated by the oil red O stained lipid accumulation. Together, the results suggest that suppression of brown adipogenesis by PRR activation is at least in part mediated through suppression of PPARγ transactivation by NF-κB pathway.

In conclusion, we have demonstrated the suppressive effects of chronic activation of selected PRR on brown adipogenesis of multipotent mesodermal stem C3H10T1/2 cells and immortalized brown preadipocytes. Our results suggest that suppression of brown differentiation could, at least in part, be mediated by suppression of PPARγ transactivation via NF-κB pathway, and anti-inflammatory therapies targeting PRRs could be beneficial for BAT development.

3.6 References

Bae, J., Ricciardi, C. J., Esposito, D., Komarnytsky, S., Hu, P., Curry, B. J., Brown, P. L., Gao, Z., Biggerstaff, J. P., Chen, J. and Zhao, L. 2014. Activation of pattern recognition receptors in brown adipocytes induces inflammation and suppresses uncoupling protein 1 expression and mitochondrial respiration. Am. J. Physiol. Cell. Physiol. 306(10): C918-930.

Chen, G., Shaw, M. H., Kim, Y. G. and Nunez, G. 2009. NOD-like receptors: role in innate immunity and inflammatory disease. Annu. Rev. Pathol. 4: 365-398.

Cypess, A. M., Lehman, S., Williams, G., Tal, I., Rodman, D., Goldfine, A. B., Kuo, F. C., Palmer, E. L., Tseng, Y. H., Doria, A., Kolodny, G. M. and Kahn, C. R. 2009. Identification and importance of brown adipose tissue in adult humans. New Engl. J. Med. 360(15): 1509-1517.

Davis, J. E., Braucher, D. R., Walker-Daniels, J. and Spurlock, M. E. 2011. Absence of Tlr2 protects against high-fat diet-induced inflammation and results in greater insulin-stimulated glucose transport in cultured adipocytes. J. Nutr. Biochem. 22(2): 136-141.

Ehses, J. A., Meier, D. T., Wueest, S., Rytka, J., Boller, S., Wielinga, P. Y., Schraenen, A., Lemaire, K., Debray, S., Van Lommel, L., Pospisilik, J. A., Tschopp, O., Schultze, S. M., Malipiero, U., Esterbauer, H., Ellingsgaard H., Rutti, S., Schuit, F. C., Lutz, T. A., Boni-Schnetzler, M., Konrad, D. and Donath, M. Y. 2010. Toll-like receptor 2-deficient mice are protected from insulin resistance and beta cell dysfunction induced by a high-fat diet. Diabetologia, 53(8): 1795-1806.

Gregoire, F. M., Smas, C. M. and Sul, H. S. 1998. Understanding adipocyte differentiation. Physiol. Rev. 78(3): 783-809.

Harms, M. and Seale, P. 2013. Brown and beige fat: development, function and therapeutic potential. Nature Med. 19(10): 1252-1263.

Himes, R. W. and Smith, C. W. 2009. Tlr2 is critical for diet-induced metabolic syndrome in a murine model. FASEB J. 24(3): 731-739.

Imai, T., Takakuwa, R., Marchand, S., Dentz, E., Bornert, J. M., Messaddeq, N., Wendling, O., Mark, M., Desvergne, B., Wahli, W., Chambon, P. and Metzger, D. 2004. Peroxisome proliferator-activated receptor gamma is required in mature white and brown adipocytes for their survival in the mouse. Proc. Natl. Acad. Sci. U. S. A. 101(13): 4543-4547.

Jin, C., Henao-Mejia, J. and Flavell, R. A. 2013. Innate immune receptors: key regulators of metabolic disease progression. Cell Metb. 17(6): 873-882.

Jobin, C., Panja, A., Hellerbrand, C., Iimuro, Y., Didonato, J., Brenner, D. A. and Sartor, R. B. 1998. Inhibition of proinflammatory molecule production by adenovirus-mediated expression of a nuclear factor kappaB super-repressor in human intestinal epithelial cells. J. Immunol. 160(1): 410-418.

Kajimura, S., Seale, P., Tomaru, T., Erdjument-Bromage, H., Cooper, M. P., Ruas, J. L., Chin, S., Tempst, P., Lazar, M. A. and Spiegelman, B. M. 2008. Regulation of the brown and white fat gene programs through a PRDM16/CtBP transcriptional complex. Genes Dev. 22(10): 1397-1409.

Kawai, T. and Akira, S. 2009. The roles of TLRs, RLRs and NLRs in pathogen recognition. Int. Immunol. 21(4): 317-337.

Klein, J., Fasshauer, M., Klein, H. H., Benito, M. and Kahn, C. R. 2002. Novel adipocyte lines from brown fat: a model system for the study of differentiation, energy metabolism, and insulin action. Bioessays, 24(4): 382-388.

Konieczny, S. F. and Emerson, Jr. C. P.. 1984. 5-Azacytidine induction of stable mesodermal stem cell lineages from 10T1/2 cells: evidence for regulatory genes controlling determination. Cell, 38(3): 791-800.

Mikami, Y., Ishii, Y., Watanabe, N., Shirakawa, T., Suzuki, S., Irie, S., Isokawa, K. and Honda, M. J. 2011. CD271/p75(NTR) inhibits the differentiation of mesenchymal stem cells into osteogenic, adipogenic, chondrogenic, and myogenic lineages. Stem Cells Dev. 20(5): 901-913.

Nicholls, D. G. and Locke, R. M. 1984. Thermogenic mechanisms in brown fat. Physiol. Rev. 64(1): 1-64.

Petrovic, N., Shabalina I. G., Timmons J. A., Cannon B.and Nedergaard J. 2008. Thermogenically competent nonadrenergic recruitment in brown preadipocytes by a PPARgamma agonist. Am. J. Physiol. Endocrinol. Metab. 295(2): E287-296.

Purohit, J., Hu, P., Burke, S. J., Collier, J. J., Chen, J. and Zhao, L. 2012. The Effects of NOD Activation on Adipocyte Differentiation. Obesity (Silver Spring), 21(4): 737-747.

Richard, D. and Picard, F. 2011. Brown fat biology and thermogenesis. Front. Biosci. 16: 1233-1260.

Ricquier, D. 2005. Respiration uncoupling and metabolism in the control of energy expenditure. Proc. Nutr. Soc. 64(1): 47-52.

Rosen, E. D., Sarraf, P., Troy, A. E., Bradwin, G., Moore, K., Milstone, D. S., Spiegelman, B. M. and Mortensen, R. M. 1999. PPAR gamma is required for the differentiation of adipose tissue in vivo and in vitro. Mol. Cell, 4(4): 611-617.

Saito, M., Okamatsu-Ogura, Y., Matsushita, M., Watanabe, K., Yoneshiro, T., Nio-Kobayashi, J., Iwanaga, T., Miyagawa, M., Kameya, T., Nakada, K., Kawai, Y. and Tsujisaki, M. 2009. High incidence of metabolically active brown adipose tissue in healthy adult humans: effects of cold exposure and adiposity. Diabetes, 58(7): 1526-1531.

Satterfield, M. C. and Wu, G. 2011. Brown adipose tissue growth and development: significance and nutritional regulation. Front. Biosci. 16: 1589-1608.

Schertzer, J. D., Tamrakar, A. K., Magalhaes, J. G., Pereira, S., Bilan, P. J., Fullerton, M. D., Liu, Z., Steinberg, G. R., Giacca, A., Philpott, D. J. and Klip, A. 2011. NOD1 Activators Link Innate Immunity to Insulin Resistance. Diabetes, 60(9): 2206-2215.

Seale, P., Bjork, B., Yang, W., Kajimura, S., Chin, S., Kuang, S., Scime, A., Devarakonda, S., Conroe, H. M., Erdjument-Bromage, H., Tempst, P., Rudnicki, M. A., Beier, D. R. and Spiegelman, B. M. 2008. PRDM16 controls a brown fat/skeletal muscle switch. Nature, 454(7207): 961-967.

Seale, P., Kajimura, S., Yang, W., Chin, S., Rohas, L. M., Uldry, M., Tavernier, G., Langin, D. and Spiegelman, B. M. 2007. Transcriptional control of brown fat determination by PRDM16. Cell Metab. 6(1): 38-54.

Shi, H., Kokoeva, M. V., Inouye, K., Tzameli, I., Yin, H. and Flier, J. S. 2006. TLR4 links innate immunity and fatty acid-induced insulin resistance. J. Clin. Invest. 116(11): 3015-3025.

Shin, C. S., Lecanda, F., Sheikh, S., Weitzmann, L., Cheng, S. L. and Civitelli, R. 2000. Relative abundance of different cadherins defines differentiation of mesenchymal precursors into osteogenic, myogenic, or adipogenic pathways. J. Cell Biochem. 78(4): 566-577.

Song, M. J., Kim, K. H., Yoon, J. M. and Kim, J. B. 2006. Activation of Toll-like receptor 4 is associated with insulin resistance in adipocytes. Biochem. Biophys. Res. Commun. 346(3): 739-745.

Takeuchi, O. and Akira, S. 2010. Pattern recognition receptors and inflammation. Cell, 140(6): 805-820.

Tang, Q. Q. and Lane, M. D. 2012. Adipogenesis: from stem cell to adipocyte. Annu. Rev. Biochem. 81: 715-736.

Taylor, S. M. and Jones, P. A. 1979. Multiple new phenotypes induced in 10T1/2 and 3T3 cells treated with 5-azacytidine. Cell, 17(4): 771-779.

Timmons, J. A., Wennmalm, K., Larsson, O., Walden, T. B., Lassmann, T., Petrovic, N., Hamilton, D. L., Gimeno, R. E., Wahlestedt, C., Baar, K., Nedergaard, J. and Cannon, B. 2007. Myogenic gene expression signature establishes that brown and white adipocytes originate from distinct cell lineages. Proc. Natl. Acad. Sci. U. S. A. 104(11): 4401-4406.

Tseng, Y. H., Kokkotou, E., Schulz, T. J., Huang, T. L., Winnay, J. N., Taniguchi, C. M., Tran, T. T., Suzuki, R., Espinoza, D. O., Yamamoto, Y., Ahrens, M. J., Dudley, A. T., Norris, A. W., Kulkarni, R. N. and Kahn, C. R. 2008. New role of bone morphogenetic protein 7 in brown adipogenesis and energy expenditure. Nature, 454(7207): 1000-1004.

Tsukumo, D. M., Carvalho-Filho, M. A., Carvalheira, J. B., Prada, P. O., Hirabara, S. M., Schenka, A. A., Araujo, E. P., Vassallo, J., Curi, R., Velloso, L. A. and Saad, M. J. 2007. Loss-of-function mutation in Toll-like receptor 4 prevents diet-induced obesity and insulin resistance. Diabetes, 56(8): 1986-1998.

van Marken Lichtenbelt, W. D., Vanhommerig, J. W., Smulders, N. M., Drossaerts, J. M., Kemerink, G. J., Bouvy, N. D., Schrauwen, P. and Teule, G. J. 2009. Cold-activated brown adipose tissue in healthy men. New Engl. J. Med. 360(15): 1500-1508.

Vijgen, G. H. and van Marken Lichtenbelt, W. D. 2013. Brown adipose tissue: clinical impact of a re-discovered thermogenic organ. Front. Biosci. E5: 823-833.

Virtanen, K. A., Lidell, M. E., Orava, J., Heglind, M., Westergren, R., Niemi, T., Taittonen, M., Laine, J., Savisto, N. J., Enerback, S. and Nuutila, P. 2009. Functional brown adipose tissue in healthy adults. New Engl. J. Med. 360(15): 1518-1525.

Vosselman, M. J., van Marken Lichtenbelt, W. D. and Schrauwen, P. 2013. Energy dissipation in brown adipose tissue: From mice to men. Mol. Cell Endocrinol. 379(1-2): 43-50

Wu, Z., Puigserver, P., Andersson, U., Zhang, C., Adelmant, G., Mootha, V., Troy, A., Cinti, S., Lowell, B., Scarpulla, R. C. and Spiegelman, B. M. 1999. Mechanisms controlling mitochondrial biogenesis and respiration through the thermogenic coactivator PGC-1. Cell, 98(1): 115-124.

Xue, R., Wan, Y., Zhang, S., Zhang, Q., Ye, H. and Li, Y. 2014. Role of bone morphogenetic protein 4 in the differentiation of brown fat-like adipocytes. Am. J. Physiol. Endocrinol. Metab. 306(4): E363-372.

Zhao, L., Hu, P., Zhou, Y., Purohit, J. and Hwang, D. 2011. NOD1 activation induces proinflammatory gene expression and insulin resistance in 3T3-L1 adipocytes. Am. J. Physiol. 301(4): E587-598.

Zingaretti, M. C., Crosta, F., Vitali, A., Guerrieri, M., Frontini, A., Cannon, B., Nedergaard, J. and Cinti, S. 2009. The presence of UCP1 demonstrates that metabolically active adipose tissue in the neck of adult humans truly represents brown adipose tissue. FASEB J. 23(9): 3113-3120.

3.7 Appendix

Figure 9 Selected PRRs are expressed and functional during commitment and differentiation of multipotent mesodermal stem C3H10T1/2 cells

C3H10T1/2 cells were committed with BMP4 for 5 days until confluency, and then were differentiated into brown-like adipocytes for another 6 days, as shown in the diagram. Total RNA were collected at after plating (D-5), commitment (D0), and differentiation (D6) according to the diagram. (A, B) mRNA expression of PRRs were evaluated by semi-quantitative RT-PCR (A), and relative mRNA expression of PRRs at D-5, D0, and D6 were compared (B). The relative mRNA expression was normalized to 36B4 and expressed as fold of NOD2 value or D-5 value (set as 1). (C) Functionality of the selected PRRs was measured by NF-κB reporter assays. Data are mean±SE (n=3). Different letters indicate significant differences between bars. **, significantly different from the controls with $p<0.01$.

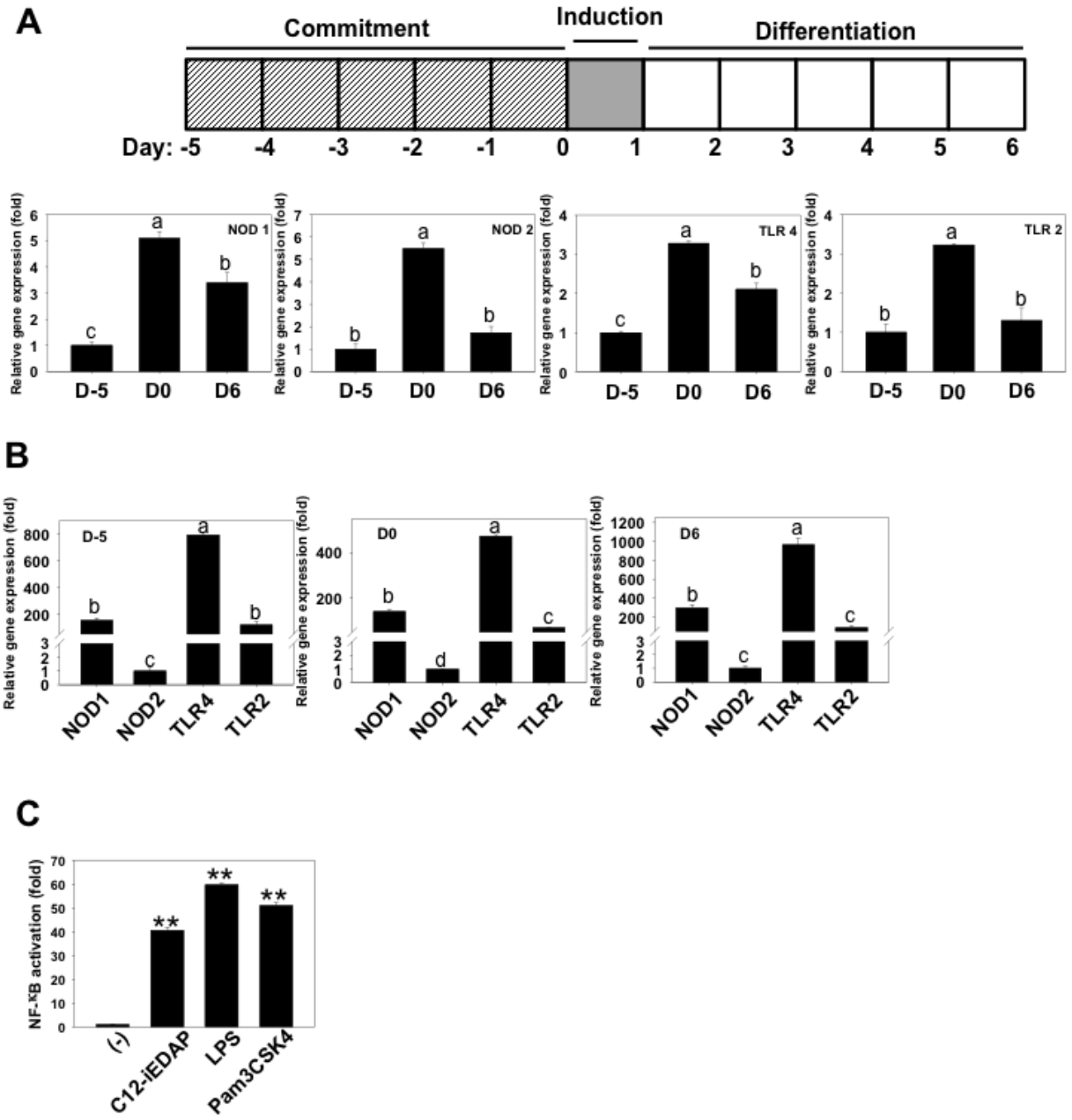
A
Commitment
Induction
Differentiation
Day: -5 -4 -3 -2 -1 0 1 2 3 4 5 6
Relative gene expression (fold)
NOD 1
NOD 2
TLR 4
TLR 2
D-5 D0 D6
B
D-5
D0
D6
NOD1 NOD2 TLR4 TLR2
C
NF-κB activation (fold)
(-)
C12-iEDAP
LPS
Pam3CSK4

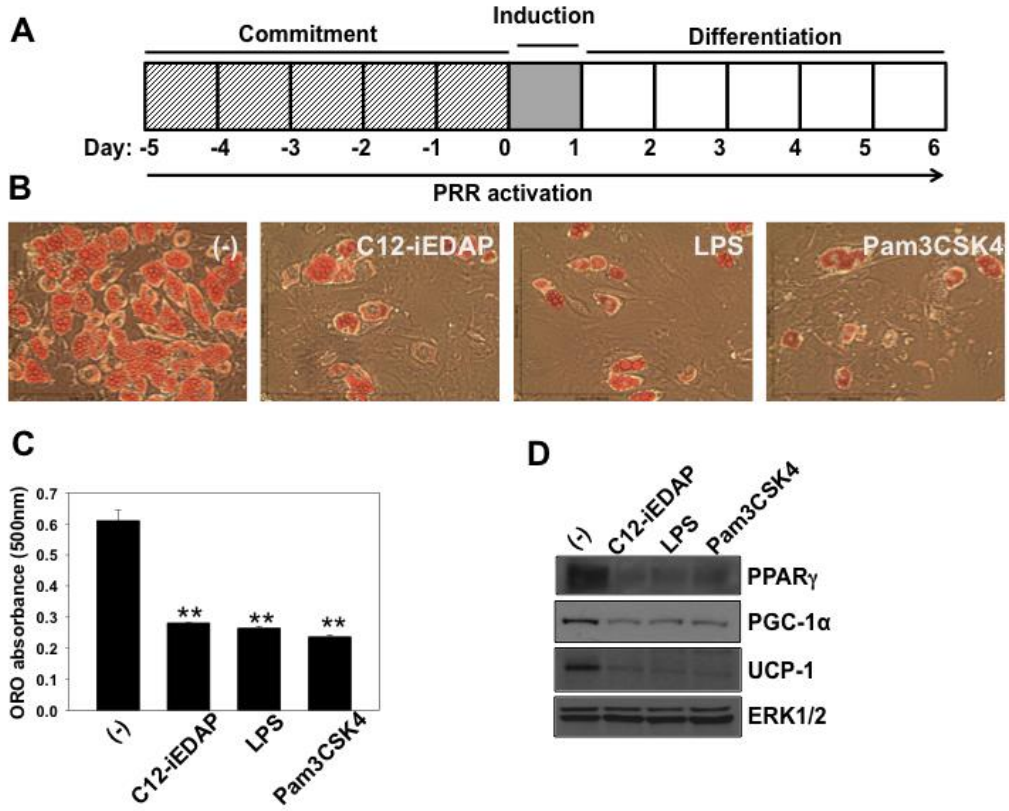

Figure 10 Chronic activation of NOD1, TLR4, or TLR2 suppresses brown-like adipocyte differentiation of C3H10T1/2 cells
C3H10T1/2 cells were committed and differentiated into brown-like adipocytes the presence of C12-iEDAP (10 µg/ml), LPS (1 µg/ml), Pam3CSK4 (10 µg/ml), or the vehicle control, as shown in (A). ORO stained cell morphology (B) and ORO absorbance (C) are shown. (D) Protein expression of established brown specific marker PPARγ, PGC-1α, and UCP-1 at D6 were analyzed by western blot. ERK1/2 is shown as a loading control. Data are mean±SE (*n*=3). **, significantly different from the controls with $p<0.01$.

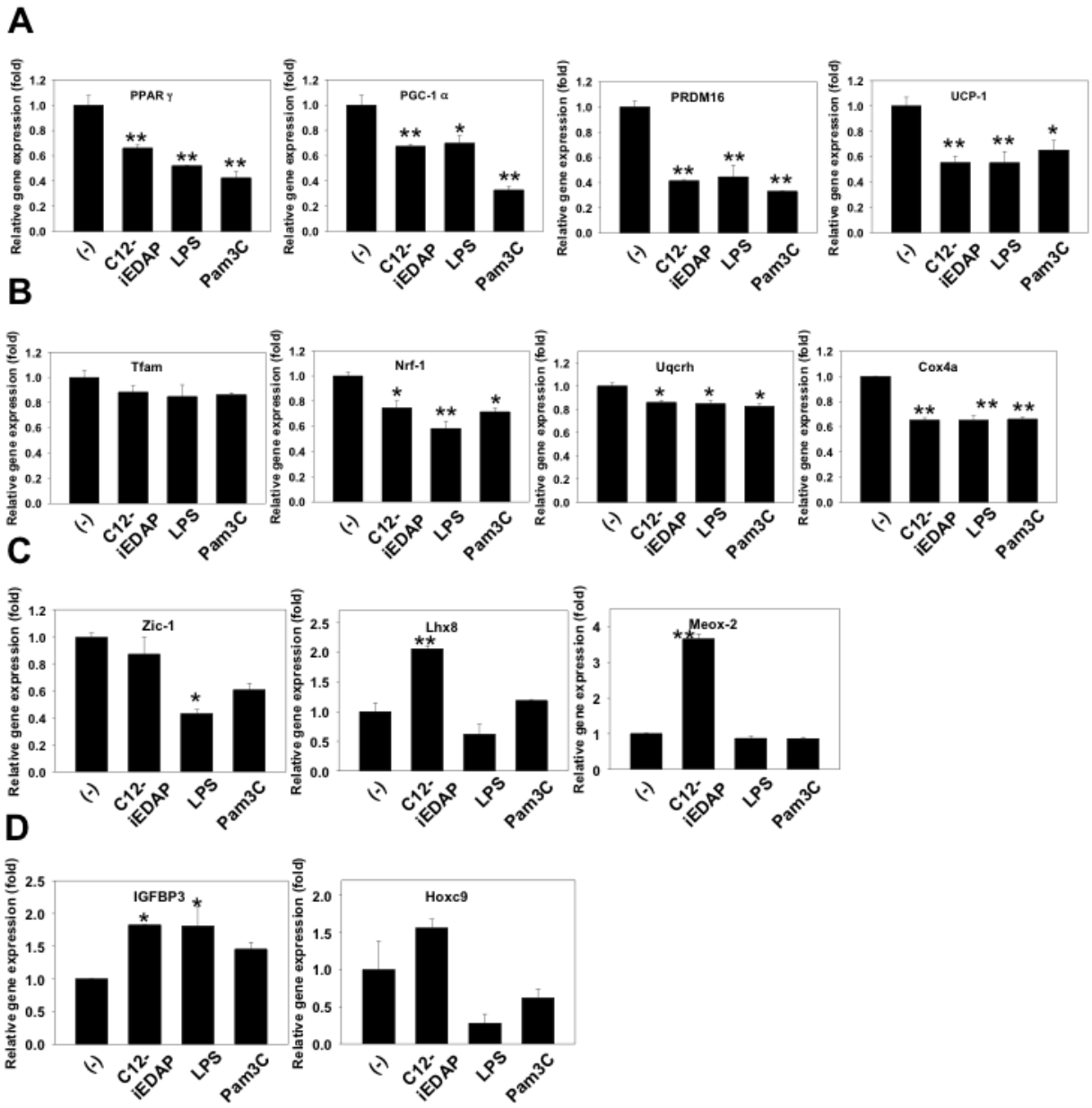

Figure 11 Molecular insights into the mechanisms by which chronic PRR activation suppresses brown-like differentiation of C3H10T1/2

C3H10T1/2 cells were committed and differentiated into brown-like adipocytes in the presence of C12-iEDAP (10 µg/ml), LPS (1 µg/ml), Pam3CSK4 (10 µg/ml), or the vehicle control. mRNA expression of established brown markers PPARγ, PGC-1α, PRDM16, and UCP-1 (A); mitochondrial transcription factors, Tfam and Nrf-1, and structural genes, Uqcrh and Cox4a (B); novel brown transcription factors, Zic-1, Lhx8, and Meox-2 (C); and white specific markers IGFBP3 and Hoxc9 (D) at D6 are shown. The relative gene expression was normalized to 36B4 gene. Data are mean±SE (n=3). *, **, significantly different from the controls with $p<0.05$ and $p<0.01$, respectively.

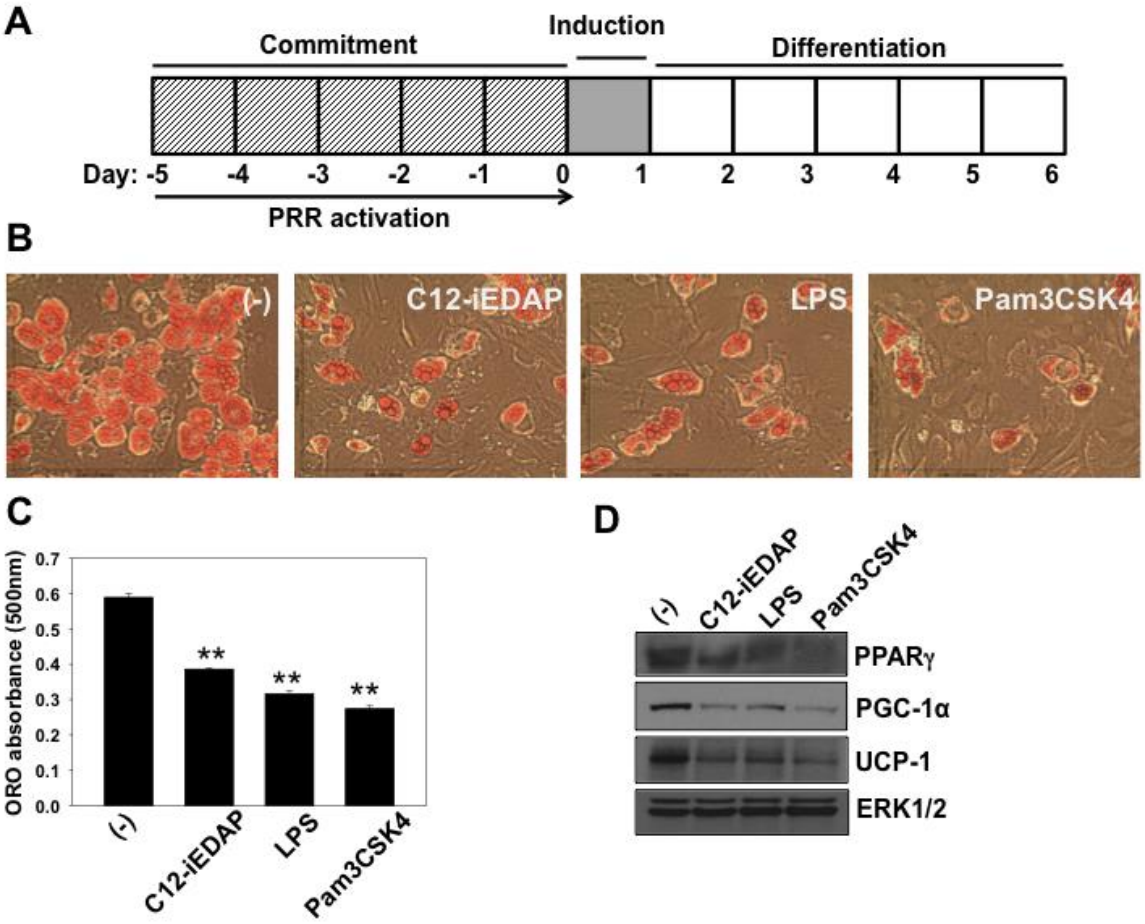

Figure 12 PRR activation only during the commitment phase is sufficient to lead to suppression of brown-like differentiation of C3H10T1/2 cells
C3H10T1/2 cells were committed with BMP4 in the presence of C12-iEDAP (10 µg/ml), LPS (1 µg/ml), Pam3CSK4 (10 µg/ml), or the vehicle control and then differentiated into brown-like adipocytes without PRR ligands until D6, as shown in (A). ORO stained cell morphology (B) and ORO absorbance (C) were measured. (D) Protein expression of established brown specific marker PPARγ, PGC-1α, and UCP-1 at D6 were analyzed by western blot. ERK1/2 is shown as a loading control. Data are mean±SE (n=3). **, significantly different from the controls with p<0.01.

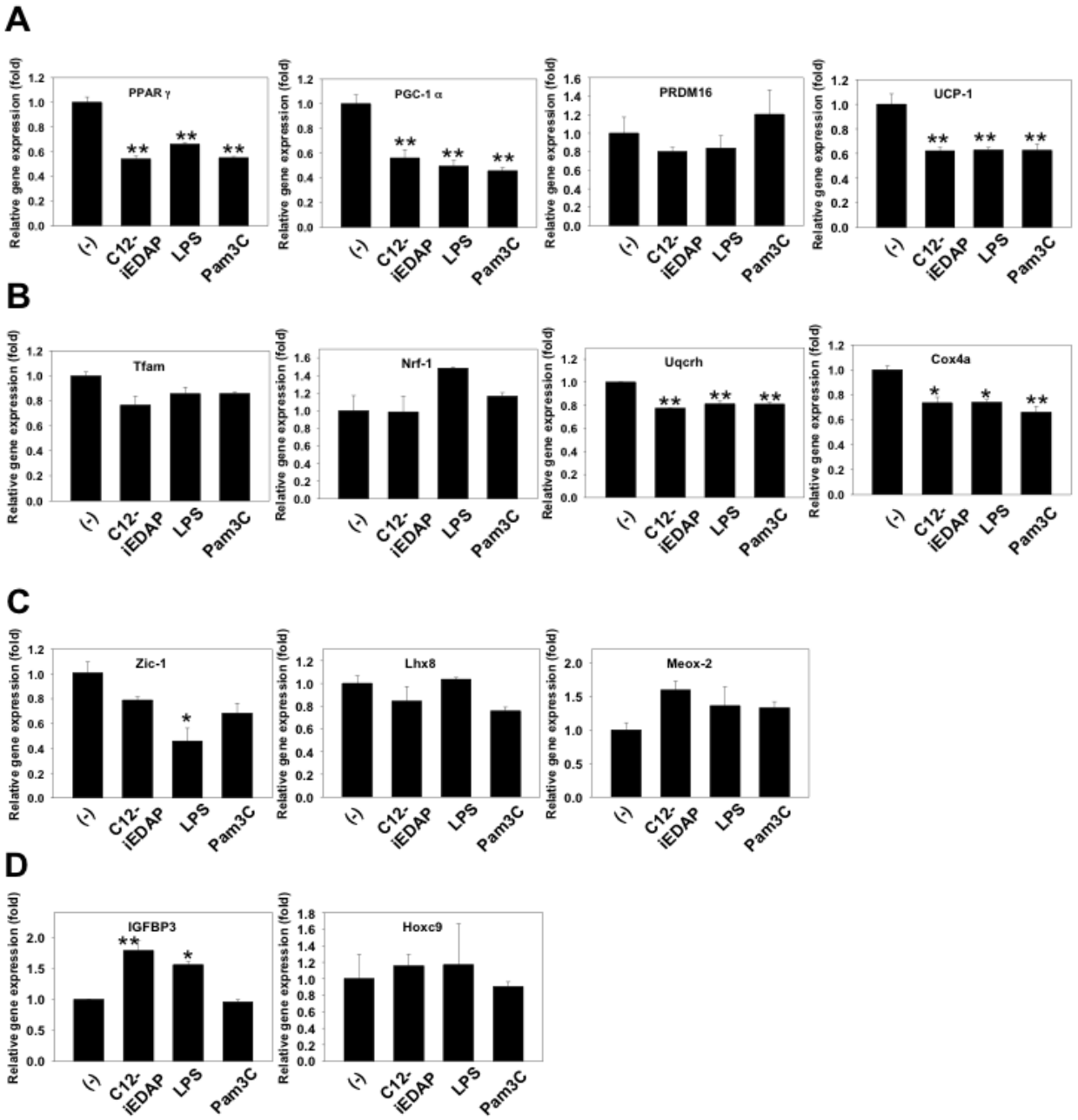

Figure 13 Molecular insights into the mechanisms by which PRR activation only during the commitment suppresses brown-like differentiation of C3H10T1/2 cells
C3H10T1/2 cells were committed with BMP4 in the presence of C12-iEDAP (10 µg/ml), LPS (1 µg/ml), Pam3CSK4 (10 µg/ml), or the vehicle control and then differentiated into brown-like adipocytes without PRR ligands until D6. mRNA expression of established brown markers (A); mitochondrial biogenesis markers (B); novel brown markers (C); and white specific markers (D) at D6 are shown. The relative mRNA expression was normalized to 36B4 and expressed as fold of the control (set as 1). Data are mean±SE (n=3). *, **, significantly different from the controls with p<0.05 and p<0.01, respectively.

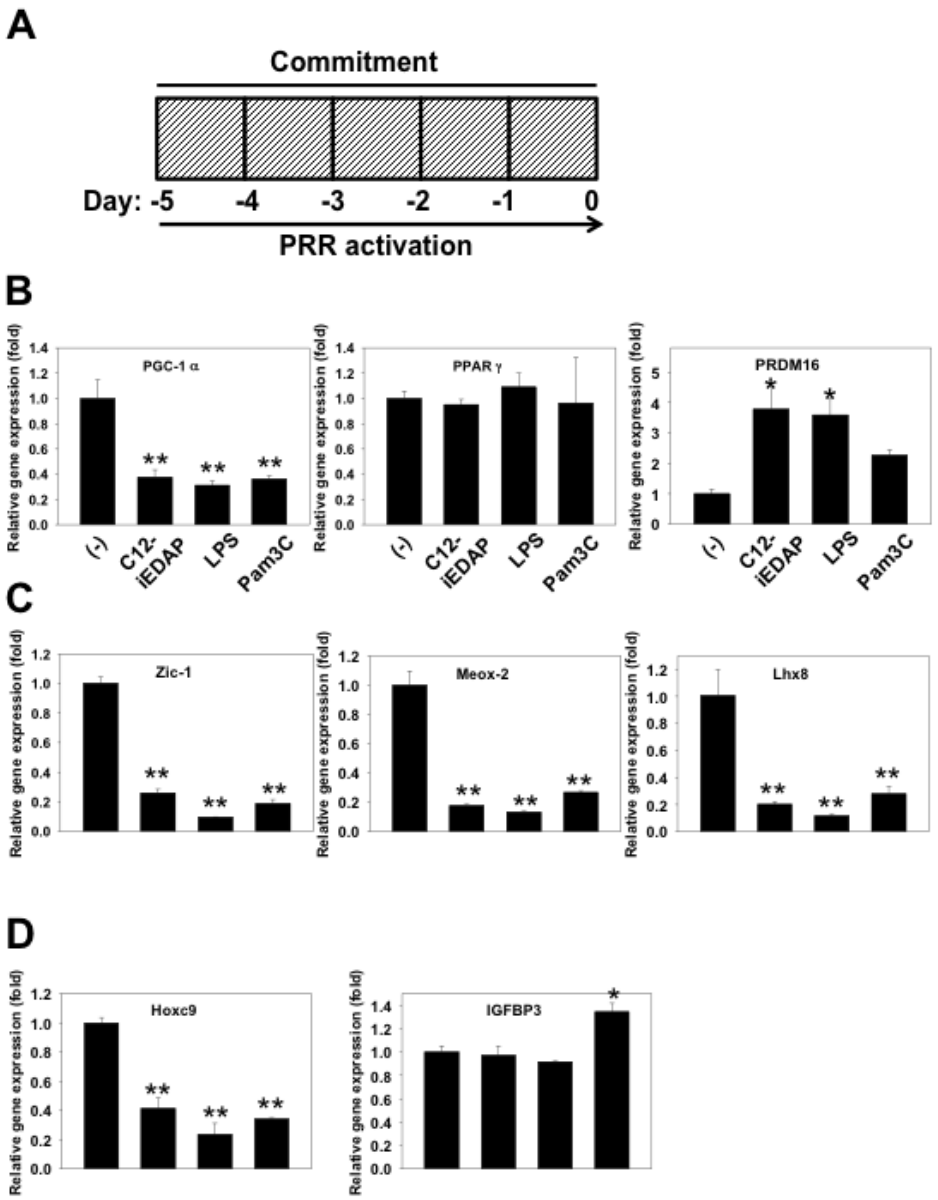

Figure 14 PRR activation suppresses the commitment to brown-like adipocytes of C3H10T1/2 cells

C3H10T1/2 cells were committed towards brown-like adipocytes with BMP4 in the presence of the C12-iEDAP (10 µg/mL), LPS (1 µg/mL), Pam3CSK4 (10 µg/mL), or the vehicle control until the cells reach confluency, as shown in (A). mRNA expression of established brown markers (B), novel brown markers (C), and white specific markers (D) at D0 are shown. The relative mRNA expression was normalized to 36B4 and expressed as fold of the control (set as 1). Data are mean±SE (*n*=3). *, **, significantly different from the controls with $p<0.05$ and $p<0.01$, respectively.

Figure 15 Chronic activation of NOD1, TLR4, or TLR2 suppresses terminal differentiation of immortalized brown preadipocytes derived from BAT of mice
Brown pre-adipocytes were differentiated in the presence of C12-iEDAP (10 µg/mL), LPS (1 µg/mL), Pam3CSK4 (10 µg/mL), or the vehicle control, as shown in (A). ORO stained cell morphology (B) and ORO absorbance (C) were measured. (D) Protein expression of established brown markers was analyzed by western blot. ERK1/2 is shown as a loading control. (E, F) mRNA expression of brown specific markers (E) and mitochondrial biogenesis markers (F) were analyzed at D6. The relative mRNA expression was normalized to 36B4 and expressed as fold of the control (set as 1). Data are mean±SE (n=3). **, significantly different from the controls with p<0.01.

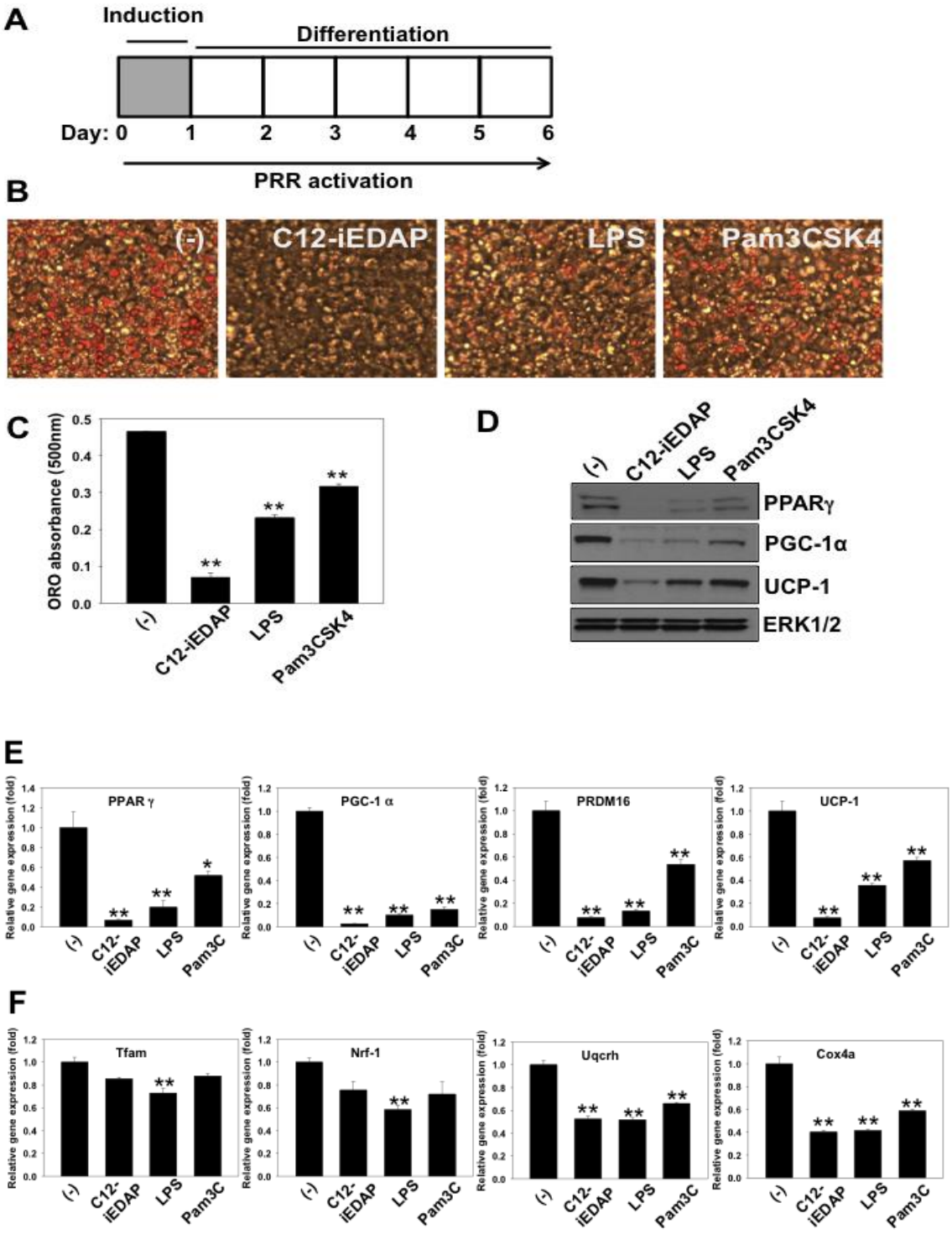
A
Induction
Differentiation
Day: 0 1 2 3 4 5 6
PRR activation
B
(-)
C12-iEDAP
LPS
Pam3CSK4
C
ORO absorbance (500nm)
(-)
C12-iEDAP
LPS
Pam3CSK4
D
(-)
C12-iEDAP
LPS
Pam3CSK4
PPARγ
PGC-1α
UCP-1
ERK1/2
E
PPAR γ
PGC-1 α
PRDM16
UCP-1
Relative gene expression (fold)
(-)
C12-iEDAP
LPS
Pam3C
F
Tfam
Nrf-1
Uqcrh
Cox4a

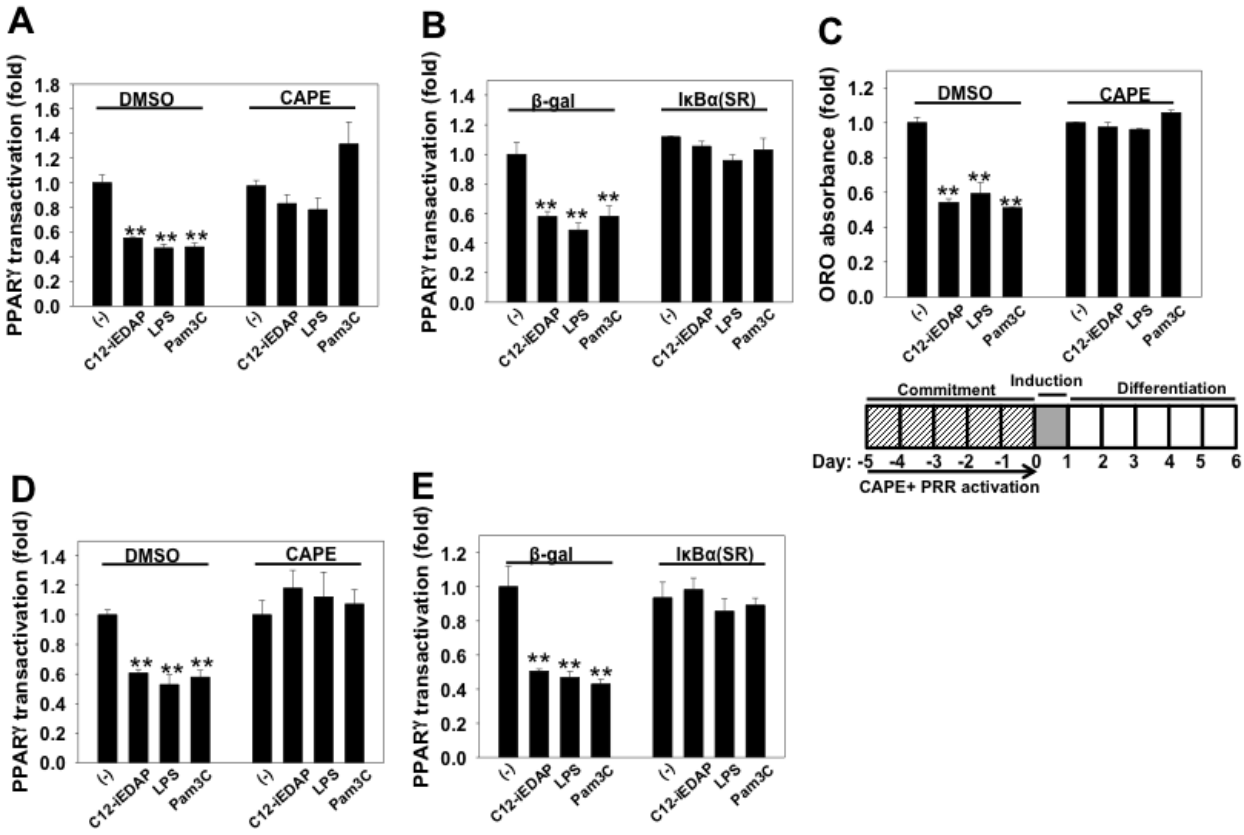

Figure 16 Activation of PRR suppresses PPARγ transactivation through NF-κB pathway

(A, B, D, E) PPARγ transactivation reporters were transfected into C3H10T1/2 (A, B) and brown pre-adipocytes (D, E). The cells were pretreated with NF-κB inhibitor CAPE or DMSO (A, D) or infected with adenovirus that encodes IκB supper-repressor IκB(SR) or the control virus (B, E) before the addition of selected PRR ligands and PPARγ synthetic ligand rosiglitazone (Rosi, 0.5 μM) together with the inhibitor or DMSO in A and D for 15 h. Cell lysate was prepared and reporter assays were performed. PPARγ transactivation normalized by the luciferase activities is presented as fold of that of the controls (set as 1). (C) C3H10T1/2 cells were committed with BMP4 in the presence of the PRR ligand and NF-κB inhibitor CAPE or DMSO during the commitment and then differentiated into brown-like adipocytes without PRR ligand and the inhibitor until D6, as shown in the diagram. ORO absorbance was measured. Data are mean±SE (n=3). **, significantly different from the controls with p<0.01.

CHAPTER IV

NARINGENIN, A CITRUS FLAVANONE, ENHANCES ISOPROTERENOL STIMULATED THERMOGENIC ACTIVATION OF 3T3-L1 ADIPOCYTES VIA PKA/P38 PATHWAYS

A version of this chapter will be submitted by Jiyoung Bae, Jiangang Chen, Ling Zhao entitled “Naringenin, a citrus flavanone, enhances isoproterenol stimulated thermogenic activation of 3T3-L1 adipocytes via PKA/p38 pathways”

4.1 Abstract

Promoting thermogenesis through increasing the activities of functional brown adipose tissues (BAT) has promised new hope for obesity treatment and prevention. Naringenin is an abundant flavanone mainly found in citrus fruits. Emerging evidence suggests that naringenin has anti-inflammatory and anti-oxidant properties and is beneficial in obesity and obesity related chronic diseases. Recently, naringenin has been reported to be capable of activating nuclear receptors, including PPAR gamma; however, it is not clear whether naringenin promotes activities of functional BAT, similar to what has been reported for rosiglitazone, a synthetic ligand for PPAR gamma. Here, we investigated the effects of naringenin on browning and isoproterenol-stimulated thermogenic activation of 3T3-L1 adipocytes. 3T3-L1 cells were differentiated into mature adipocytes with standard differentiation cocktail in the presence or absence of naringenin, followed by stimulation with β-adrenergic agonist isoproterenol. Although naringenin did not increase UCP-1 mRNA at basal condition, it significantly increased the isoproterenol-stimulated upregulation of UCP-1 and PGC-1α mRNA expression and enhanced isoproterenol-stimulated thermogenesis. Moreover, naringenin enhanced activation of PKA and phosphorylation of p38 MAPK downstream of isoproterenol stimulation; and inhibition of either PKA or p38 by their respective pharmacological inhibitors blocked naringenin-induced upregulation of UCP-1 mRNA. Taken together, our results demonstrate that naringenin enhances isoproterenol-induced thermogenic activation of 3T3-L1 adipocytes via PKA/p38 pathways.

4.2 Introduction

Obesity has been a growing problem across the globe over the past few decades, and if untreated, leads to metabolic disorders. Two types of adipose tissues, white adipose tissue (WAT) and brown adipose tissue (BAT), contribute to energy storage and expenditure. Results from recent animal and human studies, however, have identified inducible brown-like adipocytes, also known as beige adipocytes, in WAT (Giralt & Villarroya, 2013; Lo & Sun, 2013; A. Park, Kim, & Bae, 2014; J. W. Park et al., 2015; Rosenwald & Wolfrum, 2014). When exposed to cold temperature, hormonal stimuli (e.g. irisin and T3) (Obregon, 2014a; Zhang et al., 2014), or pharmacological treatment (e.g. rosiglitazone, bone morphogenetic protein, and isoproterenol) (Elsen et al., 2014; Obregon, 2014b; J. Wu et al., 2012), beige adipocytes can adopt a brown adipocyte phenotype via browning with increased UCP-1 expression, contributing to thermogenesis and energy expenditure.

Naringenin (4',5,7-trihydroxyflavanone), a citrus flavanone found in grapefruit, has emerged as a dietary bioactive compound with myriads of beneficial effects (Alam et al., 2014; Assini et al., 2013; Coelho, Hermsdorff, & Bressan, 2013; E Orhan et al., 2015; Mir & Tiku, 2015; Sharma et al., 2015). For example, several studies have reported anti-inflammatory properties of naringenin in various cell/disease models (Chtourou et al., 2015; H. Y. Park, Kim, & Choi, 2012; Seyedrezazadeh et al., 2015; Shi et al., 2009; L.-H. Wu et al., 2015; Yu, Ma, Yue, Yao, & Mao, 2015).

It has been reported that oral administration of naringenin in rodents decrease WAT adipose mass (Assini et al., 2013; Ke et al., 2015), reduce adipose tissue inflammation (Ke et al., 2015; Hiroki Yoshida et al., 2014; H. Yoshida et al., 2013) and

macrophage infiltration (Hiroki Yoshida et al., 2014) in high-fat induced obesity. Naringenin suppressed Toll-like receptor 2 (TLR2) expression induced by TNFα and high fat feeding (H. Yoshida et al., 2013). Recently, naringenin has been reported to activate nuclear receptors, including PPARγ (Goldwasser et al., 2010). PPARγ agonist rosiglitazone induced “browning” in primary culture derived from subcutaneous white fat (Petrovic et al., 2010) and induced UCP-1 expression and thermogenesis (Petrovic, Shabalina, Timmons, Cannon, & Nedergaard, 2008). However, it is not clear whether naringenin has such effects.

In this report, we investigated the impact of naringenin treatment on browning and thermogenic activation by isoproterenol, a β-adrenergic receptor agonist, in 3T3-L1 adipocytes. We report naringenin at 10 μM significantly promoted the isoproterenol-stimulated upregulation of UCP-1 and PGC-1α mRNA expression and thermogenesis in the 3T3-L1 adipocytes. We further demonstrated the effects by naringenin are mediated through the activation of PKA/p38 MAPK signaling pathways.

4.3 Materials and Methods

Reagents

Murine 3T3-L1 cells were obtained from ATCC (Manassas, VA). Naringenin, Dulbecco's modified Eagle's medium (DMEM), 3-Isobutyl-L-methylxanthine, dexamethasone, insulin, isoproterenol (ISO), and rosiglitazone (Rosi) were from Sigma (St. Louis, MO). Calf serum (CS) was purchased from Hyclone (Logan, UT) and fetal bovine serum (FBS) was purchased from Atlas Biologicals (Fort Collins, CO). The pharmacological inhibitors for p38 (SB203580) and PKA (H-89) were from Tocris Bioscience (Ellisville, MI). Anti-phospho-p38 (Thr180/Tyr182) (no. 9211), anti-p38 (no. 9212) antibodies, and horseradish peroxidase-conjugated goat anti-rabbit were from Cell Signaling Technology (Danvers, MA).

Naringenin was dissolved in dimethyl sulfoxide (DMSO, Sigma, St. Louis, MO) to make 50 mM concentration followed by dilution in DMSO to make 0, 5 and 10 mM for treatment. The final DMSO concentration in cell culture medium was ≤ 0.1%.

Cell culture and treatment

Murine 3T3-L1 cells were grown in DMEM supplemented with 10% CS at 37°C humidified atmosphere of 5% CO_2 in air until they reached confluence [designated as day 0 (D0)]. The cells were differentiated in DMEM containing 10% FBS, 1 μM/L dexamethasone, 0.5 mM/L 3-isobutyl-1-methylxanthine (IBMX) and 10 μg/mL insulin (Cohen et al.) for 3 days, followed by treatment with 10 μg/mL insulin in DMEM containing 10% FBS for an additional 2 days. The cells were then maintained in DMEM containing 10% FBS until fully differentiated at day 7 (D7).

To examine the effects of naringenin on browning of 3T3-L1 adipocytes, confluent 3T3-L1 cells were differentiated with DMI in the presence or absence of various doses of naringenin starting on D0 as indicated in the figure legends. Fresh naringenin was replaced at each change of the media during the entire differentiation process. Rosi (1 μM) was used as a positive control. On D7, the cells were stimulated with Isoproterenol (ISO, 1 μM) or the vehicle control for 6 h. Pharmacological inhibitors, SB203580 and H-89, were applied one hour before the ISO stimulation as indicated in the figure legends.

PKA activity

On D7, 3T3-L1 adipocytes differentiated in the presence or absence of naringenin (10 μM), or Rosi (1 μM) were serum starved in 0.25% FBS containing DMEM for 1 h. The cells were stimulated with or without ISO (1 μM) for further 6 h. PKA activities were measured from total cell lysates using DetectX PKA activity kit (Arbor Assays, Ann Arbor, MI) according to the manufacturer's instructions.

Western blot analysis

Total cell lysates were prepared using 1X lysis buffer (Cell Signaling, Danvers, MA) and protein concentration were determined by the BCA assay kit (Thermo Scientific, Waltham, MA). Twenty micrograms of total cell lysates were subjected to 10% SDS-PAGE and transferred to polyvinylidene difluoride membrane (Bio-Rad, Hercules, CA). The membrane was blocked in 20 mM Tris·HCl, 137 mM NaCl, and 0.1% Tween 20 (pH 7.4) containing 5% nonfat milk. The membrane was immunoblotted with primary antibodies at 4°C overnight followed by secondary antibody conjugated with horseradish peroxidase for 1 h. The membrane was exposed on X-ray film after

developed by ECL Western blot detection reagents (GE Healthcare, Piscataway, NJ). The membranes was stripped in stripping buffer (62.5 mM Tris-HCl, 2 % SDS, and 100 mM 2-mercaptoethanol) at 50 °C for 10 min.

RNA preparation and quantitative real-time PCR analysis

Total RNA was prepared using TRI reagent (Molecular Research Center, Cincinnati, OH) according to the manufacturer's instructions. Total RNA abundance was quantified using NanoDrop ND-1000 spectrophotometer (NanoDrop Technologies, Wilmington, DE). Reverse transcription was carried out using High capacity cDNA Reverse Transcription kit (Thermo Scientific, Pittsburgh, PA) according to the manufacturer's instructions. mRNA expression of target genes and the housekeeping gene 36B4 was measured quantitatively using Absolute Blue QPCR SYBR Green ROX mix (Thermo Fisher Scientific, location). PCR reactions were run in a 96-well format using an ABI 7300HT instrument. Cycle conditions were 50°C 2 min, 95°C 15 min and then 40 cycles of 95°C for 15 s/60°C for 1 min. Relative gene expression was calculated using the $2^{-\Delta\Delta Ct}$ method (Dawson et al., 2012), which normalizes against a house keeping gene 36B4.

Reporter gene assays

3T3-L1 preadipocytes were seeded in 24-well plates were transiently transfected with PPAR response element-driven luciferase reporter (PPRE-Luc) (PPRE-Luc was a gift from Bruce Spiegelman (Addgene plasmid # 1015) or murine PPARγ ligand binding domain (LBD) coupled to the Gal4 DNA binding domain (DBD) (mPPARγ-Gal4) and a reporter construct containing an upstream activating sequence linked luciferase, 4xUAS-TK-luc (TK: thymidine kinase) (gifts from Dr Susanne Mandrup at University of

Southern Denmark, Denmark) (Taxvig et al., 2012) with Fugene HD transfection reagent (Promega, Madison, WI). The cells were then treated with naringenin or the vehicle control DMSO for 18 h. Reporter luciferase activities were measured from cell lysates with GloMax Luminometer (Promega, Madison, WI). Relative luciferase activities were normalized by total protein concentrations measured by BCA assay kit.

Cellular bioenergetics measurements

3T3-L1 preadipocytes were differentiated in the presence or absence of naringenin, or Rosi for 7 days. Then adipocytes were replated and seeded in 24-well XF assay plates in DMEM containing 10% FBS for overnight followed by treated with ISO (1 μM) for 6 h. After treatment, cells were rinsed with XF assay buffer (DMEM without $NaHCO_3$, 10 mM glucose, 2 mM pyruvate, and 2 mM GlutaMAX, pH 7.4) 3 times. A 500 μl of XF assay buffer was then added into each well, and equilibrated at non-CO_2 incubator at 37°C for 1 h. Real-time measurements of oxygen consumption rate (OCR) was conducted using XF24 Extracellular Flux Analyzer (Seahorse Biosciences, North Billerica, MA). For the mitochondria stress test, mitochondrial complex inhibitors were injected to sequentially in the following order: oligomycin (1 μM), carbonyl cyanide-ptrifluoromethoxyphenylhydrazone (FCCP; 0.75 μM), antimycin A/rotenone (1 μM each), and 3 readings were taken after each injection. OCR was automatically recorded by XF24 software v1.8 provided by the manufacturer.

Calculations of proton leak, coupling efficiency, maximal respiration, and ATP production were performed according to the manufacturer's instructions.

Statistical analysis

All data are presented as mean±SE. Measurements were performed in triplicates. Statistical analysis was performed using SigmaPlot 13.0 (Systat Software). One-way ANOVA with repeated measures followed by multiple comparisons test (Student-Newman-Keuls method) was performed to determine the differences of group mean between the treatment groups and/or time points. Student's *t*-tests were performed when appropriate. The level of significance was set at $P<0.05$.

4.4 Results

Naringenin dose-dependently enhances UCP-1 and PGC-1α mRNA in ISO-stimulated 3T3-L1 adipocytes.

To investigate the browning effect of naringenin on white adipocytes, 3T3-L1 cells were differentiated in the presence or absence of naringenin (5, 10 μM). Rosi was included as a positive control in the studies. At basal (e.g., non-stimulated) condition, Rosi induced mRNA expression of established brown specific markers UCP-1, PGC-1α, and induced novel brown marker PRDM16, and suppressed Meox-2, as reported (Petrovic et al., 2010). Also, Rosi suppressed white specific marker IGFBP3, as reported (Petrovic et al., 2010). In contrast, naringenin did not increase UCP-1 and PGC-1α mRNA even when used up to 20 μM at the basal condition (data not shown); however, at 10 μM, naringenin significantly increased mRNA expression of PRDM16 and suppressed Meox-2 and IGFBP3 mRNA (Figure 17A).

When stimulated with isoproterenol (ISO), naringenin at 10 μM, significantly promoted ISO-induced UCP-1 activation, as demonstrated by the enhanced mRNA expression of brown adipocyte specific genes, UCP-1 and PGC-1α (Figure 17B).

Naringenin enhances thermogenesis in ISO-stimulated 3T3-L1 adipocytes.

To determine whether the upregulation of UCP-1 mRNA by naringenin leads to increase in mitochondrial uncoupling and thermogenesis, we examined oxygen consumption rates coupled with mitochondrial stress tests in ISO-stimulated 3T3-L1 adipocytes which have been differentiated in the presence or absence of naringenin by cellular bioenergetics measurements using XF24 Extracellular Flux Analyzers (Figure 18A-D). Naringenin at 10 μM significantly increased isoproterenol-stimulated oxygen

consumption from proton leak (Figure 18A) and decreased coupling efficiency (Figure 18B); however, naringenin did not affect the ISO-stimulated maximal respiration (Figure 18C) and oxygen consumption from ATP production (Figure 18D).

Naringenin enhances isoproterenol-stimulated PKA activation and phosphorylation of p38 MAPK.

Beta-adrenergic activation induces increase in cAMP levels, leading to PKA activation and downstream p38 MAPK phosphorylation. ISO stimulation resulted in ~3 folds of PKA activities, compared to non-stimulated controls in mature 3T3-L1 adipocytes (Figure 19). Both Rosi and naringenin induced significant enhancement of PKA activation induced by ISO (Figure 19).

We next examined whether naringenin treatment during 3T3-L1 adipocytes differentiation affects p38 MAPK phosphorylation downstream of ISO stimulation. Western analysis showed that ISO induced a peak of p38 phosphorylation at 15 min upon the stimulation (Figure 20). In contrast, p38 phosphorylation was higher at the basal state (time 0), and was significantly enhanced in naringenin treated 3T3-L1 adipocytes stimulated by ISO. Rosi induced the highest p38 MAPK phosphorylation at the basal state and throughout the 60 min in 3T3-L1 adipocytes (Figure 20).

Naringenin activates PPRE reporter gene and transactivates PPARγ in 3T3-L1 cells.

To understand whether naringenin's effects were mediated through PPARγ, we performed reporter gene assays. Naringenin at 10 μM activated PPRE-Luc reporter up to ~2 fold whereas Rosi induced ~3.5 fold compared to the controls in 3T3-L1 (Figure

21A). In addition, naringenin at the same concentration transactivated PPARγ in 3T3-L1 cells (Figure 21B), consistent with the report (Goldwasser et al., 2010).

Enhancement of UCP-1 mRNA by naringenin is attenuated by inhibition of either PKA or p38 MAPK.

To investigate whether the activation of PKA/p38 MAPK underlies ISO-stimulated UCP-1 activation by naringenin, we employed the pharmacological inhibitors of PKA H89 and p38 MAPK SB203580. The PKA inhibitor H89 blocked UCP-1 mRNA expression at the basal state and the upregulation induced by naringenin and Rosi. The p38 MAPK inhibitor SB203580 also significantly blocked basal as well as naringenin and rosi-induced UCP-1 mRNA expression, although to a less extend (Figure 22).

4.5 Discussion

Increasing functional brown adipose activities has become novel targets for obesity treatment and prevention. Naringenin, a citrus flavanone, has been reported to be beneficial in obesity and obesity associated chronic diseases. Here, we report that naringenin dose-dependently enhances ISO-stimulated UCP-1 mRNA. Naringenin at 10 μM significantly increased ISO-induced uncoupled respiration from proton leak, but decreased coupled efficiency, consistent with the enhancement on UCP-1 activation in ISO-stimulated 3T3-L1 adipocytes by naringenin. Furthermore, naringenin enhanced PKA activation and phosphorylation of p38 MARK downstream of ISO. Inhibition of either PKA or p38 MARK blocked naringenin's enhancement of ISO-stimulated UCP-1 activation. Our studies suggest that naringenin promotes ISO-stimulated thermogenic activation of 3T3-L1 adipocytes via PKA/p38 MARK pathways (Figure 23).

3T3-L1 cell model, representing a very "white" cell model (Jun Wu & Spiegelman, 2014), has been used for identifying strategies to induce browning, i.e., acquiring of brown-like adipocyte characteristics. Recent studies have suggested that 3T3-L1 cells have the ability to induce UCP-1 and markers of beige adipocytes under specific environmental conditions. β-adrenergic activation by isoproterenol, a nonspecific β-adrenergic agonist, induces thermogenic activation in brown adipocytes and brown adipose tissue. It has been reported that 3T3-L1 adipocytes differentiated from standard differentiation protocol has significant increase of UCP-1 expression in response to ISO (Asano et al., 2014). ISO induced a much higher UCP-1 expression in 3T3-L1 adipocytes treated with T3, Rosi and IBMX (Asano et al., 2014). Moreover, ISO at 100 μM also enhanced UCP-1 expression, leading to increased oxygen consumption rate in

3T3-L1 adipocytes differentiated from standard differentiation protocol supplemented with only T3 (Miller et al., 2015). To our knowledge, our finding is the first to report a dietary bioactive compound naringenin at 10 μM enhances ISO-stimulated thermogenic activation in 3T3-L1 adipocytes.

It is generally believed that the most critical test for functional brown adipocytes is the ability to display induced thermogenesis by adrenergic activation (Petrovic et al., 2010). The findings that naringenin did not induce UCP-1 expression at the basal state, but enhanced UCP-1 activation and thermogenesis in response to ISO suggest that naringenin promotes the development of functional brown adipocytes. The effect of naringenin is in contrast with some of the reported “browning” agents, such as PPARγ agonist Rosi, and Irisin. Rosi induced UCP-1 expression not only at the basal state but also ISO-stimulated condition in primary adipocytes differentiated from stromal vascular fraction of white fat (Petrovic et al., 2010). In our studies, we have included Rosi as a positive control. We show that Rosi induced UCP-1 mRNA at both basal and ISO-stimulated condition in 3T3-L1 adipocytes. Recombinant form of Irisin, a newly identifies hormone secreted from skeletal muscles, upregulated UCP-1 expression in 3T3-L1 adipocytes at the basal state and induced browning of subcutaneous fat pads when injected into the mice (Zhang et al., 2014). However, whether Irisin enhances ISO-stimulated UCP-1 activation and thermogenesis has not been reported. It is worthy of noting that naringenin exposure during differentiation increased PRDM16 mRNA and suppressed mRNA expression of Meox-2, and IGFBP3, similar to those of Rosi at the basal state, suggesting that naringenin promotes the acquiring of some of the characteristics of brown-like adipocytes induced by Rosi. However, it remains to be

determined whether naringenin induces development of functional brown adipocytes in vivo.

To explore the mechanisms by which naringenin promotes ISO-stimulated thermogenic activation, we examined the effects on naringenin on the signaling events downstream of ISO. It has been reported that adrenergic activation in brown adipocytes induces cAMP accumulation, leading to PKA activation, which indirectly leads to phosphorylation and activation of p38 MAPK. Activation of p38 leads to upregulation and activation of PGC-1α, coactivator of PPARγ on the PPRE site in the promotor of UCP-1 gene, leading to UCP-1 transcription (Cao et al., 2004; Cao, Medvedev, Daniel, & Collins, 2001). Our results indicate that naringenin enhanced PKA activation downstream of ISO to a level that is similar to that of Rosi. Moreover, naringenin exposure induced a higher level of phosphorylation of p38 at the basal state and further enhanced phosphorylation of p38 stimulated by ISO. We also show, for the first time, that Rosi also enhanced basal phosphorylation of p38 to a much higher level and further maintained a strong phosphorylation of p38 stimulated with ISO. Phosphorylation of p38 MAPK leads to upregulation of PGC-1α transcription and enhanced interaction between PGC-1α and PPARγ, leading to UCP-1 transcription in response to ISO (Cao et al., 2004; Cao et al., 2001). Our results demonstrating enhanced upregulation of PGC-1α mRNA and increased of PPARγ transactivation by naringenin are consistent with the effects of enhanced phosphorylation of p38 by naringenin. Furthermore, we show that inhibition of PKA or p38 suppressed ISO-stimulated UCP-1 activation. Together, these results suggest that the enhancement of ISO-stimulated thermogenic activation by naringenin is mediated through PKA/p38 MAPK pathways (Figure 23).

In conclusion, we have demonstrated that naringenin at 10 μM enhances ISO-stimulated UCP-1 activation and thermogenesis in 3T3-L1 adipocytes, possibly through enhancement of PKA/p38 MAPK pathways downstream of ISO. Our results suggest that naringenin may be beneficial in promoting activities of functional brown adipose tissue in vivo. Further studies of naringenin in the development of functional brown adipose tissue and promote thermogenesis in vivo are warranted.

4.6 References

Alam, M. A., Subhan, N., Rahman, M. M., Uddin, S. J., Reza, H. M., & Sarker, S. D. (2014). Effect of citrus flavonoids, naringin and naringenin, on metabolic syndrome and their mechanisms of action. *Adv Nutr, 5*(4), 404-417. doi:10.3945/an.113.005603

Asano, H., Kanamori, Y., Higurashi, S., Nara, T., Kato, K., Matsui, T., & Funaba, M. (2014). Induction of Beige-Like Adipocytes in 3T3-L1 Cells. *The Journal of Veterinary Medical Science, 76*(1), 57.

Assini, J. M., Mulvihill, E. E., Sutherland, B. G., Telford, D. E., Sawyez, C. G., Felder, S. L., . . . Huff, M. W. (2013). Naringenin prevents cholesterol-induced systemic inflammation, metabolic dysregulation, and atherosclerosis in Ldlr−/− mice. *Journal of lipid research, 54*(3), 711-724.

Cao, W., Daniel, K. W., Robidoux, J., Puigserver, P., Medvedev, A. V., Bai, X., . . . Collins, S. (2004). p38 mitogen-activated protein kinase is the central regulator of cyclic AMP-dependent transcription of the brown fat uncoupling protein 1 gene. *Molecular and cellular biology, 24*(7), 3057-3067.

Cao, W., Medvedev, A. V., Daniel, K. W., & Collins, S. (2001). β-adrenergic activation of p38 MAP kinase in adipocytes cAMP induction of the uncoupling protein 1 (UCP1) gene requires p38 map kinase. *Journal of Biological Chemistry, 276*(29), 27077-27082.

Chtourou, Y., Fetoui, H., Jemai, R., Slima, A. B., Makni, M., & Gdoura, R. (2015). Naringenin reduces cholesterol-induced hepatic inflammation in rats by modulating matrix metalloproteinases-2, 9 via inhibition of nuclear factor κB pathway. *European journal of pharmacology, 746*, 96-105.

Coelho, R. C. L. A., Hermsdorff, H. H. M., & Bressan, J. (2013). Anti-inflammatory properties of orange juice: possible favorable molecular and metabolic effects. *Plant foods for human nutrition, 68*(1), 1-10.

Cohen, P., Levy, J. D., Zhang, Y., Frontini, A., Kolodin, D. P., Svensson, K. J., . . . Khandekar, M. J. (2014). Ablation of PRDM16 and beige adipose causes metabolic dysfunction and a subcutaneous to visceral fat switch. *Cell, 156*(1), 304-316.

Dawson, K., Zhao, L., Adkins, Y., Vemuri, M., Rodriguez, R. L., Gregg, J. P., . . . Hwang, D. H. (2012). Modulation of blood cell gene expression by DHA supplementation in hypertriglyceridemic men. *The Journal of nutritional biochemistry, 23*(6), 616-621.

E Orhan, I., F Nabavi, S., Daglia, M., C Tenore, G., Mansouri, K., & M Nabavi, S. (2015). Naringenin and Atherosclerosis: A Review of Literature. *Current pharmaceutical biotechnology, 16*(3), 245-251.

Elsen, M., Raschke, S., Tennagels, N., Schwahn, U., Jelenik, T., Roden, M., . . . Eckel, J. (2014). BMP4 and BMP7 induce the white-to-brown transition of primary human adipose stem cells. *Am J Physiol Cell Physiol, 306*(5), C431-440. doi:10.1152/ajpcell.00290.2013

Erlund, I., Meririnne, E., Alfthan, G., & Aro, A. (2001). Plasma kinetics and urinary excretion of the flavanones naringenin and hesperetin in humans after ingestion of orange juice and grapefruit juice. *The Journal of nutrition, 131*(2), 235-241.

Giralt, M., & Villarroya, F. (2013). White, brown, beige/brite: different adipose cells for different functions? *Endocrinology, 154*(9), 2992-3000. doi:10.1210/en.2013-1403

Goldwasser, J., Cohen, P. Y., Yang, E., Balaguer, P., Yarmush, M. L., & Nahmias, Y. (2010). Transcriptional regulation of human and rat hepatic lipid metabolism by the grapefruit flavonoid naringenin: role of PPARalpha, PPARgamma and LXRalpha. *PLoS One, 5*(8), e12399. doi:10.1371/journal.pone.0012399

Kajimura, S., Seale, P., Tomaru, T., Erdjument-Bromage, H., Cooper, M. P., Ruas, J. L., . . . Spiegelman, B. M. (2008). Regulation of the brown and white fat gene programs through a PRDM16/CtBP transcriptional complex. *Genes & development, 22*(10), 1397-1409.

Ke, J.-Y., Kliewer, K. L., Hamad, E. M., Cole, R. M., Powell, K. A., Andridge, R. R., . . . Belury, M. A. (2015). The flavonoid, naringenin, decreases adipose tissue mass and attenuates ovariectomy-associated metabolic disturbances in mice. *Nutrition & metabolism, 12*(1), 1-10.

Lo, K. A., & Sun, L. (2013). Turning WAT into BAT: a review on regulators controlling the browning of white adipocytes. *Biosci Rep, 33*(5). doi:10.1042/BSR20130046

Miller, C., Yang, J.-Y., England, E., Yin, A., Gajjar, V., & Rayalam, S. (2015). Isoproterenol Induces Beiging and Thermogenesis in Mature 3T3-L1 Adipocytes. *The FASEB Journal, 29*(1 Supplement), LB274.

Mir, I. A., & Tiku, A. B. (2015). Chemopreventive and Therapeutic Potential of “Naringenin,” a Flavanone Present in Citrus Fruits. *Nutrition and cancer, 67*(1), 27-42.

Obregon, M. J. (2014a). Adipose tissues and thyroid hormones. *Front Physiol, 5*, 479. doi:10.3389/fphys.2014.00479

Obregon, M. J. (2014b). Changing white into brite adipocytes. Focus on "BMP4 and BMP7 induce the white-to-brown transition of primary human adipose stem cells". *Am J Physiol Cell Physiol, 306*(5), C425-427. doi:10.1152/ajpcell.00015.2014

Park, A., Kim, W. K., & Bae, K. H. (2014). Distinction of white, beige and brown adipocytes derived from mesenchymal stem cells. *World J Stem Cells, 6*(1), 33-42. doi:10.4252/wjsc.v6.i1.33

Park, H. Y., Kim, G.-Y., & Choi, Y. H. (2012). Naringenin attenuates the release of pro-inflammatory mediators from lipopolysaccharide-stimulated BV2 microglia by inactivating nuclear factor-κB and inhibiting mitogen-activated protein kinases. *International journal of molecular medicine, 30*(1), 204-210.

Park, J. W., Jung, K. H., Lee, J. H., Quach, C. H., Moon, S. H., Cho, Y. S., & Lee, K. H. (2015). 18F-FDG PET/CT monitoring of beta3 agonist-stimulated brown adipocyte recruitment in white adipose tissue. *J Nucl Med, 56*(1), 153-158. doi:10.2967/jnumed.114.147603

Pellegrini, M., Bulzomi, P., Galluzzo, P., Lecis, M., Leone, S., Pallottini, V., & Marino, M. (2014). Naringenin modulates skeletal muscle differentiation via estrogen receptor α and β signal pathway regulation. *Genes & nutrition, 9*(5), 1-13.

Petrovic, N., Shabalina, I. G., Timmons, J. A., Cannon, B., & Nedergaard, J. (2008). Thermogenically competent nonadrenergic recruitment in brown preadipocytes by a PPARγ agonist. *American Journal of Physiology-Endocrinology and Metabolism, 295*(2), E287-E296.

Petrovic, N., Walden, T. B., Shabalina, I. G., Timmons, J. A., Cannon, B., & Nedergaard, J. (2010). Chronic peroxisome proliferator-activated receptor γ (PPARγ) activation of epididymally derived white adipocyte cultures reveals a population of thermogenically competent, UCP1-containing adipocytes molecularly distinct from classic brown adipocytes. *Journal of Biological Chemistry, 285*(10), 7153-7164.

Rosenwald, M., & Wolfrum, C. (2014). The origin and definition of brite versus white and classical brown adipocytes. *Adipocyte, 3*(1), 4-9. doi:10.4161/adip.26232

Seyedrezazadeh, E., Kolahian, S., Shahbazfar, A. A., Ansarin, K., Pour Moghaddam, M., Sakhinia, M., . . . Vafa, M. (2015). Effects of the Flavanone combination Hesperetin-Naringenin, and Orange and Grapefruit Juices, on Airway inflammation and Remodeling in a murine asthma model. *Phytotherapy Research, 29*(4), 591-598.

Sharma, M., Akhtar, N., Sambhav, K., Shete, G., K Bansal, A., & S Sharma, S. (2015). Emerging Potential of Citrus Flavanones as an Antioxidant in Diabetes and its Complications. *Current topics in medicinal chemistry, 15*(2), 187-195.

Shi, Y., Dai, J., Liu, H., Li, R.-R., Sun, P.-L., Du, Q., . . . Yin, K.-S. (2009). Naringenin inhibits allergen-induced airway inflammation and airway responsiveness and inhibits NF-κB activity in a murine model of asthma. *Canadian journal of physiology and pharmacology, 87*(9), 729-735.

Taxvig, C., Dreisig, K., Boberg, J., Nellemann, C., Schelde, A. B., Pedersen, D., . . . Vinggaard, A. M. (2012). Differential effects of environmental chemicals and food contaminants on adipogenesis, biomarker release and PPARγ activation. *Molecular and cellular endocrinology, 361*(1), 106-115.

Wu, J., Bostrom, P., Sparks, L. M., Ye, L., Choi, J. H., Giang, A. H., . . . Spiegelman, B. M. (2012). Beige adipocytes are a distinct type of thermogenic fat cell in mouse and human. *Cell, 150*(2), 366-376. doi:10.1016/j.cell.2012.05.016

Wu, J., & Spiegelman, B. M. (2014). Irisin ERKs the fat. *Diabetes, 63*(2), 381-383.

Wu, L.-H., Lin, C., Lin, H.-Y., Liu, Y.-S., Wu, C. Y.-J., Tsai, C.-F., . . . Lu, D.-Y. (2015). Naringenin suppresses neuroinflammatory responses through inducing suppressor of cytokine signaling 3 expression. *Molecular neurobiology*, 1-12.

Yoshida, H., Watanabe, H., Ishida, A., Watanabe, W., Narumi, K., Atsumi, T., . . . Kurokawa, M. (2014). Naringenin suppresses macrophage infiltration into adipose tissue in an early phase of high-fat diet-induced obesity. *Biochemical and biophysical research communications, 454*(1), 95-101.

Yoshida, H., Watanabe, W., Oomagari, H., Tsuruta, E., Shida, M., & Kurokawa, M. (2013). Citrus flavonoid naringenin inhibits TLR2 expression in adipocytes. *J Nutr Biochem, 24*(7), 1276-1284. doi:10.1016/j.jnutbio.2012.10.003

Yu, D.-h., Ma, C.-h., Yue, Z.-q., Yao, X., & Mao, C.-m. (2015). Protective Effect of Naringenin Against Lipopolysaccharide-Induced Injury in Normal Human Bronchial Epithelium via Suppression of MAPK Signaling. *Inflammation, 38*(1), 195-204.

Zhang, Y., Li, R., Meng, Y., Li, S., Donelan, W., Zhao, Y., . . . Tang, D. (2014). Irisin stimulates browning of white adipocytes through mitogen-activated protein kinase p38 MAP kinase and ERK MAP kinase signaling. *Diabetes, 63*(2), 514-525. doi:10.2337/db13-1106/-/DC1

4.7 Appendix

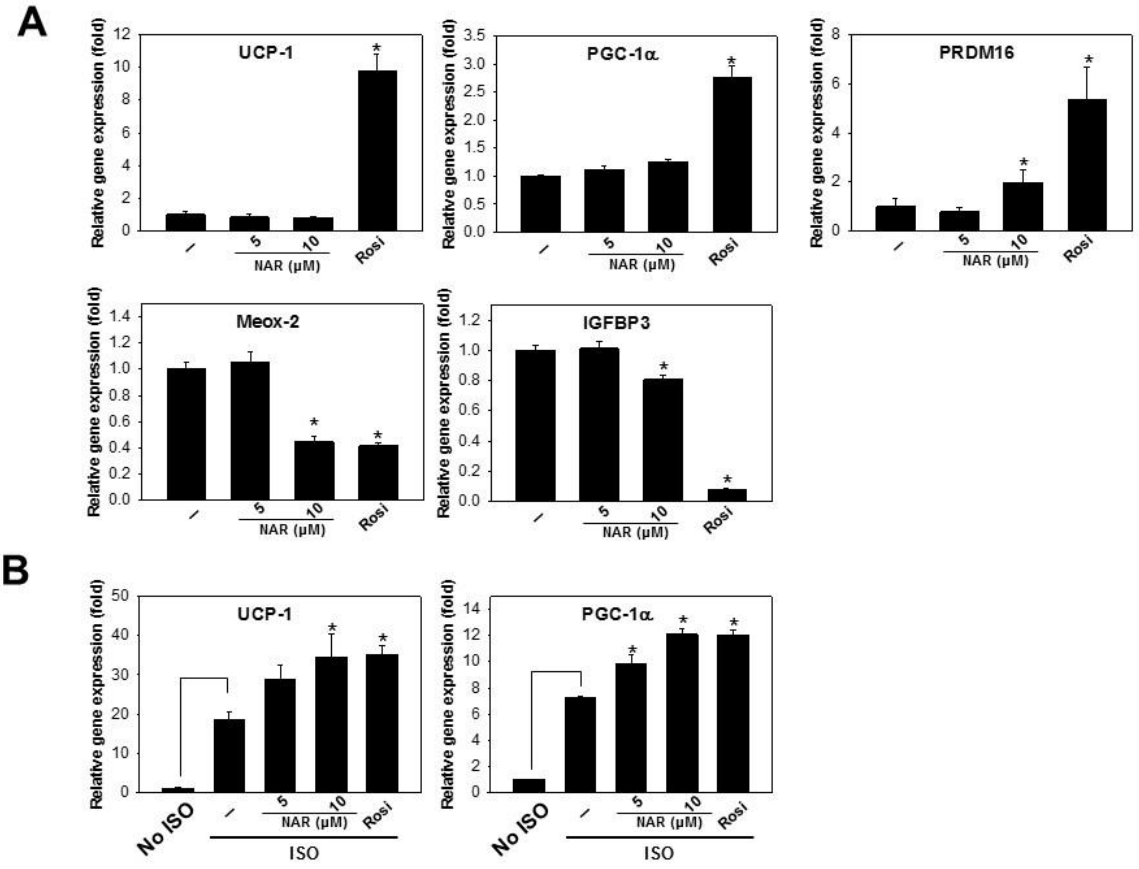

Figure 17 Effect of naringenin on mRNA expression of brown adipose specific markers

3T3-L1 preadipocytes were induced to differentiation in the presence of various doses of naringenin (NAR, 0, 5, 10 μM) for 7 days. On day 7, matured 3T3-L1 adipocytes were treated with or without isoproterenol (ISO) for 6 h. Total RNA was extracted and mRNA expression of target genes were quantified and normalized by 36B4. The relative mRNA expression was expressed as fold of changes compared to that of DMSO control (-, set as 1). (A) mRNA expression of brown adipose specific markers UCP-1, PGC-1α, PRDM16, novel brown marker Meox-2, and white adipose specific markers IGFBP3 at basal level; (B) mRNA expression of thermogenic markers UCP-1 and PGC-1α at ISO-stimulated level. Rosiglitazone (Rosi) was used as a positive control. Data were presented as mean±SE (n=3). *, significantly different from the DMSO controls (-) with $p<0.05$.

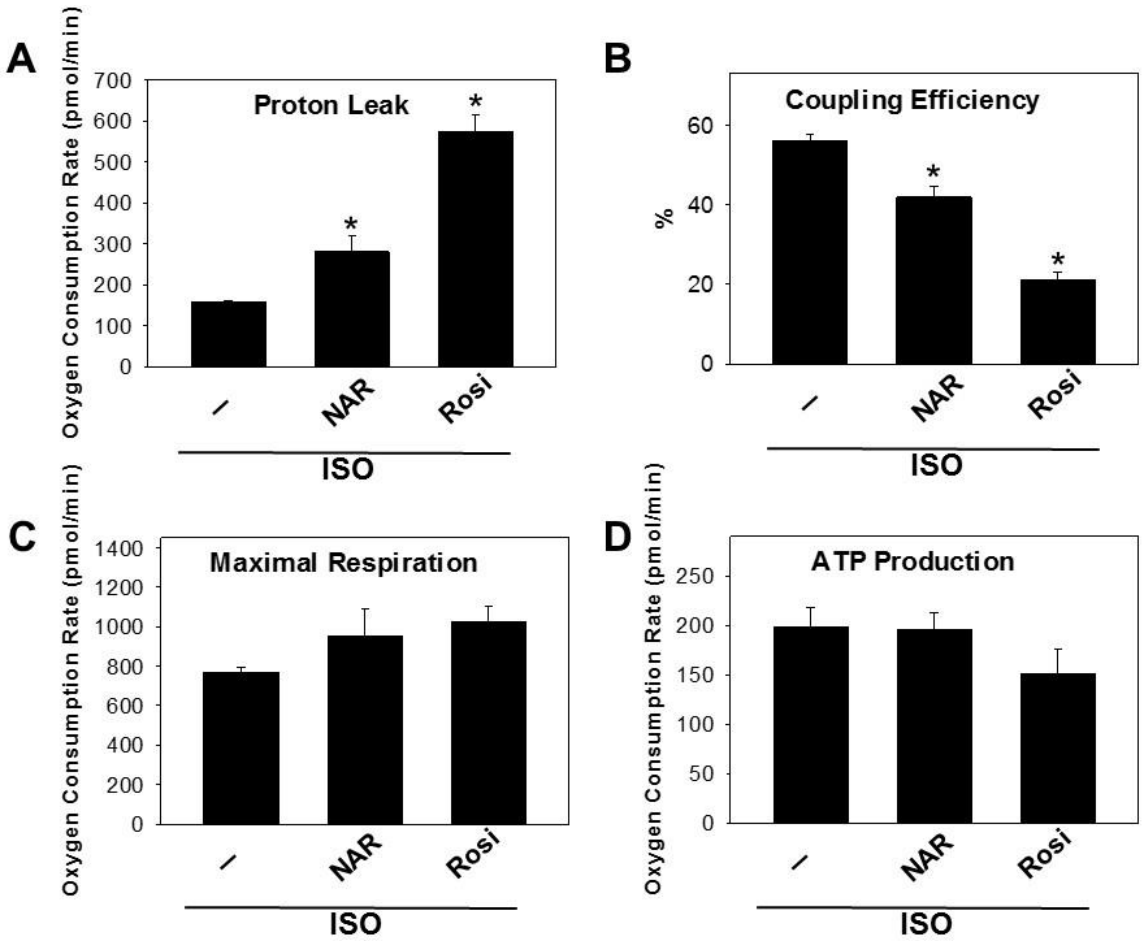

Figure 18 Effect of naringenin on mitochondrial respiration in isoproterenol induced 3T3-L1 adipocytes

3T3-L1 cells were differentiated in the presence or absence of naringenin (NAR, 10 µM) until day 7. The cells were then sub-cultured in 24-well XF assay plates overnight, followed by stimulation of isoproterenol (1µM) for 6 h. Real-time measurements of oxygen consumption rate (OCR) coupled with mitochondrial stress tests were conducted. The mitochondrial complex inhibitors were injected sequentially in the following order: oligomycin (1 µM), FCCP (0.75 µM), antimycin A/rotenone (1 µM each), and three readings were taken after each inhibitor. (A) OCR from proton leak, (B) coupling efficiency, (C) maximal respiration, and (D) ATP production. Rosiglitazone (Rosi) was used as a positive control. Data were presented as mean±SE (n=3). *, significantly different from the DMSO controls (-) with $p<0.05$.

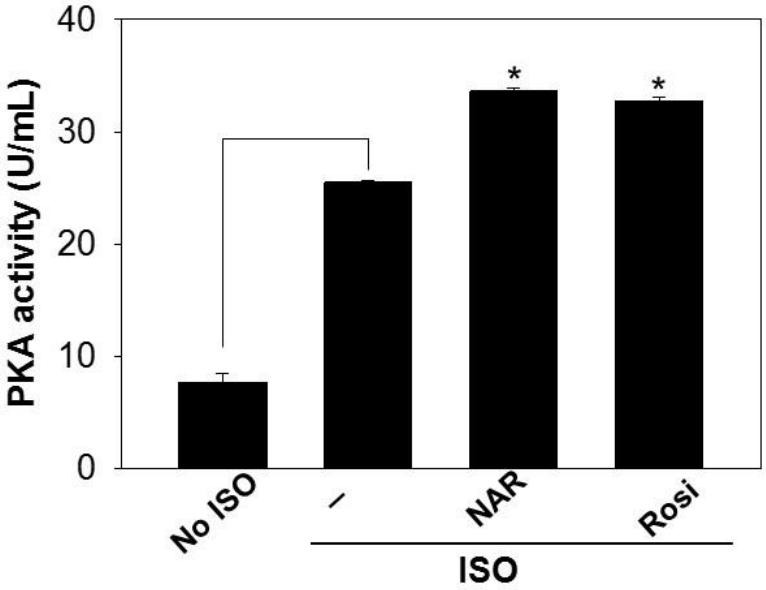

Figure 19 Effect of naringenin on PKA activation
3T3-L1 cells were differentiated in the presence or absence of naringenin (NAR, 10 µM) followed by costimulated with or without isoproterenol for 6 h. Total cell lysate was prepared and PKA activity was measured as described in materials and methods. Rosiglitazone (Rosi) was used as a positive control. Data were presented as mean±SE (n=3). *, significantly different from the DMSO control (-) with $p<0.05$.

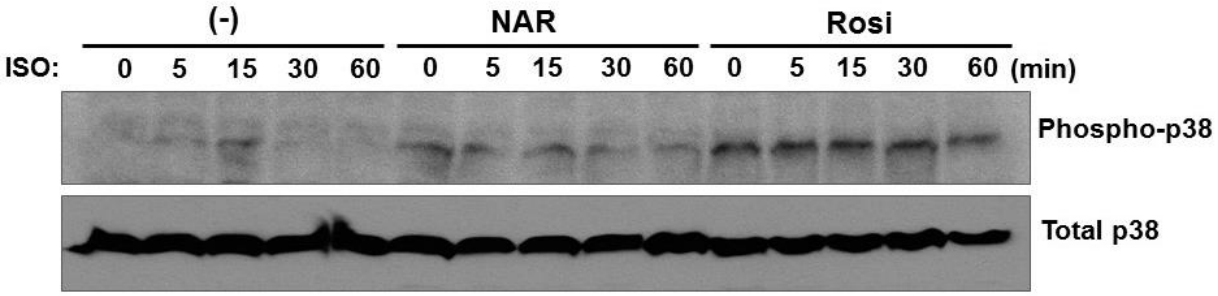

Figure 20 The effect of naringenin on the phosphorylation of p38 MAPK
3T3-L1 cells were differentiated in the presence or absence of naringenin (NAR, 10 µM) until day 7 followed by isoproterenol treatment for different times as indicated in the figure. Total cell lysate was prepared and analyzed by Western blot with specific antibodies against phospho-p38 MAPK and total-p38 MAPK. Rosiglitazone (Rosi) was used as a positive control. The experiments were performed 3 times. Results from a representative experiment was shown here.

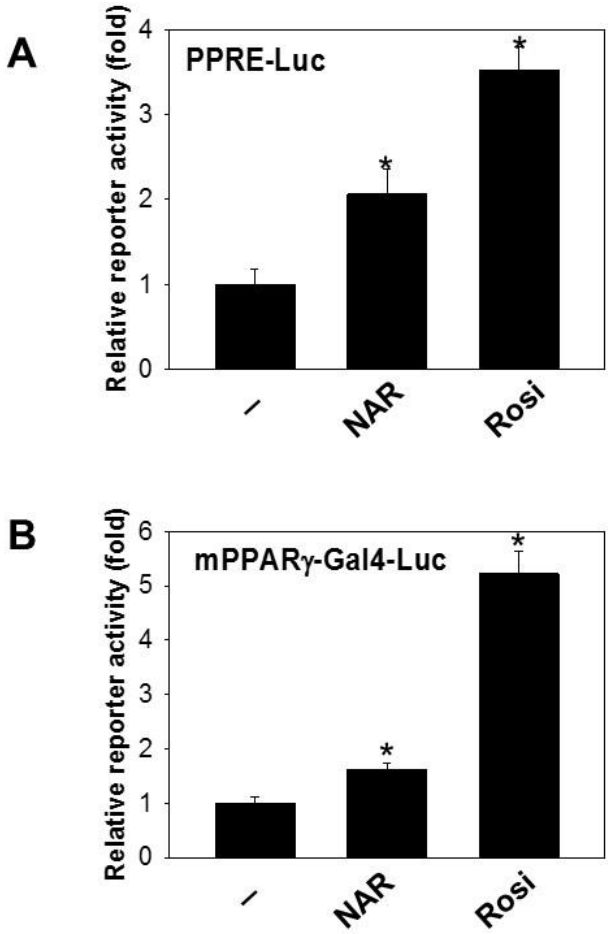

Figure 21 Effect of naringenin on PPARγ and PPRE transactivation
3T3-L1 preadipocytes were transfected with (A) PPARγ-gal4 and (B) PPRE transactivation reporters. Cells were treated with or without naringenin (NAR, 10 μM) for 18 h in 0.25% FBS containing DMEM. Cell lysate was prepared and reporter gene assay performed. Rosiglitazone (Rosi) was used as a positive control. PPRE transactivation normalized by total protein concentration is presented as fold of that of the control (set as 1). Data were presented as mean±SE (n=3). *, significantly different from the DMSO control (-) with $p<0.05$.

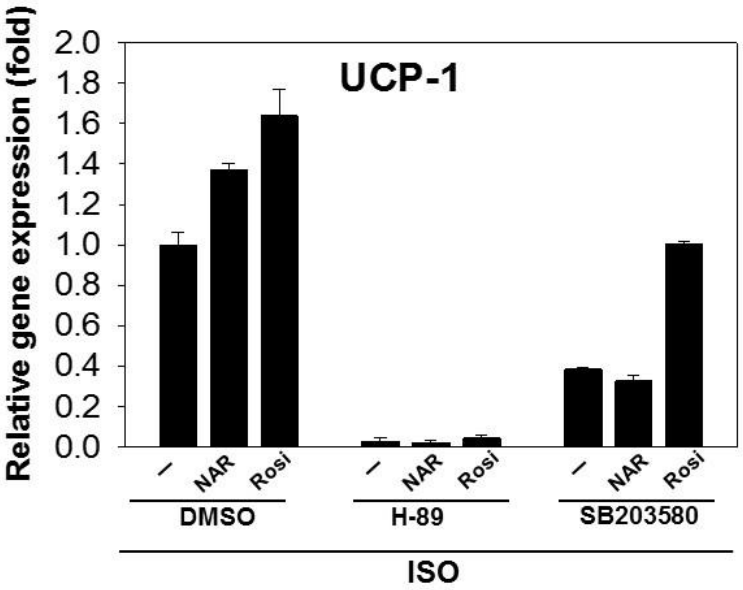

Figure 22 Regulation of UCP-1 gene expression by pharmacological inhibitors for PKA/p38 MAPK signaling pathway

3T3-L1 cells were differentiated in the presence of naringenin (NAR, 10 μM) or rosiglitazone (Rosi) until fully differentiated. The differentiated cells were pretreated with PKA inhibitor H-89 (20 μM), SB203580 (10 μM), or DMSO for 1 h followed by isoproterenol (1 μM) treatment for 6 h. Rosiglitazone (Rosi) was used as a positive control. mRNA expression of UCP-1 was evaluated by semi-quantitative RT-PCR. The relative mRNA expression was normalized with 36B4 and expressed as fold of the vehicle value (set as 1). Data were presented as mean±SE (n=3). *, significantly different from the DMSO control (-) with $p<0.05$.

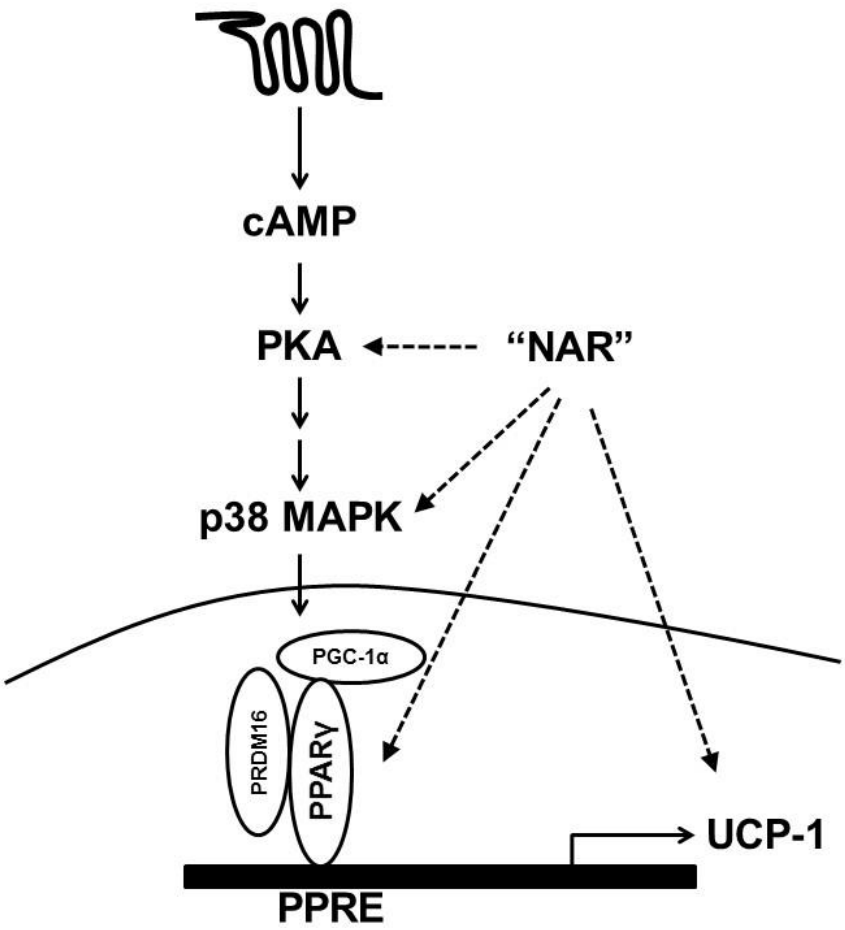

Figure 23 Schematic diagram of activation of β-adrenergic receptor-stimulated signaling pathway and naringenin effects

CONCLUSION AND FUTURE DIRECTION

In this dissertation, it has been reported that (1) mRNA of selected PRRs and inflammatory cytokines/chemokines are upregulated in the BAT of both DIO and ob/ob mice; (2) activation of PPRs induces activation of NF-κB and MAPK signaling pathways, leading to upregulation of the proinflammatory genes MCP-1, IL-6, RANTES, and TNF-α in mature brown adipocytes; (3) activation of PRRs suppresses UCP-1 expression, leading to decreased mitochondrial respiration and thermogenesis in mature brown adipocytes; (4) chronic activation of PRRs reduces adipogenesis and suppresses expression of brown-specific genes in both classic brown adipocytes and multipotent stem cells, suggesting that chronic activation of PRRs negative affect BAT development; lastly, (5) naringenin, a citrus flavanone, enhances thermogenic activation in isoproterenol-stimulated 3T3-L1 adipocytes through PKA/p38 MAPK activation.

Our results suggest that PRR-mediated inflammation in brown adipocytes may be potential targets to regulate BAT development and function for obesity treatment and prevention. Dietary bioactive compound naringenin may be beneficial in promoting functional BAT, contributing to energy expenditure.

In the future, the studies of the role of PRRs in brown adipose inflammation in vivo using the animal models would be needed to confirm the results using the cell culture models reported in chapter I and II. Selected PRR knockout animal with high fat diet could be used to determine the role of PRR in brown adipose inflammation and obesity. Since specific PRR knockout mice have been used to examine body weight, plasma inflammatory cytokines, and adipose inflammation in WAT, BAT inflammation and function can be examined in the same animal models. Moreover, these models can

be used to screen dietary bioactive compounds with anti-inflammatory properties for the activities to reduce BAT inflammation and promote BAT development and function. Furthermore, the effects of naringenin in promoting thermogenic activation in white adipocytes should be tested and extended in the animal models. Successful completion of naringenin studies in these preclinical models will provide justification to test the efficacy of naringenin in promoting functional BAT in human clinical trials.

VITA

Jiyoung Bae was born in South Korea on August 27, 1983. She obtained a Master of Science degree in Food Science and Nutrition from Hallym University in 2007. Jiyoung began her doctoral program at the University of Tennessee at Knoxville in 2011 and completed in 2015.